DUAL MODIFIED LIPOSOMES FOR DRUG AND GENE DELIVERY TO BRAIN

A Dissertation
Submitted to the Graduate Faculty
of the
North Dakota State University
of Agriculture and Applied Science

By

Gitanjali Sharma

In Partial Fulfillment of the Requirements
for the Degree of
DOCTOR OF PHILOSOPHY

Major Department:
Pharmaceutical Sciences

May 2014

Fargo, North Dakota

North Dakota State University
Graduate School

Title

Dual-modified liposomes for drug and gene delivery to brain

By

Gitanjali Sharma

The Supervisory Committee certifies that this ***disquisition*** complies with North Dakota State University's regulations and meets the accepted standards for the degree of

DOCTOR OF PHILOSOPHY

SUPERVISORY COMMITTEE:

Prof. Jagdish Singh
Chair

Prof. Chengwen Sun

Prof. Sanku mallik

Prof.Rhonda Magel

Approved:

May 14, 2014
Date

Prof. Jagdish Singh
Department Chair

ABSTRACT

The overall goal of our research was to design a vector for efficient delivery of therapeutic genes/drugs to brain. Specifically, this research work was focused on designing PEGylated liposomes surface modified with the receptor targeting protein, transferrin and cell penetrating peptides (CPPs) for targeting and improving the delivery of desired therapeutic agent to brain. Various CPPs including poly-L-arginine, TAT, Penetratin and Mastoparan were investigated for their influence on transport of transferrin receptor targeted liposomes across brain endothelial cells. The dual-modified liposomes were synthesized using thin film hydration and post-insertion technique. The biocompatibility of the liposomes was evaluated at increasing concentrations to obtain an optimum value for safe and effective delivery of drugs or genes. The liposomes showed excellent cellular, blood and tissue compatibility at the optimized concentration. In addition, the combination of targeting ligand transferrin and CPPs resulted in considerable translocation of the therapeutic agent across cellular and brain endothelial barriers both *in vitro* and *in vivo*.

Among different Tf-CPP liposomes, the Tf-Penetratin liposomes showed maximum translocation of the drug across the brain endothelial barrier (approximately 15% across *in vitro* and 4% across *in vivo* BBB) and efficient cellular transport of the encapsulated drug (approximately 90-98%) in various cell lines. In addition, Tf-poly-L-arginine and Tf-Penetratin liposomes showed improved transfection efficiencies in various cell lines. The Tf-Penetratin and Tf-TAT liposomes demonstrated excellent cellular biocompatibility and no hemolytic activity upto 200nM phospholipid concentration. *In vivo* efficacy of the liposomes was evaluated by performing biodistribution studies in in adult Sprague Dawley rats. The liposomes were intended for delivery of small molecule drug, doxorubicin and pDNA to brain. The dual modified

liposomes showed significantly ($p<0.05$) higher transport of encapsulated agents in rat brain as compared to single ligand (Tf) or plain liposomes. Histological examination of the tissues, from various organs, did not show any signs of toxicity including necrosis, inflammation, fibrosis etc. The study underlines the potential of bifunctional liposomes as high-efficiency and low-toxicity gene delivery system for the treatment of central nervous system disorders.

ACKNOWLEDGEMENTS

Gratitude is a feeling hard to express verbally. Still, I am making an attempt. Thank you God for giving me the vision to unravel the mysteries of life, the wisdom to choose what is right and the courage to stick by my principles.

Foremost, I would like to express my heartfelt gratitude to my advisor Dr. Jagdish Singh for his continuous support, patience, motivation and enthusiasm. It has been truly a wonderful and rewarding experience for me to work under the able guidance of Dr. Singh who gave me my academic life. I could not have imagined having a better advisor and mentor for my PhD study. As a very good and rigorous scientist, he taught me many different aspects of science and brought out the best in me. Dr. Singh is also an excellent life coach. He continuously influenced and inspired me by telling his past experiences. Dr. Singh has always given the great freedom and encouraged the innovative ideas. He has created a rich and fertile environment to study and explore new ideas in the lab. I am very fortunate for having known to him and being his student. I am eternally grateful to Dr. Singh for providing an excellent environment and research facilities for conducing pharmaceutical research.

My sincerest thanks are also due to my advisory committee which includes Dr. Chengwen Sun, Dr. Sanku Mallik and Dr. Rhonda Magel for their timely support and guidance. I am grateful for their deep and insightful questions about the subject which helped me to shape my research work and always make me think beyond my imagination. It was really helpful for me to prepare for my interviews and to develop as a better scientist. I extend most cordial thanks to all the teachers of my institute.

My warm and sincere thanks are due to my lab colleagues and friends: Buddhadev Layek, Moyna Layek, Mayura Oak, Ruchi, Anil Wagh, Neha Singh, Varsha Meghnani, Teicheng Zhong, Rahul Nahire, Erin, Sushant Lakkadwala and Lindsey Lipp and Dr. Manas.

The cooperation and affection of the administrative and library staff is kindly acknowledged. In this regard, Janet Krom and Jean Trautmann deserve special attention. I am eternally grateful to Janet and Jean for their constant help, information, patience & support. They have created a wonderful environment for graduate students, I'd say home away from home. 'Thank You for making this time nostalgic with lots of sweet reminiscences to look back at.

Words fail to express my sentiments for my parents Mr. Surinder Avinash Sharma & Mrs. Prem Lata Sharma for sowing in me the strength, the determination and the will to adapt to every situation in my life. My husband, Amit Modgil, whose love and support helped me to finish this journey. His love provided me inspiration and was my driving force. I also want to thank to my father & mother in-law Mr. Avinash Modgil and Mrs. Rekha Modgil for their unconditional love and support. The love, kindness, support & guidance I have received from my sisters Chayanika, Bhoomika, Saakshi and Shivani and my sister in-laws Sonali and Anubha, and my loving nephews Aryan, Shaurya, Tejas and Naman will always be fondly remembered. A very special thanks to my lovely and adorable son Ansh Modgil for making the final defense and thesis submission of my PhD degree happy and memorable.

Last but not the least; I duly acknowledge all the faculty, graduate students, administrative staff and department of pharmaceutical sciences. Though, I have not named everyone, whose kind help aided in the compilation of this work, gratitude towards them is heart-felt.

Thank you everyone, once again.

DEDICATION

I dedicated this dissertation to my family. I am extremely grateful to my parents, Mr. Surinder Avinash Sharma and Mrs. Prem Lata Sharma, who encouraged me to pursue higher education and supported me emotionally and financially. A special feeling of gratitude to my husband, Amit Modgil, whose words of encouragement, emotional support and guidance have always been an inspiration for me. Also, I would like to dedicate to my son; Ansh Modgil who is a wonderful blessing in my life.

TABLE OF CONTENTS

LIST OF TABLES

LIST OF FIGURES

CHAPTER I. INTRODUCTION

Over the recent years, there has been a considerable progress in the field of neuroscience leading to an improved understanding of disorders of central nervous system (CNS). In contrast, the development of successful strategies for treating these disorders is limited due to the protective function of blood brain barrier (BBB).The concept of BBB originated in late 19^{th} and early 20^{th} centuries, when Paul Ehrlich and his colleagues discovered that some dyes could stain the brain cells after direct injection into brain, but were not able to penetrate the brain after peripheral administration (Bradbury et al. 1979). A parallel study revealed that bile salts induced seizures after direct injection into brain but did not show any related symptoms after peripheral administration (Roth et al. 1961; Banks et al. 2012). Since then, there have been comprehensive efforts to provide a scientific definition of BBB and to elucidate the mechanisms of transport of different molecules across this barrier (Davson et al. 1969; Cserr et al. 1992; Knopf et al. 1995; Chen et al. 2012). More restrictively, BBB is defined as the microvasculature of brain that is composed of endothelial cells having tight intracellular junctions and absence of any fenestrea (Davson et al. 1969). However, the vascular BBB does not explain all facets of conceptual BBB. The choroid plexus with cerebrospinal fluid, referred to as the cerebrospinal fluid barrier (CSFB), is another important gateway to reach brain parenchyma (Johanson et al. 2008, Townsend et al. 2007). The entry of any molecule into brain, after parenteral administration, is largely controlled by BBB and CSFB (Chen et al. 2012). However, the CSFB faces a ventricle that flushes the drug, injected in the back of the ventricle, back into the blood (Rip et al. 2009; Pathan et al. 2009). Moreover, there are about 100 billion capillaries with a surface area of $20m^2$ that contribute to the formation of BBB (Pardridge et al. 2003). Therefore, BBB is universally

considered the most important barrier in restricting the transport of molecules into brain (Hawkins et al. 2008).

BBB is a highly regulated and tightly controlled barrier that provides a safe asylum to the brain. It plays a vital role in maintaining brain homeostasis and allows selective transport of essential nutrient molecules into brain (Chen et al. 2012). However, the high impermeability and selectivity of this barrier prevents the transport of many drugs and other therapeutic molecules into brain (Serwer et al. 2012; Scherrmann et al. 2002). The delivery of therapeutic agents across BBB has engendered substantial interest over past decades (Kohane et al. 2002; Qin et al. 2011;Townsend et al. 2007). BBB possesses unique biological characteristics that contribute to restricting the movement of molecules to brain:

1) Brain endothelial cells lack fenestrations and have very few pinocytotic vesicles and larger number of mitochondria (Stewart et al. 2000; Abbott et al. 2005; Oldendorf et al. 1997).
2) Occurrence of an intricate complex of transmembrane proteins (e.g. occludins, claudins), forming intimate intracellular connections, called tight junctions (TJ).
3) The expression of different transport proteins on brain endothelial cells like p-glycoproteins (efflux transporters) and multidrug resistance proteins (MRPs) (Rip et al. 2009; Abbott et al. 2006).
4) Synergistic influence of astrocytes, pericytes, astrocytic perivascular end feet, macrophages and neurons on BBB functions (Ramsauer et al. 1998; Ramsauer et al. 2002; Dohgu et al. 2005).
5) The immune barrier of brain is formed by tightly packed endothelial cells, perivascular macrophages and mast cells and is further reinforced by the macroglial cells. This barrier

limits the passage of external immune cells, especially lymphocytes across BBB (Wekerle et al. 2002; Daneman et al. 2009; Williams et al. 2001; Streit et al. 2005; Levin et al. 1980).

This unique environment of CNS presents a formidable barrier to the delivery of a wide number of therapeutic molecules to brain. With the exception of small lipophilic drug molecules having molecular mass of less than 400-600 Da, most of the drugs in circulation do not penetrate the BBB (Levin et al. 1980; Pardridge et al. 1998). More than 98% percent of the drugs are halted mid-development due to poor brain permeability (Terasaki et al. 2003). Also, recent statistics from National Cancer Institute show about 22,910 new cases of brain tumor leading to 13,700 deaths, each year. In addition, neuro-degenerative diseases like Alzheimer's disease have become the most common cause of dementia among the elderly and have been reported to affect about 5% of Americans over age of 65, and 20% over the age of 80 years (Roney et al. 2005). These factors have triggered extensive efforts, by scientists across the globe, in developing safe and efficient vectors for delivery of therapeutics to brain. Viruses are equipped with different molecular mechanisms to overcome these hurdles and can therefore, serve as efficient delivery vectors (Foust et al. 2009). Yet, the potential application of viruses as delivery agents and their further investigation in clinical research is impeded by the associated immune response and cytotoxicity thereby, accentuating the need for synthesis of safe and efficient non-viral delivery vectors. Multidisciplinary approaches involving biology, nanotechnology and biophysics need to be considered to accomplish the goal of improving the delivery of therapeutic drugs and genes across BBB (Chen et al. 2012).

1.1. Strategies for delivery of therapeutics to brain

1.1.1. Modulation of tight junction barrier

Various chemical and biological substances and physical stimuli have been reported to cause temporary opening of the BBB by modulating the TJ (Hynynen et al. 2008; Stam et al. 2010). It has been previously reported that cyclodextrins extract cholesterol from brain capillary endothelial cell membrane and allow the penetration of water soluble drugs across the *in vitro* brain endothelial monolayer (Tilloy et al. 2006). Also, chemicals like poloxamers are co-administered with Digoxin to increase the brain permeability via inhibition of P-gp and MRP efflux transporters (Batrakova et al. 2001). Apart from this, biological viruses like adeno-associated virus cause up regulation of chemokines thereby increasing the permeability of BBB (Kuang et al. 2009; Kaplitt et al. 2007). Bradykinin agonist, Cereport (RMP-7), has been widely employed to increase the CNS delivery of carboplatin, loperamide and cyclosporine A. Physical agents like ultrasound also increase the delivery of therapeutic molecules like gene, antibodies or water soluble chemotherapeutic agents by causing partial opening of the TJ (Williams et al. 1984; Yang et al. 2007; Liu et al. 2010). Electromagnetic field causes opening of TJ via protein kinase C signaling and translocation of TJ proteins whereas, microwave increases the brain permeability by thermal effects (Moriyama et al. 1991; Qiu et al. 2010; Kuo et al. 2008). The rationale for opening the TJ barrier is based on the fact that most of the disease states are associated with leakage of BBB or TJ opening. In addition, partial opening of BBB can lead to improved passage of small water soluble drugs as well as macromolecules like liposomes, nucleic acids and antibodies (Chen et al. 2012). However, the strategy of modulating the BBB by partial opening of BBB is a dual-edged sword. On one hand it improves the permeability of water soluble molecules, antibodies, proteins, liposomes and nanoparticles without the need for

chemical modification of the drug molecule. On the other hand, temporary opening of TJ can also increase the permeability of unwanted molecules like pathogens and toxins thereby necessitating the control of the duration of TJ modulation.

1.1.2. Utilization of brain transporter systems

BBB expresses a wide variety of transporters for the movement of essential nutrients like glucose, amino acids or peptides (Tsuji et al. 1999). Therapeutic molecules mimicking the endogenous nutrients are easily transported via these transporter proteins. Levodopa is a lipid insoluble precursor of dopamine used for the treatment of Parkinson's disease. It contains carboxyl and α-amino groups that facilitate its transport via large neutral amino acid carrier (Wade et al. 1975). Although, these endogenous transport systems can be used as efficient portals for delivery of drugs, however, there practical application is limited to the peptide drugs. Also, this approach is less favored as it competes with the transport of essential nutrients to brain.

1.1.3. Inhibition of efflux pumps

Various efflux pumps on the surface of BBB like P-gp and MRP transporters inhibit the transport of drug molecules into brain (Fromm et al. 2000). Miller et al., initiated the concept of inhibiting the P-gp efflux pumps using Pluronic® P85 (poloxamer) copolymers. The study compared the accumulation of Rhodamine 123, a selective substrate of P-gp, in brain microvessel endothelial cells. Poloxamer block co polymers consist of hydrophilic ethylene oxide (EO) and hydrophobic proplylene oxide (PO) arranged in the triblock fashion thereby, imparting an amphiphilic character to the polymer. Due to the amphiphilic character of these co polymers they exhibit surfactant properties. Previous studies suggest that the inhibition of P-gp involves 1) Interaction of the copolymer with cellular membrane to increase membrane

fluidization 2) Inhibition of P-gp ATPase activity and depletion of cellular ATP (Kabanov et al. 2003). These copolymers have been reported to enhance the permeability of a wide range of drugs, including doxorubicin, etoposide, taxol, 3'-azido-3'-deoxythymidine, valproic acid and loperamide, in the bovine brain microvessel endothelial cell monolayer (Batrakova et al. 1999). It has been reported earlier that both the HLB value and PO block length are important in determining the P-gp inhibition activity of Pluronic co polymers (Batrakova et al. 2003). Even though these block co polymers have a significant potential in increasing the transport of many drug molecules across the BBB, however their direct interaction with the cell membrane and inhibition of ATP activity has raised concerns about the toxicity associated with their chronic use. Nevertheless, short term application has shown transient depletion of ATP and restoration of BBB integrity (Batrakova et al. 2001; Batrakova et al. 1999).

1.1.4. Adsorptive mediated transcytosis (AMT)

The growing evidence indicating the success of transport of therapeutic molecules into brain via cationic proteins and cell penetrating peptides (CPPs) has conveyed significant importance to AMT as route for delivery of molecules across BBB. CPPs are short cationic peptides (less than 30 amino acids) that have the ability to transport extracellular molecular cargo into the cells. These peptides are capable of entering the cells without producing cytolytic effects. In addition, they effectively by pass P-gp in the BBB and are therefore used as vectors for delivery of drugs that are substrates for P-gp (Rousselle et al. 2000). Table 1 illustrates commonly used CPPs with their features. Despite the variation in length and sequence of amino acids, these peptides share some common features like their amphipathic nature, net positive charge, theoretical hydrophobicity and helical moment, the ability to interact with lipidic membranes, and to adopt a distinct secondary structure upon association with lipids (Deshayes et

al. 2005). The CPPs are primarily considered to be transported via receptor and energy dependent pathways but the exact mechanism is not yet fully understood. While for some CPPs endocytosis is the exclusive mechanism of uptake however for others it is an alternative mechanism (Drin et al. 2003).The use of CPPs is based on the fact that these peptides can be linked to the therapeutically active molecules and can transported across the cell membrane. This linkage can either be covalent or non-covalent. Various cargo molecules and delivery agents have been delivered into the cells using CPPs e.g. proteins, small drug molecules, nucleic acids, liposomes and nanoparticles. Adenot et al., have previously reported an increase in the penetration of various chemotherapeutic agents across BBB in situ and *in vitro* cell based model, after conjugation with SynB3 CPP (Adenot et al. 2007). They reported an increase in brain delivery of doxorubicin by factor of 30, benzylpenicillin by factor of 7, paclitaxel by factor of 22, dalargin by factor of 18 and morphine 6-glucoronide by factor of 50 without disrupting the function of BBB. Another study reported a significant increase in the uptake of dalargin after conjugation with SynB on intravenous injection into mice (Rousselle et al. 2003).

In addition TAT conjugated nanoparticles and liposomes have been used for deliveryof therapeutic agents across BBB. Qin et al., reported enhanced penetration of Choletrol-PEG_{2000}-TAT into brain as compared to Cholesterol-PEG^{2000} and conventional cholesterol liposomes (Qin et al. 2011). Sharma et al., reported enhanced penetration of CPP-transferrin-liposomes into brains of adult Sprague Dawley rats as compared to transferrin conjugated and conventional plain liposomes (Sharma et al. 2012; Sharma et al. 2013). A recent study demonstrated significantly ($p<0.001$) higher accumulation of Penetratin functionalized PEG-PLA (poly lactic acid) nanoparticles in rats as compared to the low molecular weight protamine nanoparticles (Xia et al. 2012).

Apart from the CPPs, cationic proteins have also been employed to increase the penetration of therapeutic agents across BBB via adsorptive-mediated mechanism. Poduslo and Curran demonstrated that polyamine modification of proteins (albumin, insulin and IgG) dramatically increased their penetration across BBB. The permeability of insulin increased by 1.7-2.0 fold, albumin increased by 54-165 fold and IgG increased by 111-349 fold (Poduslo et al. 1996). A previous study compared cationic bovine serum albumin conjugated PEG-PLA nanoparticles (CBSA-NP) with the native bovine serum albumin conjugated NP (BSA-NP) and unconjugated nanoparticles (NP) for brain delivery in mice (Lu et al. 2007). The results demonstrated that the penetration of CBSA-NP increased by 2.3 fold as compared to NP. Although cationic proteins have shown considerable improvement in delivery of molecules or delivery vectors across BBB, however the toxicity or immunogenicity associated with this chemical modification cannot be ruled out (Roney et al. 2005).

Table 1. Properties of some naturally occurring cell penetrating peptides

CPP	Amino acid Sequence	Net charge	Cell Lysis activity
MAP	KLALKLALKALKAALKLA	+5	Yes
$pAntp_{43-68}$(Penetratin)	RQIKIWFQNRRMKWKK	+8	No
SynB1	RGGRLSYSRRFSTSTGR	+6	Yes
SBP	MGLGLHLLVAAALQGAWSPKKKRKV	+6	No
SynB3	RRLSYSRRRF	+6	-
Transportan	GWTLNSAGYLLGKINLKALAALAKKIL	+4	No
FBP	GALFLGWLGAAGSTMGAWSQPKKKRKV	+6	-
TAT_{48-60}	GRKKRRQRRRPPQ	+8	No

(Batrakova et al. 2003; Zorkoet al. 2005; Rousselle et al. 2000; Deshayes et al. 2005)

The delivery of small molecules, vectors and other protein and nucleic acid drugs that are associated with poor brain penetration can be efficiently transported across BBB via AMT. However, the non-specific uptake of the CPP or cationic proteins can result in higher accumulations in blood vessels and peripheral organs. In addition, the toxicity and immunogenicity associated with chemical modifications of proteins can pose a challenge to practical application of these agents in improving brain delivery. Previous studies have reported membrane toxicity and tissue inflammation using CPPs and cationic albumin nanoparticles (Drin, et al. 2003; Lu et al. 2007). A recent report has indicated that is non-toxic up to a concentration of 100μM however after peptide bound TAT demonstrated significant and chain length dependent toxicity irrespective of the sequence of peptide (Cardozo et al. 2007). A study indicated toxicity associated with a very high dose of TAT46–60 peptide (Sabatier et al. 1991).

1.1.5. Receptor mediated transcytosis (RMT)

RMT overcomes the limitation of non-specific uptake by peripheral tissues and blood vessels thus reducing the side effects associated with AMT. Up regulation of certain receptor types in a diseased condition further enhance the opportunity for active targeting of therapeutic molecules to specific sites and tissues e.g. transferrin receptors are over expressed on brain endothelium and the receptor expression is significantly up regulated in tumor conditions (Huwyler et al. 1996; Oba et al. 2007). Cargo molecules like proteins, peptides, delivery vectors can be linked with an active targeting ligand and transported across BBB via RMT. Therefore, this approach is also called as Trojan horse approach (Pardridge et al. 2002; Pardridge et al. 2003). Increased understanding of BBB biology and genomics has led to the discovery of a large number of transporters and receptors that can be used for delivery of molecules across BBB. In general there are three steps involved in RMT (Pardridge et al. 2002; Pardridge et al. 2003):

a) Endocytosis of the molecules on the luminal(blood) side after binding of the ligand to the targeted receptor.

b) Movement of the molecules across the endothelial cytoplasm

c) Exocytosis of the drug/ ligand-attached drug or delivery vector on the abluminal (brain) side.

The second step sometimes leads endosomal/lysosomal degradation of the drug molecules or cargo. This fate is overcome by using pH sensitive liposomes or cationic peptides/molecules (Bartsch et al. 2005; Shir et al. 2006). Certain targeting ligands like diphtheria toxin have endosomal escaping ability (Boer et al. 2007). Advantageously, lysosomal/endosomal escaping phenomenon is not required for brain delivery and successful

transport of small drug molecules, liposomes, nanoparticles and polymeric complexes to brain (Gabathuler et al. 2010; Boer et al. 2007).

Various receptors involved in RMT for delivery of molecules across BBB are listed below:

a) Insulin receptors: Insulin receptor is a heterotetramer protein of molecular weight 300kDa and consists of two extracellular alpha and two transmemberane beta subunits (Boer et al. 2007). This receptor has been widely evaluated for RMT and is used for transporting drugs into brain. Pardridge and colleagues extensively investigated this receptor system and successfully developed a radiolabelled amyloid-β-peptide, 125I-Abeta1–40 conjugated to 83–14 monoclonal antibody(mAb) that was used to target human insulin receptor and was used as a diagnostic probe for Alzheimer's disease (AD) (Pardridge et al. 1985; Pardridge et al. 1995; Zhang et al. 2003; Xia et al. 2009; Wu et al. 1997; Frolich et al. 1998). The same group also investigated human insulin receptor monoclonal antibody in adult Rhesus monkey and observed wide distribution of the antibody in all parts of the primate brain and thus confirmed the potential of the antibody in delivering therapeutic molecules across BBB. Insulin receptors on BBB are involved in transport of glucose to brain and therefore, these receptors play an important role diabetes and obesity. Frolich et al., reported that the expression of insulin receptors is altered in AD (Frolich et al. 1998). A previous study also reported that amyloid-β peptide, an important mediator of AD, can compete with the endogenous insulin and interfere insulin metabolism thereby leading to impaired glucose utilization in the brain of AD patients (Recht et al. 1990). These results suggested the profound implications of using insulin receptor of transporting receptor targeted therapeutic molecules or delivery vectors across BBB. The approach is likely to affect the most important pathway for glucose utilization.

b) Transferrin receptors (TfR): Transferrin receptors are the widely studied systems for RMT of delivery vectors and therapeutic agents across BBB. The receptor is a transmembrane glycoprotein with two subunits of 90kDa that are linked by disulfide bridge and each of these subunits can bind to one molecule of transferrin (Moos et al. 2000). In addition to the BBB, this TfR is also expressed on hepatocytes, monocytes, erythrocytes, intestinal cells, epithelial cells of choroid plexus and neurons. TfRs on BBB mediate the transport of iron bound to transferrin into the brain. Nanoparticles, liposomes, therapeutic drug molecules can be conjugated to either transferrin protein or transferrin monoclonal antibody (OX-26). The TfR targeted monoclonal antibody binds to a different site as compared to transferrin protein and therefore, is less likely to interfere with the endogenous transferrin in circulation. A recent study reported an improvement in the expression of luciferase gene in C6 glioma cells, primary hippocampal neurons and primary cortical neurons on transfection with transferrin modified cationic liposomes as compared to conventional plain liposomes. However, the transfection levels were low with the conjugation of transferrin protein. There low transfection levels with transferrin conjugated delivery vector were attributed to the high concentration of transferrin protein in circulation which competes with the transferrin on the nanoparticle system (Cruz et al. 2004). Another limitation of using transferrin as a delivery system is that exogenously supplied transferrin can lead to overdose of iron transport into brain. In order to avoid the limitations of using transferrin as a delivery system, transferrin receptor targeted antibodies have been used that bind to a receptor binding site different as compared to the transferrin protein. Different antibodies that have been evaluated include OX26 (anti-rat TfR monoclonal antibody), R17-217 and 8D3 (anti mouse TfR monoclonal antibody) were all examined. Comparison of the brain uptake of R17-217 and 8D3 revealed a higher uptake of 8D3 (3.1% injected dose/gram of tissue) as compared

to R17-217 (1.7% injected dose/gram of the tissue) (Lee et al. 2000). Ulbrich et al., investigated the distribution and brain targeting properties of human serum albumin nanoparticles conjugated to transferrin protein or transferrin monolclonal antibodies (OX26 or R17-217) for delivery of loperamide (does not cross BBB) (Ulbrich et al. 2009). The results demonstrated significant anti-nociceptive effects with loperamine loaded HAS nanoparticles after covalent modification with transferrin or antibodies (OX-26 or R17-217). The study also showed enhanced transport of transferrin monoclonal antibody modified nanoparticles across BBB as compared to the IgG2a antibody or transferrin modified nanoparticles thus further confirming the efficacy of monoclonal antibodies over transferrin protein for delivery of therapeutic agents to brain (Ulbrich et al. 2009). A recent report showed a comparison of different targeting ligands in improving the transport of molecules to brain. Five different targeting ligands were compared for their ability to target brain both *in vitro* and *in vivo*: transferrin, R17-217 (against TfR), COG 133 (against low density lipoprotein receptor -LDLR and lipoprotein receptor protein-LRP), Angioprep-2 (against LRP) and cross reacting material (CRM)197(against diphtheria toxin receptor-DTR). The *in vitro* results showed that only R17-217 and CRM197 were observed to be associated with human endothelial cells and only R17-217 showed enhanced brain uptake of liposomes in Balb/c mice at all time-points after intravenous injection (Rooy et al. 2011). The authors studied the distribution of ^{3}H-labelled liposomes in brain capillaries using capillary depletion method and observed that the distribution of R17-217 liposomes was 10 times more than the untargeted liposomes. In addition, R17-217 liposomes were the only ones whose concentration was maintained in the brain over a period of 6h and was 0.18% of the injected dose/gram of tissue after 12h. The authors also suggested that the higher accumulation of this antibody in comparison to the other groups could be due the higher molecular weight and higher

affinity of the antibody to the receptors leading to stronger brain targeting ability and lower rate of elimination (Rooy et al. 2011). Although targeting ligand has a significant contribution in improving the delivery of molecules to brain, there are other parameters like matrix material, particle size, surface properties, the density and conformation of targeting ligand that also play an important role in brain delivery. A recent study performed by Sharma et al., also showed higher accumulation of transferrin-CPP modified liposomes in rat brain after 24h of intravenous administration (Sharma et al. 2013). The authors proposed a dual mechanism for improved and targeted delivery of transferrin modified liposomes. The conjugation of CPP with transferrin-liposomes enhanced the penetration of transferrin liposomes into brain by overcoming receptor saturation versus the transferrin conjugated or untargeted liposomes. Transferrin has been evaluated to be an important target for delivery to brain. However, more studies need to be conducted in order to fully understand the function and performance of targeting ligands. The expression of TfR on brain endothelial cells was observed to decrease in brain ischemia (Moos et al. 2004). In contrast, the expression was observed to be decreased in the hippocampus of patients with AD as compared to normal humans (Morris et al. 2004; Kalaria et al. 1992). However, there was a marked increase in the expression of transferrin receptors during brain injury and after intra cerebral hemorrhage (Wu et al. 2003). An immunohistochemical evaluation of normal brain tissue and tumor biopsy revealed a differential staining pattern for TfRs on brain endothelial cells of normal and tumor tissue indicating a higher level of expression in tumor associated brain endothelial cells (Recht et al. 1990).

c) Low-density lipoprotein receptor related proteins 1 and 2 (LRP1 and LRP2) receptors: These are multi-ligand, multifunctional scavengers and signaling receptors. They can interact with a diverse range of molecules and/or mediators like ApoE, tissue plasminogen

activator(tPA), plasminogen activator inhibitor 1 (PAI-1), amyloid precursorprotein (APP), lactoferrin, melanotransferrin, α2 macroglobulin(α2 M), receptor associated protein (RAP), HIV-1 TAT protein, Heparin, cofactor II, heat shock protein 96 (HSP-96) and engineered angiopeps (Gabathuler et al. 2010; Boer et al. 2007). Recently, a wide number of investigations have revealed the application of LRP1 and LRP 2 in targeting drugs to brain in a manner similar to the transferrin or insulin receptors. Schroder et al., first investigated the distribution of polysorbate-80 coated poly(butylcyanoacrylate-PBCA) nanoparticles *in vivo* and observed increased transport of hexapeptidedalargin after intravenous injection of the nanoparticles (Schröder et al. 1996). Similar study also indicated improved brain transport of drugs that do not cross BBB e.g. tubocurarine, loperamide, 8-chloro-4-hydroxy-1-oxol, 2-dihydropyridazino, quinoline-5-oxide choline salt (MRZ 2/576),and doxorubicin, after incorporation into polysorbate 80 coated nanoparticles. The enhanced transport across BBB was attributed to the adsorption of Apo E or B on the nanoparticles followed by LDL receptor mediated transcytosis (Blasi et al. 2007). A recent study reported enhanced uptake and intracellular localization of PEGylated albumin nanoparticles, covalently bound to ApoE, into mouse brain microvascular endothelial cells (Zensi et al. 2009). Furthermore, *in vivo* evaluation of ApoE modified albumin nanoparticles in SV129 mice showed transcytosis of the nanoparticles into brain parenchyma and transport into neurons 30 min after administration into juglar vein (Yuan et al. 2006).

Lactoferrin is another ligand that can be targeted to brain via LRP mediated transcytosis (Fillebeenet al. 1999). A group of scientists also confirmed the expression of lactoferrin receptors on mouse brain capillary endothelial cells (Huang et al. 2007). It is an iron binding glycoprotein that belongs to transferrin family. It has been implicated in a number of pathological conditions of brain. This cationic glycoprotein is found to be associated with

normal ageing and to be increased in people with AD, Pick's disease and Down Syndrome (Leveugle et al. 1994). Ji et al., demonstrated greater transport of lactoferrin into rat brain as compared to transferrin and OX26 (Ji et al. 2006). Another group of researchers showed a 3fold increase in the brain transport of PEG-PLA nanoparticles after conjugation with lactoferrin, in intravenously injected mice (Hu et al. 2009). Later the same group evaluated the biodistribution of Lactoferrin conjugated PEG-PLA nanoparticles loaded with coumarin-6 in mice and the therapeutic efficacy of the same nanoparticles loaded with urocortin in Parkinson's disease rat model (Hu e al. 2011). The data demonstrated an increase in the AUC by 2.5 times using lactoferrin conjugated nanoparticles as compared to the unmodified nanoparticles, 24h post administration. Despite the low drug loading levels of lactoferrin nanoparticles, these were successfully taken up by brain and resulted in enhanced attenuation of lesions in striatum (Hu et al. 2011). This suggests that lactoferin modified nanoparticles can serve as efficient delivery vectors for treatment of brain diseases like Parkinson's disease.

Melanotransferrin is another targeting molecule that has been evaluated to undergo transcytosisvia LRP1 receptor. It has been previously reported that recombinant human melanotransferrin was easily taken up by mouse brain after intravenous injection and in situ perfusion of brain (Demeule et al. 2002). This transcytosis across bovine brain capillary endothelial cells was atleast 14 fold higher as compared to transferrin and showed minimum intra-endothelial degradation. A previous report indicated higher efficacy of P97- adrimaycin conjugates against intracranial rat C6 glioma and human ZR-75-1 mammary tumors in athymic mice in comparison to the adriamycin alone (Gabathuler et al. 2005). The technology involving application of melanotransferrin as targeting molecule is now patented and a related product

(NeroTransTM transporter platform) is the proprietary property of Raptor Pharmaceutical Corp (Novato, CA).

Angiopeps is a group of targeting ligands that are reported to be highly effective in targeting BBB. Angiopeps have a high affinity for LRP receptors and belong to a family of peptides derived from Kunitz domains of aprotinin and other human proteins (Demeule et al. 2008). Angiopep2 (TFFYGGSRGKRNNFKTEEY, molecular weight 2.4 kDa) is a group of angiopeps that has demonstrated higher transcytosis and accumulation in brain parenchyma as compared to transferrin, lactoferrin and avidin (Demeule et al. 2008). Some recent studies have highlighted the efficiency of angiopep 2 conjugated dendrimers and amphotericin B loaded polymeric micelles in transporting across BBB (Ke et al. 2009; Shao et al. 2010). Thomas et al., reported 86 fold increase in transport of paclitaxel (3 molecules) conjugated with angiopep 2 (ANG1005) across BBB, using in situ rat brain perfusion model, as compared to free drug. The transport of angiopep conjugated drug also increased 4-54 fold as compared to free drug, after intravenous administration (Thomas et al. 2009).The therapeutic efficiency of ANG1005 was confirmed by increased survival rates of mice with implanted tumor cells (Regina et al. 2008). A recent study reported the use of dual modified PLGA naoparticles in improving the delivery of drugs or molecules into brain. The nanoparticles were surface modified with a brain penetrating peptide (similipoid, g7) and sialic acid residue for targeting receptors on brain tissue (Tosi et al. 2010). The dual modified nanoparticles showed an accumulation of ~6% of the injected dose/gram of tissue in the CNS over a period of 24h. In contrast, the single modified nanoparticles with only g7 modification showed a brain uptake of about 14%injected dose/gram of tissue at 1.5h after injection, however, they demonstrated a much shorter opioid effect (5h). Sialic acid conjugation with g7 modified nanoparticles increased the CNS activity of drug to 24h

(Tosi et al. 2010). The results established the significance of sialic acid g7 modified nanoparticles in improving the delivery of therapeutic agents to brain. The researchers confirmed the significance of sialic acid in retaining the nanoparticles in brain by slowing their clearance from brain parenchyma. The increased clearance without sialic acid was attributed more to the physical translocation rather than enzymatic degradation.

d) Diphtheria toxin receptor (DTR): This is commonly referred to as transmembrane Heparin binding Epidermal Growth factor (HB-EGF). This receptor forms a well characterized internalizing transporter on BBB and neuronal and glial cells that facilitated the transport of molecules via RMT (Mishima et al. 1996). The advantage of using DTR for RMT is that there are no endogenous ligands that can compete for transport across BBB (Gaillard et al. 2005). In addition, upregulation of this receptor is observed in various inflammatory condition associated with brain diseases (Opanashuk et al. 1999; Kawahara et al. 1999, Jin et al. 2004). However, a major disadvantage of using this receptor for targeting is that Diphtheria toxin (DT) is very toxic and not suitable for *in vivo* administration (Giannini et al. 1984). A mutated form of DT that has been used for targeting DTR is cross reacting material (CRM 197). It does not retain the toxicity associated with the enzymatic activity of DT but has the ability to bind with the DTR (Kaefer et al. 2000). CRM 197 has demonstrated efficient brain targeting both *in vitro* and *in vivo*. The safety and efficacy of CRM 197 as a carrier protein has been tested in clinical trials and has been recommended for use in human vaccines (Anderson et al. 1983; Buzzi et al. 2004). The upregulation of DTR in seizures and inflammatory brain conditions provides an opportunity for targeting in brain disease conditions and helps in maximizing the therapeutic efficacy of the conjugated therapeutic or diagnostic cargo across BBB.

1.2. Nanocarriers for delivery across blood brain barrier (BBB)

These are nanoscale carriers for delivery of therapeutic drugs or other molecules and consist of particles in the size range of 100-1000μm (Kreuter et al. 2005). These nanocarrier systems consist of polymeric nanoparticles and lipid based particles e.g. liposomes and solid lipid nanoparticles. This emerging class of delivery systems can be easily customized to transport desired therapeutic agents to specific tissues in the body. Rapid development in polymer chemistry and nanotechnology coupled with an increased understanding of the molecular biology of brain and various receptor systems that can be used to target brain, the development of nanocarriers for delivery to brain has gained increasing attention of scientists across the world. They can be surface modified for targeting specific receptors, can carry the therapeutic drugs and molecules in sufficient amounts and provide a controlled/ targeted release of the therapeutic agent. Ideal nanocarriers should have the following properties for delivery of drugs/therapeutic agents across BBB (Koo et al. 2006; Bhaskar et al. 2010):

a) They should be biodegradable, non-toxic and biocompatible,

b) Preferably a size of less than 200 nm

c) They should not aggregate/ dissociate in blood; should be stable in circulation

d) They should be non-immunogenic

e) Should have a targeting moiety coupled for delivery across BBB via receptor/adsorptive transcytosis or monocytes and macrophages.

f) The drug (small molecules, peptides, proteins, nucleic acids) carried should be stable and the drug release should be tunable

A large variety of nanocarriers have been developed so far, however only polymeric nanoparticles and amphiphilic lipids forming liposomes have been extensively exploited as

delivery of therapeutic agents to brain (Garcia et al. 2005). Several polymeric and liposomal delivery systems for treatment of brain disorders have reached clinical trials. The University of Regensburg in collaboration with Essex Pharma (Schering-Plough) has successfully completed phase 2 of clinical trials for pegylated liposomal doxorubicin and prolonged temozolamide in combination with radiotherapy in treatment of glioblastoma (ClinicalTrials.gov, 2011; Chen et al. 2012). Another pegylated doxorubicin formulation surface modified with glutathione is currently in Phase I/II of clinical trials in the Antoni van Leeuwenhoek hospital, the Netherlands. Non-amphiphilic colloidal drug carriers like dendrimers and micro emulsions are still at relatively early stage of development.

Amphiphilic molecules have been increasing investigated for development of nanocarrier systems. An amphiphilic molecule has a polar head group and a non-polar or hydrophobic tail. These agents interact with water or hydrophobic solution to orient their hydrophilic heads towards the aqueous phase and the hydrophobic tails away. At low concentrations, the amphiphilic molecules accumulate at the surface of water. The polar head of the amphiphile orients towards water while the hydrophobic tails orients towards the air. At higher concentrations above a critical concentration these amphiphilic molecules aggregate in the bulk of the aqueous phase to various structures like micelles, rods, vesicles etc (Chen et al. 2012).

Vesicles are hollow bilayer spherical structures having a hydrophilic core and the lipophilic walls. The size range of these vesicles for brain delivery varies from 20-200μm while the thickness of the membranes is approximately 3.5 nm (Chen et al. 2012). Liposomes are phospholipid bilayer vesicles that can encapsulate the hydrophilic drugs in the aqueous core and incorporate the lipophilic drugs in the membrane (Chen et al. 2011; Kateb et al. 2011). Niosomes are non-phospholipid polymeric/micellar vesicles with similar structure and function as that of

liposomes (Dufes et al. 2000, Arunothayanun et al. 2000). Xie et al., evaluated brain targeted nerve growth factor (NGF) encapsulated liposomes for delivery across BBB. The PEGylated liposomes were surface modified with RMP-7 for targeting the B2 receptors on brain endothelial cells. The results demonstrated protection of NGF from enzymatic degradation *in vivo* and increased permeability into brain after encapsulation into targeted liposomes (Xie et al. 2005). As discussed earlier, transferrin has been studied to possess significant potential for targeting the transferrin receptors on BBB. A recent study reported considerable improvement in tumor growth inhibition and increased survival rate of C6 glioma bearing rats using transferrin conjugated liposomes, with epirubicin in the hydrophilic core and tamoxifen in the lipid bilayer, as compared to the control groups administered with unconjugated liposomes or free drug (Tian et al. 2010). Another group of researchers reported that the phagocytic cells of the innate immune system, mainly neutrophils and monocytes, can be exploited as transporters of drugs to the brain. They synthesized negatively charged liposomes, encapsulating serotonin in the hydrophilic core, to target the circulating mononuclear phagocytic cells. The drug serotonin was selected as a brain impermeable neurological drug. The results indicated significantly higher uptake of liposomal serotonin after 4h and 24 of intravenous administration as compared to serotonin in solution (Afergan et al. 2008). Another very recent report illustrated the influence of incorporating a cell penetrating peptide on transferrin conjugated liposomes for improving their delivery to brain. The results showed an accumulation of ~3.8% of injected dose/gram in rat brain following 24h of intravenous injection of the transferrin-CPP modified liposomes. The accumulation was significantly greater as compared to transferrin liposomes or plain unconjugated liposomes (Sharma et al. 2012; Sharma et al. 2013).

Micelles form another group of spherical aggregates formed by the amphiphilic molecules. Micellar aggregates are formed by the amphiphilic molecules above a certain concentration called the critical micellar concentration (CMC). The most commonly known structures are the ones with their hydrophilic heads oriented towards the outer aqueous phase and the hydrophobic lipid tails directed inside. The amphiphilic molecules in the micelles are in continuous dynamic equilibrium and are in constant exchange with the outer bulk liquid (Chen et al. 2012). Polymeric micelles also known as polymersomes are self-assembled polymer shells composed of amphiphilic block co-polymers e.g. polyethylene glycol-polylactic acid and PEG-polycaprolactone (Discher et al. 2006). Block co-polymers that form the micelles have the same amphiphilic property as the lipids and differ in the fact that the block co-polymers have two distinct polymer groups that are covalently linked (Discher et al. 2006). Polymeric micelles differ from nanoparticles as the latter are either more solid (nanospheres) or contain oily/aqueous cores surrounded by the polymer shell (nanocapsules). Amphilic block co-polymers micelles have emerged as promising brain delivery vectors over the recent years. The advantage of using these polymeric micelles is that they are more stable and their molecular weights are controllable as compared to amphiphilic lipid micelle systems (Chen et al. 2012). In addition, the diversity of polymers and their block lengths provides flexibility in designing the most stable and desirable delivery systems. Some examples of hydrophobic core forming polymers include poly propylene glycol, poly caprolactone and poly D, L-lactide. Cholesterol is often employed as a hydrophobic group as it is biocompatible and possesses the potential of interacting with the cholesterol receptors on cell surface (Liu et al. 2004).

1.2.1. Surface modification of nanocarriers

1.2.1.1. PEGylation of nanocarriers

The most commonly used nanocarriers for delivery of therapeutic agents to brain include liposomes, polymer nanoparticles and polymeric micelles. These systems not only provide an advantage of protecting the encapsulated therapeutic agent from enzymatic, biological or chemical degradation in circulation they can also be manipulated as per desired application. pegylation of these agents has been reported to increase the circulation time of the nanocarriers (Maruyama et al. 2011; Sadzuka et al. 2002; Klibanov et al. 1990). Nanocarriers especially liposomes have very short half lives in circulation due to their interaction with various blood components and opsonins their elimination by the macrophage system of the body. Specifically, liposomes have a tendency to exchange their lipids with the cell membrane and are taken up by phagocytes in the body (Woodle et al. 1995). Incorporation of highly flexible and hydrophilic PEG chain on the surface of liposomes imparts the latter with steric stabilization and resistance to opsonins (Hatakeyama et al. 2007).Thus PEGylation of liposomes has become a standard platform for designing various tissue/receptor targeting nanocarrier systems (Hatakeyama et al. 2007; Li et al. 2009; Markoutsa et al. 2011). Furthermore, incorporation of PEG in block co-polymers also provides a hydrophilic head group to the polymers. PEG containing surfactants like poly oxyethylene-poly oxypropylene block co-polymers (Poloxamer 338 and Poloxamine 908) have been reported to effectively prolong the circulation life time of nanoparticles (Stolnik et al. 1995; Coombes et al. 1994). Gref et al., first reported the conjugation of PEG chains to poly (lactic acid) nanoparticles (Gref et al. 1994). Later PEG chains were also coupled to poly (hexadecyl cyanoacrylate) PHDCA nanoparticles (Perachhia et al. 1997). PEGylation resulted in an increased circulation time and decreased liver uptake of both PLA and PHDCA nanoparticles.

Another study indicated the distribution of fluorescently labeled PEG-PHDCA nanoparticles in the epithelial cells of piamater, ventricles, spinal cord surface and the ependymal cells of choroid plexus after intravenous administration in rats and mice. Also, the PEGylated nanoparticles were transported into brain at 4-8 fold higher concentration than the non-PEGylated nanoparticles (Calvo et al. 2001).

1.2.1.2. Surface modification with functional ligands

Selection and synthesis of an appropriate targeting ligand is a crucial step in formulating nanocarriers for drug delivery. Appropriate functionalization of nanocarriers is itself a challenge and requires a thorough understanding of the target organ/tissue and the transport mechanisms available for targeting. Some transport systems may get up regulated or down regulated during a diseased condition. PEG is the most common agent for surface Functionalization of nanocarriers (Woodle et al. 1995). It provides steric stabilization to the delivery vector and therefore prolongs its circulation *in vivo*. The Functionalization is s usually achieved via covalent linking of the functional groups like amines, carboxylic acid, succinimidyl ester, thiol etc. (Sharma et al. 2012; Sharma et al. 2013, Chen et al. 2004). Following are the two major concerns for surface modification of the nanocarriers:

1) Active targeting ligands like antibody, protein, peptide, sugar moiety, folate or carbohydrate attached to the surface of the delivery vector can decrease the stability of the carrier in circulation and increase the rate of elimination uptake of the vector by liver and spleen.

However, the presence of the PEG protecting polymer may compensate for this effect.

2) Prolonged circulation of the PEGylated ligand-bearing nanocarriers may result in the increased accumulation of the carrier in target organs even with low blood flow or with low concentration of the receptor antigens.

1.2.2. Solid lipid nanoparticles (SLNs)

SLNs are solid nanoparticles with a spherical lipid core matrix that can solubilize various lipophilic drugs. Various lipids have been used in the past including triglycerides, fatty acids (steric acids), waxes (bees wax, carnauba wax), cetyl alcohol and steroids (cholesterol).(Loxley et al. 2009) These lipids are stabilized in the aqueous environment by emulsifiers like soybean lecithin, poloxamers, polysorbates, Phosphatidylcholine, sodium cholate, sodium glycocholate, butanol, butyric acid etc. The SLNs are usually composed of 0.1% to 30% (w/w) of the solid lipids dispersed in an aqueous medium stabilized with 0.5% to 5% (w/w) emulsifier. The melted lipids containing the active ingredients are emulsified using different techniques like hot homogenization, cold homogenization, ultrasound and high shear homogenization (Mehnert et al. 2001). The application of SLNs for brain drug delivery started in late 90's when two independent groups of researchers showed increased accumulation of the anticancer drugs camptothecin and doxorubicin after oral and intravenous administration of drug loaded SLNs (Yang et al. 1999, Zara et al. 1999). With increasing investigation of these lipid nanoparticles as drug delivery systems, another group of scientists demonstrated prolonged release of the drugs tetracaine, etomidate and prednisolone using SLNs synthesized with Compritol 888 ATO and Dynasan112 as matrix material (Muhlen et al. 1998). In a recent study Martin et al., showed increased levels of the antitumor drug, campothecin, in brain after intravenous administration of camptothecin loaded SLNs in rats (Martins et al. 2012). The advantage of using these carriers is that they provide a controlled release of the encapsulated material and the lipids used are

biodegradable and have low systemic toxicity (Weyhers et al. 1995). They can be surface modified to increase their steric stabilization or targeting efficiency (Blasi et al. 2005). Despite their efficacy and utility, at present there are no SLN formulations for parenteral administration in the market. Certain limitations associated with SLNs include particle growth, unpredictable gelation tendency and change in lipid polymorphic state causing drug leakage (Ekambaram et al. 2012; Mehnart et al. 2001;Liet al. 2009). In addition, the toxicity associated with the surfactants used in formulating SLNs limits the *in vivo* applications. A previous report indicated toxic effects of SLN formulations composed of cetylpalmitate or Compritol® on liver and spleen of mice after intravenous administration (Weyhers et al. 1995).

1.2.3. Polymeric nanoparticles

Increased progress in understanding of the mechanism of nanoparticle transport across BBB has resulted in greater application of the polymeric nanoparticles for delivery of therapeutic agents to brain. Various nanoparticles surface modified with targeting ligands, surfactants or steric stabilizers have been used in the recent past to accomplish the formidable task of transporting hydrophilic drug molecules to brain (Wohlfart et al. 2012). Lu et al., demonstrated improved accumulation of cationized albumin conjugated pegylated nanoparticles in the glioma tumor implanted in rat brain, 1hr post intravenous administration (Lu et al. 2007). In another study, Wen et al., showed that conjugation of PEG-PLGA nanoparticles with odorranalectin resulted in increased brain delivery of the nanoparticles and improved therapeutic effect of urocortin peptide loaded nanoparticles in rat with Parkinson's disease (Wen et al. 2011). Recently, gold nanoparticles have been employed in combination with magnetic resonance imaging guided ultrasound for increasing the permeability of BBB (Etame et al. 2012). The uptake of nanoparticles into brain is now considered to be majorly regulated via receptor

mediated endocytosis followed by transcytosis across the endothelial barrier (Gabathuler et al. 2010).

Various receptors like lipoprotein and scavenger receptors and the transferrin and insulin receptors have been utilized for transport of nanoparticles to brain. One of the major prerequisite for nanoparticulate delivery of therapeutics to brain is the biodegradability and safety of the nanoparticles, both *in vitro* and *in vivo*. Non-biodegradable particles like carbon nanotubes, quantum dots and fullerenes are associated with hazardous effects and therefore, are not considered safe for *in vivo* administration. Moreover, the drug loaded into the nanoparticles is exposed to macrophages and serum proteins in circulation and is thus, often associated with the risk of *in vivo* degradation (Wohlfart et al. 2012).

1.2.4. Liposomes

Liposomes are lipid vesicles that have an inner aqueous core surrounded by the phospholipid bilayer. The pulsating development of targeted nanoparticulate systems has allowed efficient delivery of therapeutic agents to brain (Cheng et al. 2007; Jong et al. 2008).Various nano-constructs like liposomes, dendrimers, lipid-polymeric nanoparticle systems and nanocapsules have been evaluated in the recent past for the delivery of desired cargo to the target site (Allen et al. 2004; Carlmark et al. 2009; Szoka et al. 1980; Muller et al. 2000; Vauthier et al. 2009).The versatility of liposomes, their ability to efficiently protect the encapsulated therapeutic agent in circulation, and the simplicity of surface engineering, provide substantial advantage to the liposomal delivery vectors over other nanoparticle systems (Maeda et al. 2000; Vasir et al. 2005).These liposomes can be conjugated to proteins for targeting specific receptors. Furthermore, sterically stabilized liposomes, surface modified with polyethylene glycol (PEG), show a reduction in clearance by the reticuloendothelial system and

immunogenic response of the targeting proteins (Shek et al. 1986; Harasyma et al. 1998). Low elimination by the liver and spleen increases the circulation time of liposomes and improves the bioavailability of encapsulated molecules for therapeutic action (Klibanov et al. 1990; Woodle et al. 1994).

These liposomes have traditionally been used for delivery of poorly water soluble drugs by parenteral administration. Conventional liposomes, composed of cholesterol and phospholipids suffer from high plasma clearance and low transport across BBB. These liposomes can be surface modified with different ligands like proteins, peptides and antibodies for targeting specific receptors (Schnyder et al. 2005).

Furthermore, surface functionalization with steric stabilizers like poly-ethylene glycol can increase the circulation time and decrease non-specific interactions and plasma clearance of liposomes (Klibanov et al. 1990, Sadzuka et al. 2002). However, the proportion of PEGmolecules on the surface needs to be circumspectly optimized as the incorporation of hydrophilic polymers can reduce the cellular uptake of liposomes. This can be attributed to the hydrophobicity of the cell membrane that establishes an effectual barrier for many hydrophilic molecules. Xiang et al., showed increased tumor transport of chlorotoxin modified PEGylated liposomes loaded with doxorubicin and greater inhibition of the tumor growth as compared to the unmodified liposomes (Xiang et al. 2011). In another study, Ying et al., evaluated dual-targeting liposomes surface functionalized with p-aminophenyl-α-D-mannopyranoside and transferrin for crossing the BBB. The dual-modified liposomes showed enhanced transport across *in vitro* BBB model and significantly decreased the C6 glioma tumor volume in rat models (Ying et al. 2010). A recent report showed the comparison of five different targeting ligands (transferrin, RI7217, COG133, angiopep-2, and CRM197) in improving the brain delivery of liposomes (Rooy et al.

2011). RI7217 is the antibody targeted to mouse transferrin receptors, COG133 is an apo-E mimetic peptide targeted to the low density lipoprotein receptors (LDLR) on the surface of BBB, angiopep-2 can bind to the LDLR-related protein on the brain endothelial cells and CRM197 can bind to the Diphtheria toxin receptor (DTR). The results indicated that only CRM197 was able to bind to the brain endothelial receptors *in vitro* while RI7217 showed maximum uptake into brain *in vivo*.

Liposomes can be functionalized with one or more ligands for improving the delivery of the encapsulated drug or plasmid to specific cells. Conjugating to multiple ligands can help perform multiple functions, e.g. one vector can facilitate brain tissue targeting and another ligand can induce cellular uptake and/or intracellular translocation to specific cell compartments like nucleus for delivery of pDNA (Tan et al. 2003).

1.3. Cell penetrating peptides (CPPs)

Cell-penetrating peptides (CPPs) are short cationic or amphipathic peptides that have the ability to transport the associated molecular cargo (e.g., peptides, proteins, oligonucleotides, liposomes, nanoparticles, bacteriophages, etc.) inside the cells (Sharma et al. 2012). Biological evolution has conferred certain proteins with an ability to penetrate the cell membrane due to the presence of specific peptide sequences called protein transduction domains (Schmidt et al. 2010). The peptide sequences constituting these domains carry basic amino acids and possess cell penetrating properties, thus, these peptides are referred to as cell penetrating peptides (CPPs). Over the past decade, there has been a vibrant increase in the application of these CPPs for the delivery of cargo molecules inside the cells (Snyder et al. 2004).These peptide sequences have been utilized for the delivery of various molecules like proteins, nucleic acids, liposomes, and nanoparticles across the cell membrane (Lewin et al. 2000; Torchilin et al. 2001; Torchilin et

al. 2003; Huwyler et al. 1996). The profound interest evoked by the CPPs among the scientists is not only attributed to their ability of crossing the cell membrane via receptor and energy-independent processes but also their capacity to efficiently internalize the associated biomolecules without compromising with the biocompatibility (Trabulo et al. 2010). Various CPPs such as poly-L-arginine (PR), transactivator of transcription peptide (TAT), and penetratin have been conjugated to the delivery vectors to improve the delivery of therapeutic molecules (Kibria et al. 2011; Cheng et al. 2007).

1.3.1. Poly-L-arginine

Polyarginine is a synthetic cationic peptide consisting of 8 or more arginine residues and has been used to facilitate intracellular translocation of a wide variety of molecular cargo (Sharma et al. 2012; Sharma et al. 2013). This cell penetrating peptide has been used for delivery of cargo such as liposomes, nucleic acids, nanoparticles etc. into the cells. Kibria et al., (Kibria et al. 2011) showed that dual modification of liposomes with polyarginine and cyclic RGD (Arg-Gly-Asp) peptide significantly increased the transfection efficiency of liposomes in Integrin α(v)β(3) expressing cells. Later, Opanasopit et al., (Opanasopit et al. 2011) demonstrated considerable improvement in transfection efficiency of liposomes after coating with poly-L-arginine. A previous report, provided a deeper insight into the interaction of cationic peptides with the phospholipid bilayer during the surface adsorption of positively charges amino acids onto the liposomal surface (Disalvo et al. 2012). The results showed that the adsorption of cationic amino acids, like arginine was not only driven by electrostatic interactions but also by polarization forces and caused surface rearrangements in the phospholipid membrane. Zhang et al., (Zhang et al. 2006) showed that siRNA containing octarginine modified liposomes efficiently inhibited the targeted gene and significantly reduced the tumor cell proliferation.

1.3.2. HIV-1 trans-activator of transcription (TAT) peptide

TAT is a protein encoded by the TAT gene of HIV-1. TAT was discovered with the emergence of various CPPs of natural (AntP/Penetratin) and synthetic origin (Mastoparan/ transportan) that have been alternatively termed as protein transduction domains (PTDs) (Mae et al. 2009; Ziegler et al. 2005). Over the recent years, TAT peptide has gained significant attention in the field of nucleic acids and drug delivery. A previous study compared the transfection efficiencies of SLN gene delivery vector and polyethylenimine (PEI), *in vitro* and *in vivo*. The presence of TAT significantly enhanced the gene expression of SLNs in different cell lines as compared to the PEI nanoparticles (Rudolph et al. 2004). Another group of scientists reported efficient gene delivery using TAT peptide functionalized polymeric nanoparticle complexes into undifferentiated and differentiated SH-SY5Y cells (Suk et al. 2006). TAT peptide modified liposomes showed considerable improvement in the delivery of plasmid encoding green fluorescent protein (pGFP) to human brain tumor U-87 cells *in vitro* and intracranial tumor mice model (Gupta et al. 2007). TAT modified liposomes synthesized with small quantities of the cationic lipid DOTAP showed substantially higher gene expression levels in mouse fibroblast NIH3T3 and cardiac myocytes H9C2 cells and lower cytotoxic potential as compared to the commercially available transfecting reagent Lipofectin® (Torchilin et al. 2003;Wallje et al. 2005). Despite the large area of application of the TAT peptide, the exact mechanism of their cellular internalization still appears controversial. Variable results illustrating different mechanisms of uptake can result from variation in different experimental factors like wide range of the sequences of TAT peptide used, variable cell lines and different protocols for investigation of the mechanism of entry which can influence the mechanism of internalization of TAT peptide.

1.3.3. Penetratin

Penetratin is a 16-amino acid basic cationic CPP, derived from Antennapedia homeodomain, which is capable of inducing the cell uptake of a large variety of molecular cargo (Wallje et al. 2005). The peptide is translocated across the cell membranes by the third α-helix of the homeodomain of Antennapedia, known as penetratin. Previous biophysical studies have shown that even though the entry of this peptide requires initial binding to the cell membrane, binding and translocation are differentially affected by the amphiphilic nature and net charge of the peptide. Also, the internalization of penetratin is affected by the lipid composition of the plasma membrane (Drin et al. 2001; Scheller et al. 2000). A group of researchers showed that the presence of negatively charged lipids in the membrane promote the transfer of penetratin from hydrophilic to hydrophobic environment likely via charge neutralization. They showed that the transfer of penetratin can also occur in the absence of the negatively charged lipid by adding DNA oligonucleotides, by the same mechanism. Their findings further confirmed that charge neutralization and phase transfer represented only the initial step of internalization while further uptake required the presence of tryptophan at position 6 of the peptide (Dom et al. 2003). Previous study showed enhanced accumulation of penetratin functionalized PEG-PLA nanoparticles in rat brain and low uptake by non-specific organs as compared to the protamine conjugated nanoparticles (Xia et al. 2012). Another group of researchers showed improved transfection efficiency of penetratin conjugated polymethacrylates as compared to PEI-polymethacrylates and comparable to the gene expression of lipofectamine® (Christiaens et al. 2005). Conjugation of penetratin with elastin like polypeptides showed maximum reduction in growth and proliferation of SKOV-3 and HeLa cells (Massodi et al. 2005).

1.3.4. Mastoparan

Mastoparan is a 14-residue peptide from wasp (vespulalewisii) venom and belongs to a class of peptides that are more amphipathic (Yandek et al. 2007; Ha¨llbrink et al. 2001). This peptide has been used in the construction of 21 residue peptide transportan 10 (TP10) which has been widely investigated in the delivery of cargo like proteins into the cells (Pooga et al. 2001). The use of this amphiphilic peptide is restricted due its cytolytic effects (Deshayes et al. 2005; Saar et al. 2005; Cardozo et al. 2007). Previous reports have indicated the application of mastoparan peptide for mitochondrial delivery causing increased apoptosis of tumor cells (Pfeiffer et al. 1995;Hirai et al. 1979). Yamada et al., reported that the peptide caused increased permeability of mitochondrial membrane causing leakage of components from the mitochondrial matrix eventually leading to apoptosis of tumor cells (Yamada et al. 2008). Another report, showed that presence of mastoparan peptide, Transportan 10 (Tp10), significantly increased the transfection efficiency of PEI. Also, low concentration (0.6nM) of Tp10 conjugates with DNA showed efficient gene expression in HeLa cells and Murine fibroblast C3H 10T1/2 cells(Kilk et al. 2005).

1.4. Drug delivery to brain

The presence of multiple endogenous transporters and tight junctions in brain capillary endothelial cells restricts the transport of many essential therapeutic molecules across BBB thus posing a great challenge to treatment of CNS related disorders. Passive diffusion of the systemically administered therapeutic molecules across the BBB depends on the lipophilicity and the molecular weight of the drug (Ren et al. 2012). However, a large number of drugs that have very low molecular weight and high lipophilicity are also pumped back into the blood stream by the efflux pumps like multiple organic anion transporter (MOAT) especially the P-glycoprotein

(Pgp) or the multidrug resistance protein (MDR) (Begley 1996). In addition, the tight junctions between the endothelial cells of brain capillaries result in a very high electrical resistance across the brain endothelial barrier (around 1500-2000 Ωcm2) as compared to the other body tissues (approximately 33.3 Ωcm2) (Crone and Cristensen, 1981; Crone and Olesen, 1982). This has necessitated the need for developing efficient drug delivery approaches like targeted nanoparticles, liposomes etc. Poly (butyl cyanoacrylate) is one the earliest and efficient, biodegradable and biocompatible polymer that has been used in forming nanoparticles for improving the delivery of water soluble drugs to brain (Grislain et al. 1983; Couvreur et al. 1986). Dalargin, a hexapeptide (Tyr-D-Ala-Gly-Phe-Leu-Arg) with opioid activity was the first drug delivery to brain using systemically administered poly (butyl cyanoacrylate) nanoparticles (Alyautdin et al. 1995; Kreuter et al. 1995). The dalargin loaded nanoparticles showed improved brain delivery and antinociceptive activity, demonstrated by the hot plate and tail flick test, as compared to the control groups (Alyautdin et al. 1995; Kreuter et al. 1995; Schroeder et al. 1996; Ramge et al. 1999). Another study compared the development of epileptic spikes after brain perfusion of tubocurarine and after intraventricular injection of this drug. No spikes were observed after addition of the drug to the perfusate. In contrast adding of polysorbate 80 coated poly(butyl cyanoacrylate) nanoparticles loaded with tubocurarine resulted in the development of frequent severe spikes in the EEC comparable to those developed after intraventricular injection of the drug (Alyautdin et al. 1998).

Certain receptors that are present in high concentrations on the surface of tumor cells can be used for delivering the desired therapeutic agents via active targeting of these receptors (Gutman et al. 2000). Low density lipoprotein (LDL) receptors are usually overexpressed in tumors cells like gliomas and this helps in realizing the therapeutic advantage of the LDL

targeted delivery vehicle (Yamamoto et al. 1997). Gutman et al. developed boronated LDL by modifying the cholesterol group of the LDL and utilized this molecule for active targeting of LDL receptors during boron neutron capture therapy (BNCT) of glioma cells (Gutman et al. 2000). The results showed that the boronated LDL not just accumulated around the tumor but showed considerable internalization into the tumor. Transferrin is an 80kDa serum glycoprotein that facilitates the transport of iron into cells. It is transported across the cell membranes via transferrin receptor mediated transcytosis (Yoon et al. 2009). A group of researchers utilized the occurrence of transferrin receptors on the surface of brain endothelial cells for active brain targeting of the liposomes (Sharma et al. 2013). The liposomes were surface modified with transferrin protein for targeting the brain endothelial receptors and were additionally conjugated to CPP for improving their internalization into brain by overcoming receptor saturation. The results showed about 8 fold higher penetration of the liposomes into brain as compared to the unmodified liposomes. Many metabolic sugars and amino acids are able to cross the BBB via specific carrier mediated transport systems that exist on both the luminal (blood side) and abluminal (brain side) of the brain endothelial cells (Béduneau et al. 2007). Glucose transporter (GLUT) system is one such transporter of sugars into brain. The GLUT1 isoform exists on the luminal surface of the brain endothelial cells and has been reported to possess the potential of enhancing the transport of carriers into brain (Tsuji 2005; Pardridge et al. 1990). GLUT1 has been reported to facilitate the transport of sugars with structures similar to glucose like 2-deoxyglucose, galactose and mannose analogs (Pardridge 1995). A recent study reported dual-modified liposomes surface modified with a mannose analog, p-aminophenyl-α-D-manno-pyranoside (MAN) for targeting GLUT1 receptors and transferrin protein targeted to transferrin receptors on the brain endothelium for improving the delivery of the anticancer drug,

daunorubicin, into brain (Ying et al. 2010). The results showed that the dual-modified daunorubicin liposomes were able to improve the therapeutic efficacy of the drug after intravenous administration of the daunorbicin encapsulating liposomes. The C6 glioma tumor volume was reduced to 54.7% and the median survival time of the tumor bearing rats (22 days) was significantly longer than the rats administered with free daunorubicin (17 days, p= 0.001).

Effective brain targeting requires high selectivity of the BBB receptors which means that ideally the receptor should be expressed preferentially on the BBB. However, most of the receptors are nearly non-specific and therefore, limit the highly selective targeting of the delivery vectors to brain. More efforts need to be focused on exploring the BBB biology and occurrence of receptors that can be utilized for active targeting of therapeutic agents.

1.5. Gene delivery to brain

Gene therapy is an effective tool for providing lasting and notable treatment for genetic disorders like cystic fibrosis, combined immunodeficiency syndrome and many cancers that result from the presence of defective genes (Cavazzana-Calvo et al., 2000; Cavazzana-Calvo et al., 2001; Cavazzana-Calvo et al., 2007). Considering the remarkable progress in the development of efficient gene transfer vectors leading to safer transduction and robust transgene expression coupled with increased understanding of the molecular mechanisms of neurological and other CNS disorders, it is rational to believe that gene therapy can play an inevitable role in the treatment of CNS diseases by introducing genes into brain (Manfredsson et al. 2010; Costantini et al., 2007). Gene therapy can be used for the treatment of a wide range of CNS disorders like neurodegenerative diseases by increasing the expression of growth factors, anti-apoptotic molecules or antioxidants (Costantini et al., 2007; Bowers et al., 1997; Raymon et al., 1997); it can reduce the proliferation of tumor cells by producing anti-angiogenic factors or by

down regulating the expression of certain genes using antisense or siRNA (Carter et al., 1999; Fueyo et al., 1999; Boviatsis et al., 1994; Haque et al., 1997). However, the major challenge faced by the scientific community lies in the safe and efficient delivery of therapeutic genes to the brain. The transport of therapeutic agents to brain is largely inhibited by the BBB after intravenous administration. Nucleic acids are commonly administered for gene therapy via craniotomy or intracerebral injections which are extremely invasive and are useful only for local gene delivery (Schlachetzki et al. 2004; Pardridge et al. 2002). In contrast, the delivery of genes via viral and non-viral vectors leads to widespread gene expression throughout the CNS, post intravenous administration (Pardridge et al. 2001). The usefulness of a viral vector is based on the ratio of cytopathic effects to beneficial effects of the transgene. Previous reports indicate the complexity associated with generation of non-toxic replication defective viral vectors that caused neuronal cytotoxicity *in vitro* (Johnson et al. 1992). Local injection site toxicities were evident as necrosis accompanied with inflammation and gliosis during *in vivo* studies (Isacson 1995).

In mid 1990s the number of gene therapy clinical trial reached an average of 100 per year, however with the death of a patient, enrolled in an experiment for deficiency of ornithine-transcarbamylase using adenoviral vector, in 1999 and the development of leukemia in two pateints with SCID-X1 treated with gamma retroviral vector, the number of such trials declined significantly (Marshall 1999 and Buckley 2002).

Considering the side effects of viral vectors, the efforts for achieving safe and efficient gene delivery are focused on developing non-viral vectors. RVG29 is a 29-residue peptide derived from the rabies virus glycoprotein (RVG) that has been shown to specifically bind to neuronal cells expressing the nicotinic acetylcholine receptor (AchR) (Lentz et al. 1982). Also, the presence of AchRs on brain capillary endothelial cells facilitates the transport of RVG

peptide via receptor mediated transcytosis (Liu et al. 2009; Lafon 2005). A previous report showed efficient gene expression in neuro2a cells after transfection with pGFPpolyplexed RVG29-octarginine polymer (Gong et al. 2012). In addition, the polymer complexed with luciferase expressing plasmid (pGL3) showed 3fold higher gene expression in mice brain after intravenous administration as compared to the control administered with plasmid alone. Another recent study demonstrated successful delivery of desired gene to mouse brain using RVG peptide conjugated bioreduciblepolyethylenimine polymeric vectors (Son et al. 2011).The complexes showed efficient *in vitro* biocompatibility. Polymeric complexes containing 30µg of pDNA expressing red fluorescence protein (CMV-RFP) showed efficient gene expression in brain. Furthermore, PEG conjugated RVG tethered complexes showed 1.3 fold higher gene expression in mouse brain as compared to the non-RVG tethered Pegylatedpolyplexes. A group of researchers showed efficient targeted gene delivery using PEGylatedpoly(2-(dimethylamino) ethyl methacrylate)/DNA polyplex micelles surface modified with phage-displayed TGN peptide (Qian et al. 2013). The polyplex micelles were non-cytotoxic and demonstrated efficient cell uptake and transfection, *in vitro* as compared to the control polyplexes without the targeting peptide. In addition, the TGN peptide conjugated micelles showed 3 fold higher gene expression in brain as compared to the control group. Another group of scientists investigated lactoferrin modified nanoparticles for gene delivery to brain (Huang et al. 2010). The researchers utilized the brain targeting ability of lactoferrin protein for delivery across BBB. The nanoparticles loaded with ethidiummonoazide bromide (EMA)-labeled pGL2- control plasmid vector were injected into nude mice and the distribution of the nanoparticles was assessed after 4h using Cri *in vivo* imaging. The lactoferrin modified nanoparticles showed lower accumulation in peripheral organs like liver and improved transport to brain as compared to the unmodified nanoparticles.

Furthermore, the lactoferrin targeted nanoparticles showed higher pGFP (green fluorescent protein expressing plasmid) expression in the mid brain sections of balb/c mice as compared to the control nanoparticles.

Gene therapy for disorders of central nervous system is currently under investigation and the clinical trials are aimed at slowing of disease progression and safe and effective treatment of genetic abnormalities. With the advancement in the understanding of molecular mechanism underlying various neurological disorders and development of efficient gene transfer system, the success of focal and global delivery of therapeutic genes to brain appears realizable. Limitations, such as stability and regulation of transgene expression and safety of both vector and the expressed transgene are still evident. Furthermore, the heterogeneity of cell types and the existence of post mitotic cells present several challenges in successful delivery of gene to brain. Considering these factors, it is highly probable that successful delivery of genes for treatment of CNS disorders will require multiple modes of gene delivery and collaborative efforts between basic researchers and clinical scientists.

Table 2. Drug and gene delivery vectors for transport across BBB

Nanoparticles for brain delivery	Properties	References
Bolaamphilic cationic vesicles	High serum stability, efficient cell uptake and improved brain targeting	Dakwar et al. 2012;Philosof-Mazor et al. 2013
Poly(lactide-co-glycolide) (PLGA) nanoparticles	Biocompatible, biodegradable, efficient cellular uptake and delivery of therapeutic agents into cells	Jalali et al. 201; Seju et al. 2011
Angiopep-conjugated nanoparticles	Internalization by brain capillary endothelial cells, efficient cell uptake, transport across BBB and gene expression.	Ke et al. 200; Shao et al. 2010
CPP modified Tf-liposomes	Biocompatible, efficient cell uptake, transfection, transport across BBB *in vitro* and *in vivo*.	Sharma et al. 2012; Sharma et al. 2013
RVG peptide conjugated nanocarriers	High serum stability, biocompatibility, efficient transfection *in vitro* and *in vivo*	Kim et al. 2013; Son et al. 2011
Solid lipid nanoparticles	Biocompatible, efficient cell uptake and drug delivery *in vitro*, efficient brain delivery *in vivo*	Martins et al. 2012;Venishetty et a. 2013;Madan 2013
TAT-liposomes	Efficient cell uptake, low cytotoxicity, improved brain targeting and penetration	Wang et al. 2012; Qin et al. 2011
Surfactant coated nanoparticles	Efficient brain penetration and improved therapeutic efficacy.	Borchard et al. 1983;Kreuter et al. 1997; Wilson et al. 2008
Antibody conjugated nanoparticles	Significantly enhanced brain delivery, biocompatible, improved therapeutic efficacy	Pang et al. 2008; Fengetal. 2009;Furrer et al. 2009

1. 6. Statement of problems and research objectives

Over the recent years, there has been a considerable progress in the field of neuroscience leading to an improved understanding of disorders of central nervous system (CNS). In contrast, the development of successful strategies for treating these disorders is limited due to the protective function of blood brain barrier (BBB). The formidable challenge of delivering an effective therapeutic agent to brain requires collaborative multidisciplinary efforts that take into consideration the blood brain barrier (BBB) biology as well as the study of basic transport mechanisms for delivery to brain. There are about 100 billion capillaries in the human brain with a surface area of approximately 20 m^2 that constitute the BBB (Sharma et al. 2013; Chen et al. 2012; Pardridge et al. 2003). The occurrence of specific receptors on the surface of BBB facilitates the transport of various essential molecules into the brain. Transferrin receptor mediated transcytosis is the most well characterized system for transport of iron to brain (Pardridge et al. 2005). In addition, the transferrin receptors on the surface of brain endothelial cells have been widely explored for targeting various drug delivery systems to brain (Chena et al. 2010; Xie et al. 2005; Sharma et al. 2012).

Liposomes, being functionally versatile, can be engineered for targeting these receptors, thereby rendering them as promising carriers for drug and gene delivery (Peer et al. 2007). Nevertheless, this receptor facilitated uptake, being disposed to receptor saturation cannot provide adequate transport of ligand conjugated liposomes into the cells and lowers the therapeutic effect of the encapsulated agent (Huwyler et al. 1996). Therefore, in this study we have conjugated the liposomes with two ligands (1) a receptor targeting protein (transferrin) and (2) a cell penetrating peptide (Poly-L-arginine, HIV-1 TAT, Penetratin and Mastoparan). We **hypothesize** that a combination of these two ligands on PEGylated liposomes will enhance their

ability to penetrate the BBB and transfect the desired cells via receptor targeting and improved cell penetration. Our **primary aims** are: (I) to synthesize and evaluate dual-modified PEGylated liposomal delivery system, surface modified with transferrin and cell penetrating peptide (Tf-CPP-liposomes), *in vitro* (II) To investigate the bio-distribution, transfection and biocompatibility of the dual-modified delivery system *in vivo*.

The long term objective of our research is to design a vector for efficient delivery of therapeutic agents to brain. Specifically, our research work is focused on designing PEGylated liposomes surface modified with transferrin and a cell penetrating peptide for enhancing the delivery of desired therapeutic agent to brain. The contribution is significant because this is the first step in the continuum of research that is expected to illustrate the influence of grafting the targeted liposomal delivery vector to cell penetrating peptide and forming near neutral vesicles for improving the delivery of therapeutics across BBB.

1.6.1. Specific aim 1

1.6.1.1. To synthesize bi-functional liposomes targeted to brain endothelial cells

Lipid-based nanocarriers for drugs/genes, e.g., liposomes, can alter the disposition and improve the utility of variety of therapeutic agents. Several ligands like transferrin, monoclonal antibodies or peptides can be conjugated to PEG moieties on liposomal surface for active targeting of desired cells (Huwyler et al. 1996, Oba et al. 2007). In our study, we propose to conjugate transferrin-coupled liposomes to a CPP (i.e. short cationic or amphipathic peptides that have the ability to transport the associated molecular cargo such as oligonucleotides, liposomes, nanoparticles etc. inside the cells) (Bolhassani et al. 2011). The bi-functional liposomes were synthesized using post-insertion technique. Transferrin, being negatively charged protein

molecule, balanced the positive charge of cell penetrating peptides thereby imparting a near neutral charge (zeta potential in the range of 0-15 mV) to the liposomal vector.

1.6.1.2. To evaluate the biocompatibility, transfection efficiency, cellular uptake and of the bi-functional liposomes, *in vitro*

The efficiency of the delivery vector lies not only in its ability to carry the encapsulated agent into the desired cells but also its biocompatibility at the concentrations used. We evaluated the cytotoxic potential of bi-functional liposomes, in various tumor (e.g. Daoy, U87) and brain endothelial (bEnd3) cell lines using MTT assay. Hemolysis assay was performed to authenticate the biocompatibility of liposomes for *in vivo* administration. We also investigated the uptake of DiR (near infra-red indicarbocyanine) dye labeled and doxorubicin encapsulating liposomes and the transfection efficiency of Green fluorescent protein (GFP) plasmid encapsulating liposomes in these cell lines. A comprehensive investigation of the mechanism of cell uptake was also performed in different cell lines (U87, Daoy and brain endothelial cells) using various inhibitors like chlorpromazine, colchicine, methyl-β-cyclodextrin, amiloride and low temperature (4°C).

1.6.1.3. To design 2 dimensional (2D) BBB model and 3- (3D) *in vitro* brain tumor model and evaluate the transport of liposomes across the barrier layer

The transport of DiR labeled liposomes was evaluated across 2D BBB model that will be designed by co-culture of brain endothelial and primary glial cells on opposite sides of culture inserts. Despite the dubiousness associated with the feasibility of developing an *in vivo* brain tumor model, very little or no research has been done to develop efficient *in vitro* brain tumor models where the transport to the tumor is regulated via the endothelial barrier. Therefore, we designed an *in vitro* brain tumor model using biodegradable chitosan-PLGA scaffolds where the transport of liposomes to the 3-dimensional tumor was regulated via the endothelial cells

cultured on transwell inserts. We developed the 3D *in vitro* brain tumor model using PLGA based scaffold for culture of tumor cells (glioblastoma). The porous structure of the scaffold supports the growth of tumor cells in a 3-dimensional environment (Kim et al. 2005). Reportedly, the cells attach to the intertwined scaffold fibers and fill the spaces/pores within the scaffold to form 3D tumor (Sourla et al. 1996; Bell et al. 1995). These 3D tumors, cultured on the scaffold, were combined with the 2D BBB model.

1.6.2. Specific aim 2

1.6.2.1. To evaluate the *in vivo* biodistribution of bi-functional liposomes

The *in vivo* evaluation of the delivery vectors is essential for clinical translation. The presence of high serum concentrations and non-specific binding to extracellular components can interfere with the *in vivo* performance of the delivery vector. Therefore, considering the complexity of *in vivo* environment, we investigated the ability of dual-modified liposomes to target brain and deliver the desired gene across BBB, *in vivo*. Biodistrbution of DiR labeled and doxorubicin encapsulating liposomes was evaluated in adult Sprague Dawley rats. Additionally, we evaluated the *in vivo* transfection efficiency of β-gal encapsulating liposomes in adult SD rats after intravenous administration. The *in vivo* biocompatibility of the dual-modified liposomes was assessed by histological evaluation of the transfected tissue sections from different organs.

CHAPTER II. MATERIALS AND METHODS

2.1. Materials

The materials used are listed in table 3.

2.2. Cell culture

Primary glial cells were isolated from 2 to 3 weeks old rats (details of the method are provided in supporting information). Brain endothelial (bEnd.3) cells were obtained from American Type Culture Collection (ATCC, Rockville, Maryland). Human medulloblastoma (Daoy) and glioblastoma (U87) were obtained from Dr. Erxi Wu's laboratory (Department of Pharmaceutical Sciences, North Dakota State University). All cell types were cultured in Dulbecco's Modified Eagle's Medium (DMEM) with 10% FBS and 1% Psf in an atmosphere of 5% carbon dioxide (CO2) at 37°C.

2.3. Animals

All animal experiments were conducted as approved by the Institutional Animal Care and Use Committee (IACUC) at North Dakota State University (Protocol #A12024). Adult Sprague-Dawley (SD) rats were used to evaluate the biodistribution, transfection efficiency, and biocompatibility of liposomes. The animals were housed under controlled temperature conditions with 12 h light and dark cycles and were allowed free access to food and water.

Table 3. List of materials and their sources

Material	Company and location
Alexa-Fluor 594 goat anti-rabbit IgG	Abcam Inc. (Cambridge, MA)
Alexa-Fluor 488 goat anti-mouse IgG	Abcam Inc. (Cambridge, MA)
Amiloride hydrochloride	Sigma-Aldrich Co. (St. Louis, MO)
Anti-transferrin receptor antibody (OX26)	Abcam Inc. (Cambridge, MA)
β-galactosidase assay kit	Promega Corp. (Madison, WI)
Chlorpromazine HCl	Enzo Life Sciences (Farmingdale, NY)
Cholesterol	Sigma-Aldrich Co. (St. Louis, MO)
Colchicine	Enzo Life Sciences (Farmingdale, NY)
Cytoseal 60	Thermo Fisher Scientific Inc., Barrington, IL)
1,1'-dioctadecyl-3,3,3'3'-tetramethylindocarbocyanineperchlorate (DiI)	Invitrogen (CA)
1,1'-dioctadecyl-3,3,3',3'-tetramethyl-indocarbocyanine iodide (DiR)	Invitrogen (CA)
1,2-Dioleoyl-sn-glycero-3-phosphoethanolamine (DOPE)	Avanti Polar Lipids (Birmingham, AL)
1,2-dioleoyl-3-trimethylammonium-propane chloride (DOTAP)	Avanti Polar Lipids (Birmingham, AL)
1,2-distearoyl-sn-glycero-3-phosphoethanolamine-N-[carboxy(PEG)2000](DSPE–PEG–COOH)	Avanti Polar Lipids (Birmingham, AL)
3-(4,5-dimethylthiazol-2-yl) -2,5-diphenyltetrazolium bromide (MTT)	Sigma-Aldrich Co. (St. Louis, MO)
Dulbecco's modified Eagle medium (DMEM)	ATCC, Rockville, MD
Eosin Y	Alfa Aesar (Ward Hill, MA)
1-ethyl-3-(3-dimethylaminopropyl) carbodiimide hydrochloride (EDC·HCl)	Creosalus Inc. (Louisville, KY)

Table 3. List of materials and their sources (continued)

Material	Company and location
Ethylenediaminetetraacetic acid (EDTA)	Sigma–Aldrich Co. (St. Louis, MO)
Fetal bovine serum (FBS)	ATCC, Rockville, MD
gWiz™-GFP (Plasmid encoding green fluorescent protein)	Aldevron LLC (Fargo, ND)
Harris Hematoxylin solution	Sigma-Aldrich Co. (St. Louis, MO)
HIV-1 TAT peptide	Sigma-Aldrich Co. (St. Louis, MO)
Hoechst 33342 dye	Anaspec (Fremont, CA)
Mastoparan	Anaspec (Fremont, CA)
N-Hydroxysuccinimide (NHS)	Alfa Aesar (Ward Hill, MA)
Penetratin	Anaspec, Inc. (Fremont, CA)
Penicillin-streptomycin-Fungizone (Psf)	United Biochemical (Sanborn, NY)
Phloxine B	Spectrum® (New Brunswick, NJ)
Phosphate buffered saline (PBS)	ATCC, Rockville, MD
Polyethylene terephthalate (PET) transwellculture inserts	BD BioCoat™ ;BD Biosciences (NC)
Poly-L-arginine hydrochloride (Mwt. 13,300 Da)	Sigma–Aldrich Co. (St. Louis, MO)
Poly (lactic-co-glycolide) (50:50; PLGA)	Polyscitech (West Lafayette, IN)
Tissue lysis/protein extraction buffer	Fab Gennix International, Frisco, TX
Tissue-Tek® OCT™ Compound	Sakura Finetek Inc., (Torrance, CA)

2.4. Experimental methods

2.4.1. Preparation of Tf-PR-liposomes

2.4.1.1. Preparation of PR-coupled liposomes

Poly-L-arginine was coupled to DSPE–PEG phospholipid as previously reported and coupling was confirmed using 1H NMR technique (Kim et al. 2010). Briefly, the primary amino group of poly-L-arginine was coupled to the linker phospholipid, DSPE-PEG-COOH via EDC/NHS reaction to form the poly-L-arginine coupled lipid (DSPE-PEG-PR). The PR–PEG–lipid was then combined with other lipids, in the following molar ratio: DOPE/DOTAP/PR–PEG–lipid/ cholesterol 45:45:4:2 mol % in chloroform/methanol (2:1) solution and dried on a rotavapor to form a thin film of lipids. For preparation of DiI-labeled liposomes, 0.5 mol % of the dye was added to the lipid mixture prior to formation of thin lipid film.The lipid film was hydrated using 4-(2-hydroxyethyl)-1-piperazineethanesulfonic acid (HEPES)-buffered saline (pH 7.3) Plasmid GFP polyplexes (GFP-chitosan) were added to the hydration buffer at N/P ratio of 5 for encapsulation into liposomes.

2.4.1.2. Preparation of Tf–PR liposomes

Bi-functional liposomes were prepared using post-insertion technique (Visser et al. 2005).Tf was coupled to the phospholipid DSPE–PEG–COOH as reported previously (Li et al. 2009). Briefly, DSPE–PEG–COOH (remaining 4mol%of the total phospholipid content)was suspended in HEPES buffered saline (pH 5.0) to form micelles. The micellar suspension was then treated with 360 µl of both EDC (0.5 M in H_2O) and NHS (0.5 M in H_2O) per 10µmols of the phospholipid. Excess EDC was removed by dialysis and pH of the micellar suspension was adjusted to 7.3 with 0.1 N sodium hydroxide. Tf (125 µg/µmol of the lipid) was added to the resulting suspension and stirred at 25°C for about 8 h. The resulting Tf micelles were stirred

overnight with PR liposomes at room temperature and the final liposomal suspension was passed through Sephadex G-100 column.

2.4.2. Preparation of Tf-CPP (Tf-TAT, Tf-Penetratin, Tf-Mastoparan) liposomes

The dual-functionalized liposomes, conjugated with TAT, Penetratin or Mastoparan, were prepared using post insertion technique as described above for preparation of Tf-PR liposomes. Briefly, the primary amine group of the CPPs was terminally conjugated to EDC/NHS activated DSPE-PEG2000-COOH. The DSPE-PEG-CPP was then mixed with other phospholipids DOPE/DOTAP/cholesterol in chloroform: methanol (2:1) and dried to form a thin lipid film. The thin film was then hydrated using Hepes buffered saline, pH 7.4 to form CPPcoupled liposomes (CPP-liposomes). Transferrin was coupled to the distal end of DSPE-PEG-COOH via EDC/NHS reaction to form Tf-micelles. The CPP-liposomes were then stirred overnight with Tf-micelles at room temperature to form Tf-CPP-liposomes. The free Tf-micelles were separated from the Tf-CPP liposomes by passing the liposomes through sepahadex G-100 column

2.4.3. Loading of doxorubicin into Tf-CPP-liposomes

Doxorubicin encapsulating liposomes were generated using pH gradient drug loading. The thin phospholipid film was hydrated using citric acid buffer, pH 5.0 (to form CPP-liposomes) followed by stirring with Tf-micelles in the citric acid buffer. The final liposomes were passed through sephadex G-100 column pre-equilibrated with Hepes buffered saline, pH 7.4 to remove any extra liposomal Tf-PEG-lipid and to exchange the extra liposomal citric acid buffer with the Hepes buffered saline. Therefore a pH gradient was generated between the outer aqueous buffer at pH 7.4 and the intra liposomal citric acid buffer at pH 5.0. The drug doxorubicin was added to the liposomal suspension and incubated at 50°C for 60 min. The drug

loaded liposomes were then cooled to room temperature and passed through sephadex columns to remove the unencapsulated drug. Encapsulation efficiency of the liposomes was determined using high performance liquid chromatography (HPLC). A solution of 10µl of the liposomes, before and after passing through the column, was prepared in 380µl of phosphate buffer (pH 5.5) with 10µl of 0.1%tritonX-100 and 100µl of methanol. The samples were analyzed using HPLC system equipped with UV-visible detector (Yamano et al. 2011). The analysis was performed at a wavelength of 234 nm using C18 column and phosphate buffer pH 5.5: Acetonitrile (75:25) mixture as mobile phase with a flow rate of 0.5 ml/min. In addition, doxorubicin release studies were performed by diluting the liposomal samples in PBS with 10% FBS and incubating the samples at 37°C (Supplementary Material Fig. S10). Samples were withdrawn at different time points, passed through sephadex columns and analyzed using HPLC.

2.4.4. Physical characterization of liposomes

2.4.4.1. Characterization of Tf-PR-liposomes

We evaluated the morphologic appearance and shape of liposomes with and without Tf and PR conjugation using AFM (VeecoDI-3100 Veeco, St Paul, MN) (Anabousi et al. 2000; Nakano et al. 2008). Freshly cleaved mica(grade V-4; 15 × 15 × 0.15 mm^3) was used as a substrate for AFM imaging. The liposomal suspensions were diluted with HEPES-buffered saline (pH 7.4). Approximately, 10µl of the diluted suspension was placed on the surface of thin mica film followed by air drying. Images were recorded in tapping contact mode at scan rate and scan size of 1Hz and 1µm, respectively. The average hydrodynamic diameter and zeta potential of liposomes were determined using Zetasizer Nano ZS 90 (Malvern Instruments, Worcestershire, UK) at 25°C. The Tf content of the liposomes was determined using micro

bicinchoninic acid (BCA) assay (PR liposomes were used as control). Pure bovine serum albumin was used as a standard.

Additionally, we determined the pDNA (β-gal plasmid) loading efficiency of liposomes. Briefly, 100 µl of the liposomal suspension was diluted (1:3) with HEPES buffered saline, pH 7.4. The evaluation of pDNA loading was performed under three conditions: after liposome preparation, after storage at 4 °C for 30 days and after incubation at 37 °C for 7 days in the presence of 10% FBS. Poly aspartic acid was used to maintain free DNA and Hoechst dye 33342was used for fluorescent staining of released pDNA. The fluorescence intensity of the samples was measured at excitation and emission wavelengths of 354 and 450 nm, respectively (Spectra Max M5microplate spectrofluorometer (Molecular Devices, Sunnyvale, CA)). The percent pDNA encapsulated (EE) and percent pDNA released (RL) were determined using the following equations:

$$EE\ (\%) = [F(t)-F(0)]/F(t)]x100 \quad (1)$$

$$RL(\%) = 1-EE(\%) \quad (2)$$

where, F(t) is the fluorescence of the sample after lysis of the liposomes using methanol and F(0) is the fluorescence intensity of the sample before lysis of liposomes.

2.4.4.2. Characterization of Tf-CPP liposomes

The Tf-CPP-liposomes were characterized for size and charge using zetasizer. The coupling efficiency of transferrin to the liposomes was determined using microbicinchonic acid assay as described earlier (Sharma et al. 2012). The conjugation of CPPs to the DSPE-PEG lipid was confirmed using fluorescamine assay (Rea et al. 2008). Stock solution of fluorescamine (Fluram®) was prepared in acetone at a concentration of 1 mg/ml. A fixed volume (50µl) of fluorescamine stock solution was added to each standard or sample prepared in sodium borate

buffer, pH8.5 (Miedel et al. 1989; Yuba et al. 2008). The standard curve was generated using varying concentrations of free CPPs. DSPE-PEG-lipid without CPP conjugation was used as a control. The fluorescence of the samples and standards was measured at excitation and emission wavelengths of 365 and 470 nm, respectively. In addition, doxorubicin release studies were performed by diluting the liposomal samples in PBS with 10% FBS and incubating the samples at 37°C. Samples were withdrawn at different time points, passed through sephadex columns and analyzed using HPLC.

2.4.5. Qualitative evaluation of Tf-receptor expression in brain

We confirmed the presence of high density of transferrin receptors in rat brain sections using immunohistochemistry. Anti-transferrin receptor antibody (OX26), anti-CD31 antibody, Alexa-Fluor 594 goat anti-rabbit IgG (excitation 590 nm and emission 617 nm) and Alexa-Fluor 488 goat anti-mouse IgG (excitation: 494 nm and emission: 517 nm) were used to confirm the presence of transferrin receptors. Rat brain tissue was obtained from the breeding colony which originated from Charles River laboratories (Wilmington, MA). The tissue was embedded in Tissue-Tek® OCT compound (Ted Pella Inc., CA) and snap frozen in liquid nitrogen. The frozen brain tissue was sectioned using cryostat (Leica 1950, Nussioch, Germany) to obtain 10µm sections. These tissue sections were then fixed for 15 min with 4% paraformaldehyde in phosphate buffered saline (PBS, pH 7.4) containing 0.1% Tween 20 (PBS-Tween). The tissue sections were washed twice for 10 min with PBS-Tween and incubated with PBS-Tween containing 5% bovine serum albumin (BSA) to block non-specific binding sites. The sections were then incubated overnight at 4ºC with rabbit anti-CD31 Ab (1:400, diluted in PBS-Tween with 1% BSA) and mouse anti-transferrin receptor Ab (OX26, 1:400, diluted in PBS-Tween with 1% BSA) followed by washing with PBS-Tween (two washings for 10 min each). On the next

day, the sections were counter-stained with secondary antibodies (Alexa-Fluor 594 goat anti-rabbit IgG, 1:800 and Alexa-Fluor 488 goat anti-mouse IgG, 1:800, diluted with PBS containing 0.1% tween 20 and 1% BSA) for 1 hour at room temperature. The staining of endothelial cells and transferrin receptors was observed under FV300 confocal fluorescence microscope (Olympus, NY, USA). Brain capillary endothelial cells were stained with the endothelial marker, CD-31 antibody and counter stained with secondary antibody, Alexa fluor 594. Transferrin receptors, on the rat brain sections, were similarly stained with transferrin receptor antibody, OX26 and counterstained with secondary antibody, Alexa fluor 488.

2.4.6. Measurement of pDNA encapsulation efficiency

The pDNA (pGFP or β-gal plasmid) encapsulation efficiency of the liposomes was calculated based on the previously reported method (Zhang et al. 2007). Briefly, 100µl of the liposomal suspension was diluted (1:3) with HEPES buffered saline, pH 7.4. The evaluation of pDNA loading was performed under three conditions: after liposome preparation, after storage at 4 °C for 30 days and after incubation at 37°C for 7 days in the presence of 10% FBS.DNA intercalating dye Hoechst 33342 was used to fluorescently stain the encapsulated DNA. Poly aspartic acid was used to maintain free pDNA. The fluorescence was measured using Spectra Max M5microplatespectrofluorometer (Molecular Devices, Sunnyvale, CA) at excitation and emission wavelengths of 354 and 450 nm, respectively. Percent pDNA encapsulation (EE) was calculated by using the following equation:

$$EE\ (\%) = [FI(t) - FI(0)]/FI(t) \qquad (3)$$

Where, FI(t) is the total fluorescence intensity of the sample after lysis of the liposomes using 1% Triton X-100 (St Louis, MO) and FI(0) is the fluorescence intensity of the sample before lysis of liposomes. The percent pDNA released (RL) was calculated as follows:

$$RL(\%) = 1\text{-}EE(\%) \quad (4)$$

2.4.7. Evaluation of cytotoxicity

MTT assay, apart from being a rapid and reliable method for estimation of cell viability, also allows for multiple sample concentrations to be evaluated spectrophotometrically on a single 96-well plate (Edmondson et al. 1998). Biocompatibility of the formulated liposomes was therefore evaluated in both glial and endothelial cells using MTT assay based on previously reported method (Lila et al. 2009).Cell viabilities of Tf-PR liposomes were evaluated in bEnd3 and primary glial cells at varying phospholipid concentrations (100, 200, 400, and 600 nM) prepared by serial dilution of liposomes in a serum-free medium, that is, DMEM. Similarly, the biocompatibilities of the CPP-liposomes and Tf-CPP liposomes (Tf-TAT, Tf-Penetratin and Tf-Mastoparan) were evaluated in three different cell lines, Daoy (medulloblastoma), U87 (glioblastoma), and bEnd.3 (brain endothelial). The cytotoxic potential of the liposomes was assessed at 50, 100, 200, 400 and 600 nM concentrations of phospholipids. For evaluation of the biocompatibilities of both Tf-PR and TF-CPP liposomes, the cells were plated in 96-well plates at a density of 5×10^2 cells/ well 24 h prior to addition of liposomes. Following this, the culture medium was replaced with serum free medium containing different concentrations of either plain, Tf, PR, CPPs (TAT, Penetratin or Mastoparan), Tf–PR or TF-CPP liposomes. Followingincubation for 2 h, the liposomes were removed and fresh DMEM containing 10% FBS was added. Thecells were incubated further for a total of 48 h. Themedium was then removed and 25 µl of MTT (2mg/ml in PBS, pH 7.4) was added to the wells. After 3 h, the MTT solution was removed and the formazan crystals were dissolved in 200 µl of DMSO. The absorbance of the cells was measured at 570 nm. Untreated cells (without exposure to liposomes) were used as controls.

2.4.8. Evaluation of cell uptake

Cellular uptake of *DiI*-labeled liposomes (Plain, Tf, Tf-PR and PR) was evaluated in bEnd.3 cells, while the uptake of doxorubicin encapsulating (Plain, Tf, Tf-CPP and CPP) liposomes was evaluated in Daoy, U87 and bEnd3 cells.Qualitative investigation of liposomal uptake was performed using fluorescence microscopy. The cells ($6x10^4$/well) were seeded onto 35 mm culture dishes 24h prior to the uptake analysis. Doxorubicin encapsulating liposomes were incubated with the cells at a concentration of 100nM and the uptake of liposomes was investigated at different time intervals. Following liposomal uptake, the cells were rinsed with PBS, pH 7.4. The nuclei of the cells were stained with 4',6-diamidino-2-phenylindole (DAPI) dye and fluorescence of the cells was evaluated using fluorescence microscope (Olympus, Melville, NY).Quantitative estimation of *DiI* labeled liposome uptake was performed by lysis of cells in PBS containing 0.1% Triton X-100 followed by extraction of the fluorescent dye in methanol. The fluorescence intensity of samples was measured spectrofluorometrically (excitation wavelength: 553 nm and emission wavelength: 570 nm).The uptake of doxorubicin carrying liposomes was quantified by lysis of the cells in triton X-100 followed by extraction in methanol. The solution was centrifuged at 3000 rpm for 15 min at 4°C and the supernatant was analyzed using HPLC system equipped with UV-visible detector. The analysis was performed as described above for evaluation of doxorubicin loading.

2.4.9. Measurement of transfection efficiency

The transfection potential of Tf–PR liposomes was evaluated in primary glial cell cultures using GFP plasmid. To protect the gene from acidic pH of the endosome, the gene of interest was further complexed with chitosan and subsequently added to the hydration buffer for encapsulation into Tf–PR liposomes. Transfection efficiency of bifunctional liposomes was

compared with that of plain and Tf liposomes. The cells were seeded onto 35 mm culture dishes (6×10^6 cells/dish) precoated with poly-L-lysine and cultured in DMEM containing 10% FBS at 37°C in 5% CO_2 until approximately 80% confluent. Liposomal formulations containing pGFP chitosan complexes were then added to these cells in serum-free medium.After 2 h, the medium containing liposomes was removedand the cells were further incubated for a totalof 48 h in serum-containing medium. The cellswere then analyzed for GFP expression using confocal laser scanning microscope, and quantitative evaluation was performed using FACS analysis (AccuriC6 flow cytometer (Accuri cytometers, Ann Arbor,MI),laser excitation wavelength: 488 nm, emission detection wavelength using optical filter: FL1 533/30 nm).

The transfection efficiency of the Tf-CPP liposomes was assessed using gWiz GFP and β-galactosidase expressing plasmids (Aldevron LLC, Fargo, North Dakota). The cells were seeded onto poly-L-lysine coated 35 mm dishes and cultured in DMEM containing 10% FBS at 37°C in 5% CO2 until approximately 85% confluent. The cells were then incubated with either GFP or β-galactosidase(β-gal) expressing plasmid (pGFP/pβ-gal) encapsulating liposomes in serum free media for 1h following which the liposomes were removed and the cells were incubated with fresh serum containing media for further 48 h. The cells were then evaluated for expression of GFP using fluorescence microscopy. The gene expression was quantified using β-gal assay kit (Promega, Madison, WI). The β-gal assay was based on the enzymatic hydrolysis of the colorless substrate ONPG to the yellow colored product o-nitrophenol by β-gal enzyme. The hydrolytic reaction was stopped by the addition of sodium carbonate following which the absorbance of the sample was measured at 420 nm. Control samples consisted of the cells exposed to naked β-gal pDNA (not encapsulated into liposomes). Cells not exposed to DNA were similarly processed to determine the endogenous β-gal activity of different cells.

2.4.10. Design of *in vitro* BBB model

The *in vitro* BBB model was constructed using a combination of bEnd.3 and primary glial cell cultures. Glial cells ($1.5 \times 10^4/cm^2$) were seeded on the bottom side of collagen-coated polyethylene terepthalate (PET) membrane (0.4 μm pore size; effective growth area 4.2 cm^2) of Transwell inserts (BD BioCoat™; BD Biosciences, North Carolina) in DMEM with 20% FBS. The cells were allowed to adhere firmly to the membrane overnight. Following this, the endothelialcells ($1.5 \times 10^6/cm^2$ per culture insert) were seeded on the inside of culture inserts placed in six-well plates and cultured in DMEM with 20% FBS and 1% Psf. The cell culture inserts were kept in six-well plates in the culture medium for 6–7 days to allow the formation of tight barrier layer. As a control, models with only bEnd.3 cells on the upper side of the culture inserts, without any glial cells on the underside of the membrane, were also constructed and maintained similarly. The cells were regularly checked for confluency under the microscope, and the cell culture medium was replaced every other day during the incubation period.

2.4.11. Evaluation of barrier integrity

The intactness of the barrier layer was calculated by measuring the transendothelial electrical resistance (TEER) using patch clamp technique.33 Briefly, the culture inserts were filled with 1.5 mL of PBS (with Ca^{2+} and Mg^{2+} ions), and electric pulses with duration of 100 ms were applied through cell layer and voltage generated across the layer was recorded. The current density between 2.0 and 20 $\mu A/cm^2$ was selected depending on the resistance (greater than or less than 1000 Ωcm2). The paracellular transport across the *in vitro* models was evaluated by measuring the flux of sodium–fluorescein (Na–F) across the barrier layer as previously reported (Nakagawa et al. 2009; Veszelka et al. 2007).Cell culture inserts with both glial and endothelial cells (co-culture)or only endothelial cells (monolayer) were transferred to six-well plates

containing 1.5 mL of PBS (pH 7.4) in the lower compartment. In the upper compartment of the inserts, the culture medium was replaced with 1 mL of PBS containing 10μg/mL Na–F. The culture inserts were transferred to new wells containing buffer at specific time intervals of 5, 15, 30, and 45 min. The concentrations of the fluorescent molecule in samples from the upper and the lower compartments were determined by fluorescence SpectraMax®M5 multimode micro plate reader (Molecular devices, Sunnyvale, CA)excitation wavelength: 485 nm, emission wavelength: 535 nm). Flux was also measured across cell-free inserts and the transendothelial permeability coefficients (Pe) were determined for both model types (glial-bEnd.3 and bEnd.3) as previously described (Veszelka et al. 2007; Deli et al. 2005).All experiments were performed in quadruplicates and each experiment involved a set of four culture inserts($n = 4 \times 4$).

2.4.12. Transport across the i*n vitro* BBB model

The transport of four types of DiI-labeled liposomes (plain, Tf liposomes, PR liposomes, and Tf–PR liposomes) was measured across the *in vitro* BBB model (Qin et al. 2011).To mimic the *in vivo* environment, flux of these liposomes was evaluated in sterile PBS (pH 7.4) containing10% FBS. The inserts were transferred to six well plates containing 1.5 mL of PBS in the lower compartment. The culture medium inside the inserts was replaced with liposomal suspensions (100 nM) in 1mL of fresh serum-containing buffer. The inserts were transferred at 15, 30, 60 min, 2, 4, and 8 h to new wells with serum–PBS. The concentrations of the liposomes in the upper and the lower compartments were determined by measuring the fluorescence intensity of the dye molecule in the samples using fluorescence Spectra Max®M5 multimode microplate reader(excitation wavelength: 553 nm, emission wavelength:570 nm). Apparent permeability coefficient (P_{app}) for each liposomal formulation was calculated, according to Gaillard et al. by using the following equation:

$$P_{aap} = dQ/dt1/AC_0.60cm/s \quad (5)$$

Where dQ/dt is the amount of liposomes transported per minute (µg/min), A is the surface area of the transwell membrane (cm^2), C_0 is the initial concentration of liposomes (µg/mL), and 60 is the conversion factor from minute to second. P_{aap} for liposomes wasalso evaluated across cell-free inserts. This apparent permeability was termed as P_t for the permeability coefficient of the total system (*in vitro* model) and P_f for the permeability coefficient across cell-free inserts. The permeability of the endothelial barrier was then calculated using the following equation (Xie et al. 2005; Fenke et al. 2000):

$$1/P_e = 1/P_t - 1/P_f cm/s \quad (6)$$

The percent transport, for all four types of liposomes, was also calculated over a period of 8 h.

2.4.13. Design of 3D *in vitro* BBB model

2.4.13.1. Construction of porous scaffold

The porous scaffold for the growth of tumor cells was generated using emulsion freeze drying technique (Fenke et al. 2000). Poly(D,L-lactide-co-glycolide) (PLGA, lactic acid/glycolic acid 50:50) was dissolved in dichloromethane at a concentration of 0.2 g/ml. This solution (5 ml) was added to a mixture of 500 mg of Chitosan (50 kDa) and 150 mg poly vinyl alcohol (PVA) in 10 ml of acetic acid buffer, pH 4.5 at 2 ml/min with constant stirring using a glass rod. Five hundred microliter solution of collagen in 0.1 M acetic acid (0.1%w/v) was added to the above mixture with stirring to form an emulsified paste. The paste was then poured into rod shaped moulds and freeze dried to form the chitosan-PLGA scaffold. The scaffolds were sectioned into discs of 2 mm thickness which were used for the culture of tumor cells.

2.4.13.2. Growth of tumor cells in 3D microenvironment

The scaffold discs were rinsed with PBS, pH 7.4 and the glioblastoma cells were added to the scaffold surface and incubated overnight. Fresh media containing 20–30% serum was added the following day and the cells were cultured for approximately 35 days to form 3D tumors on scaffold. The cellular biocompatibility was assessed using MTT assay and the cell growth was monitored by hematoxylin-eosin stainingof the frozen scaffold sections. The scaffold sections, atdifferent time points, were embedded in Tissue Tek OCT™ compound and snap frozen in dry ice. The scaffold with tumor cells was sectioned using cryostat, mounted on polylysine coated slides and stained using hemotoxylin-eosin (Sharma et al. 2013). The scaffold was assessed for continuous pore formationand 3D tumor growth using scanning electron microscopy(SEM). The scaffold sections were attached to the sample stubswith carbon paint and were sputter coated with gold. Thesesections were evaluated under JEOL JSM-6490LV highperformancevariable pressure SEM. The tumor cells growingin 3D environment on the scaffolds were then combined with the culture inserts (0.4μm pore size) carrying bEnd.3 cells onthe luminal surface of the insert membrane(Sharma et al. 2012) to forma 3Dbrain tumor model. Culture inserts with brain endothelialcells were placed above the scaffold and different liposomes(TAT, Penetratin and Mastoparan peptides conjugated to Tf-liposomes)were evaluated for transport across the *in vitro* braintumor model.

2.4.13.3. Evaluation of liposomal transport across 3D brain tumor model

The culture inserts seeded with mouse brain endothelial cells (bEnd.3) were placed above the tumor scaffolds on day 28 of tumor growth and cultured for about 7 days to form a brain tumor barrier model. Brain tumor model was designed to simulate *in vivo* tumor conditions where the permeability of the brain endothelial barrier is compromised by the glioblastoma

tumor growth. The intactness of the barrier was determined by measuring the transendothelial electrical resistance (TEER) and the sodium fluorescein (Na-F)permeability coefficient across the endothelial cell layer. The TEER of culture inserts was measured using patch clamp technique (Sharma et al. 2012; Erben et al. 1995). However, in this study the TEER values were determined across the endothelial cell layer on the culture inserts after removing the inserts from the scaffold containing wells and transferring them to the 24-well plates containing PBS (with Ca^{2+} and Mg^{2+} ions). The presence of scaffold with the inserts caused physical contact of the electrodes with the scaffold and interfered with the measurement of resistance resulting in very high resistance values. The Na-F permeability of the barrier was assessed by replacing the media inside the culture inserts with 500µl of PBS, pH 7.4 containing 10µg/ml of Na-F. The media in the lower compartment of the inserts, for the culture of tumor cells, was also replaced with PBS (pH 7.4). The paracellular transport of Na-F was assessed by measuring the fluorescence intensity of the samples from the upper and the lower compartment using fluorescence Spectra Max®M5multimodal micro plate reader (Molecular devices, Sunnyvale, CA) at excitation/emission wavelength: 485/535 nm. Following transport, the scaffolds were rinsed with PBS and approximately 50µl of 0.1% w/v Triton X-100 was added to tumor cells on scaffold with 500µl of PBS, pH 7.4and incubated for ~1 h at 37°C to lyse the tumor cells. The fluorescence of the lysate was measured at different time points to calculate the amount of Na-F transported across the endothelial barrier. The flux measured across cell free inserts and across the total model system was used to calculate the endothelial permeability coefficients (Pe) using equation (4), as described above. The permeability coefficients were assessed across the culture inserts with only endothelial cells and across the *in vitro* brain tumor model and were compared with the permeability coefficient values across the *in vitro* BBB model. The liposomal transport

was similarly assessed by adding different liposomes to the culture inserts seeded with brain endothelial cells and placed on the 3D tumor scaffolds. The media in surrounding the scaffold in the lower compartment was replaced with fresh serum containing PBS (pH 7.4). Also, the media inside the culture inserts was replaced with the liposomal suspensions (200nM) in 1 ml of fresh serum containing buffer. The doxorubicin containing liposomes were transported across the endothelial barrier into the 3Dtumor cell mass growing within the porous scaffold. Following the transport of liposomes, the tumor cells were lysed as described above and the lysates were analyzed using HPLC system equipped with UV-visible detector. The analysis was performed at wavelength of 234 nm using C18 column and phosphate buffer pH 5.5: Acetonitrile (75:25) mixture as described earlier for cell uptake analysis.

2.4.14. Hemolysis assay

To study the interaction of CPP modified liposomes with the negatively charged erythrocytes, we performed the hemolysis assay at increasing phospholipid concentrations. Blood was collected from an adult rat into tubes containing EDTA solution and centrifuged at 2000 rpm for 10 min. The pelleted erythrocytes were washed three times with phosphate buffered saline (PBS), pH 7.4. The erythrocyte count was determined using a hemocytometer. The liposomes, at different concentrations in PBS, were added to pre-determined number of erythrocytes and incubated at 37 °C for 60 min. The samples were centrifuged at 2000 rpm for 10 min and absorbance (A) of the supernatant was analyzed at 540 nm by spectrophotometric analysis. Triton X-100 and PBS treated erythrocytes were used as controls for 100% and 0% hemolysis, respectively. The percent hemolysis was calculated as:

$$\text{Hemolysis (\%)} = \{[A(\text{experimental group}) - A(\text{PBS})]/[A(\text{Triton X-100})]\} * 100 \qquad (7)$$

Less than 10% hemolysis was regarded as non-toxic (Fischer et al. 2003; Lee et al. 2004). The microscopic examination of erythrocytes, exposed to varying liposome concentrations, was performed to further confirm the results from spectrophotometric measurements. Erythrocytes, subjected to different liposomes at increasing concentrations, were observed under light microscope (Olympus DP72,Melville, NY) equipped with a 12.8 megapixel digital colored camera. The images were captured and analyzed using Olympus Cell Sens Version 1.5 Software. All experiments were performed in triplicate and repeated four times to obtain statistically relevant results.

2.4.15. *In vivo* evaluation of liposomes

2.4.15.1. Evaluation of Tf and Tf-PR liposomes

After a seven day acclimation period, the rats were injected via tail vein with either DiR-labeled liposomes or β-gal plasmid encapsulating liposomes. Animals injected with phosphate buffered saline (PBS), pH 7.4, or with β-gal plasmid alone were used as control.

2.4.15.1.1. Biodistribution of DiR labeled liposomes

Animals were divided into four groups where each group, consisting of 6 rats, was administered with either PBS, plain liposomes, Tf-liposomes or Tf-PR-liposomes. The biodistribution profiles of the liposomal formulations were investigated by injecting the animals with DiR-labeled liposomes via tail vein at a dose of ~15.2 μmoles phospholipids/kg body weight. At time points of 12, 24, 48, and 72 h, different organs such as brain, heart, liver, spleen, lungs, and kidneys were excised and rinsed with PBS (n=6 for each time point). Qualitative evaluation of liposomal distribution was performed by acquiring *ex vivo* fluorescent images of the organs using NIR imaging. The system was equipped with a halogen lamp (150 W) as the excitation light source and the band pass filters were adjusted for excitation and emission at720

and 790 nm, respectively. Tissue samples from different organs were weighed, homogenized with PBS (200 µl), and the fluorescent dye was extracted in 3 fold excess of chloroform: methanol (3:1). The homogenized samples were centrifuged at 4000 rpm for 10 min and fluorescence intensity of the supernatant (100 µl) was measured using spectrophotometric analysis. Standard curve for the measurement of the dye extracted from each organ was generated by vortexing free DiR in methanol with the tissue samples from the corresponding organs of the control rat. The organs were homogenized and the dye was extracted as described above. All data were normalized in units of percentage of injected dose per gram of the tissue (% ID/g).

2.4.15.1.2. Transfection efficiency of Tf and Tf-PR liposomes

After a seven day acclimation period, the rats were injected via tail vein with β-gal plasmid encapsulating liposomes. Animals injected with β-gal plasmid alone were used as control. The transfection efficiencies of Tf-liposomes, Tf-PR-liposomes, and naked DNA were assessed by administering the rats with β-gal plasmid encapsulating formulations via tail vein, at a dose of 50µg of DNA/rat (n=6). After five days, different organs (i.e., brain, liver, spleen, heart, lungs and kidneys) were isolated and snap frozen in liquid nitrogen. Tissue samples from different organs were excised, weighed, transferred to 200µl of tissue lysis/protein extraction buffer (Fab Gennix International Inc., Frisco, TX), and homogenized using a high speed homogenizer (Biospec products, Inc., Bartlesville, OK). The homogenized samples were centrifuged at 4000 rpm, 4 °C for 15 min. The supernatant was separated and stored in ice for further processing with the β-gal assay kit. The homogenates extracted from the tissue samples were diluted with an equal volume of assay buffer containing the substrate, o-nitrophenyl-β-D-galactopyranoside (ONPG), and incubated at 37 °C for 60 min. The tissue samples transfected

with β-gal plasmid express the enzyme β-gal. The β-gal activity of the transfected tissues was quantified using the β-gal assay kit (Promega, Madison, WI).The transfection efficiency was determined by evaluating the enzymatic hydrolysis of the colorless substrate ONPG to the yellow colored product o-nitrophenol by β-gal enzyme. The reaction was terminated by the addition of sodium carbonate and the absorbance was measured at 420 nm. Tissue samples fromcontrol rats (without administration of DNA or liposomes) were similarly processed to quantify the endogenous activity of individual organs.

2.4.15.1.3. Histological evaluation of tissues

The biocompatibility of liposomes, *in vivo*, was evaluated by histological examination of tissue sections transfected with β-gal plasmid encapsulating liposomes. The transfected tissue sections from different organs were embedded in Tissue-Tek® OCT™ Compound (Sakura Finetek USA, Inc., Torrance, CA) and snap frozen in dry ice. The frozen tissues were sectioned using cryostat, mounted on poly lysine coated slides and fixed in 4% paraformaldehyde (prepared in PBS, pH 7.4). The sections were stained with Harris hematoxylin solution, washed in running tap water and differentiated in 1% acid alcohol for 10 seconds. The stained tissue section was then rinsed in tap water and blued in 1.36% lithium carbonate solution. The slides were then dehydrated in 95% alcohol and counter stained with eosin Y-phloxine B solution for 5–10 s. The stained tissue sections were cleared in xylene, mounted with Cytoseal 60 (Thermo Fisher Scientific Inc., Barrington, IL) and observed under light microscope. Since, the liver and spleen were exposed to highest concentration of liposomes, therefore, these tissue were carefully examined for any signs of toxicity. The liver sections were observed for ballooning of hepatocytes, enlargement of nuclei or kupffer cells, and granulomas (Semete et al. 2010; Tseng et al. 2012). Similarly, the splenic tissue was evaluated for necrosis and inflammation (Kanth et

al. 2010). Heart and lungs were also examined for signs of necrosis or extravasation of red blood cells(Abdelhalim 2011) and thickening of alveoli (Kamata et al. 2011), respectively. Kidneys were observed for inflammation and necrosis(Kanth et al. 2010) and brain tissue for any signs of lesions (Cole et al. 2011).

2.4.15.2. Biodistribution of Tf-CPP liposomes

After 7 days of acclimation period, the rats were intravenously injected with either free doxorubicin or doxorubicin loaded liposomes. Animals were divided into 7 groups and each group was injected with either free doxorubicin, doxorubicin loaded plain, Tf, Tf-TAT, Tf-Penetratin, or Tf-Mastoparan liposomes at a dose of 15.2μmols of phospholipids/kg body weight. Animals injected with PBS, pH 7.4 were used as control. At time points of 12, 24 and 48h various organs including brain, liver, heart, lungs, kidneys and spleen were isolated and blood samples were withdrawn. The distribution of drug to various organs was determined by homogenization of tissue samples and extraction of the drug in chloroform: methanol (3:1). The extracted samples were then dried in a vacuum drier and the residue was reconstituted in phosphate buffer pH5.5:methanol(4:1). The reconstituted samples were vortexed to allow complete re-suspension of the residue followed by centrifugation of the samples at 10,000 rpm and 4°C to remove any unwanted proteins. The supernatant was then analyzed using HPLC system equipped with UV-visible detector at 234 nm as described for cell uptake analysis. A standard curve for the measurement of the drug extracted from each organ was generated by vortexing free doxorubicin in methanol with the tissue samples from different organs of control rat. The samples were homogenized and the drug was extracted as illustrated above. All data were normalized in units of percentage of injected dose per gram of the tissue (%ID/g).

2.4.16. Statistical analysis

The statistical data were processed using Microsoft Excel 2010 software and presented as mean ± standard deviation (S.D.). The treatment and control groups were compared using two tailed student's t-test and analysis of variance (ANOVA).

CHAPTER III. RESULTS

3.1. Characterization of liposomes

The liposomes were characterized for hydrodyanamic size and zeta potential values. The conjugation of peptides to the surface of liposomes was determined using fluorescamine assay. Surface properties of Tf-PR liposomes were characterized using AFM techniques. The amount of transferrin protein conjugated with the functional lipid DSPE-PEG-COOH was determined using micro BCA assay. Cytotoxic and hemolytic potential of the liposomes was assessed via MTT and hemolysis assay, respectively. *In vivo* biodistribution and transfection of the liposomes was evaluated in adult SD rats.

3.2. Physical properties of liposomes

The phase image analysis using AFM revealed spherical morphology with uniformly dispersed liposomal vesicles as shown in Figure 1. The conjugation of Tf protein and PR did not cause any apparent change in the shape or aggregation of liposomes. The overall morphological appearance for the two types of liposomes was observed to be same. Because the AFM analysis involved drying of the liposomal samples; therefore, this technique was used only for the evaluation of shape and morphological appearance. The average hydrodynamic particle size and zeta potential of liposomes were evaluated in HEPES-buffered saline (pH 7.4), using Zetasizer Nano ZS 90 (Malvern Instruments), at 25°C. The overall size of the liposomes was less than 200nm. The average size for plain unconjugated and Tf–PR liposomes was observed to be in the range of 172.3±3.77 and 196.2±9.5 nm, respectively, and zeta potential was in the range of 6.21±1.2 and 11.19 ± 2.7 mV (mean ± SE), respectively. The results showed that conjugation of transferrin protein to the liposomes significantly ($p < 0.05$) increased the particle size of the liposomes. The sizes of TAT, Penetratin, and Mastoparan conjugated liposomes did not differ

significantly ($p > 0.05$) from each other. Also, the incorporation of Tf decreased the zeta potential to a negative value. This negative zeta potential was attributed to the presence of negatively charged protein on the surface of the liposomes. This negative charge was balanced by the positively charged PR or other CPPs in dual-modified liposomes, thereby imparting a near-neutral zeta potential to the Tf-CPP liposomes. Table 4 summarizes the size and zeta potential values for different liposomes.

No significant ($p > 0.05$) change in size of Tf-CPP liposomes was observed after incubation of the liposomes at 37°C in PBS containing 10% serum. However, the size of CPP-liposomes increased significantly ($p < 0.05$) after incubation in PBS containing serum (Table 5). This was ascribed to the adsorption of negatively charged serum proteins onto CPP-liposomes (due to the presence of only cationic CPPs on the liposomal surface leading to higher positive zeta potential). The presence of polyethylene glycol on the liposomes prevented their aggregation in the presence of serum. However, the presence of serum proteins in the buffer resulted in slightly negative zeta potential values.

Micro BCA assay for Tf content of liposomes revealed that 58±1.6% of the Tf was coupled to the Tf–PR liposomes. The coupling efficiency indicated a slight decrease in the incorporation of Tf-PEG-lipid micelles to the liposomes in the presence of PEGylated PR. The Tf content was approximately 69.82±5.2%, 63.21±5.1%, 60.13±4.9%, and 61±5.8% for Tf-liposomes, Tf-TAT, Tf-Mastoparan and Tf-Penetratin liposomes, respectively. Fluorescamine assay showed a coupling efficiency of approximately 85±4.3%, 82.88± 5.2% and 83.31±4.8% for TAT, Penetratin and Mastoparan, respectively. Coupling of PR was to the PEG lipid was confirmed using 1H NMR technique. The results indicated that approximately 55.6% of the PR was coupled to the PEG–lipid. The pDNA encapsulation efficiencies of plain, Tf, PR, and Tf–PR

liposomes were 35±3.8%, 36±5.4%, 42±2.2%, and 39.6±4.2%, respectively. The loading efficiencies of different liposomes were not significantly ($p>0.05$) different. No significant difference ($p>0.05$) was observed in the encapsulation efficiencies of the liposomes. The drug encapsulation efficiencies were observed to be 78±5.3%, 74.82±4.6%, 76.33±3.8%, and 77.98±4.3% for plain, TAT, Penetratin, and Mastoparan liposomes, respectively. The doxorubicin encapsulation efficiencies were 68.38±6.3%, 65.81±5.2%, and 66.73±5.8% for Tf-TAT, Tf-Penetratin and Tf-Mastoparan liposomes, respectively.

The release of pDNA from the liposomes stored at 4°C was also determined after two weeks. The percentage of pDNA released from plain, Tf, PR, and Tf-PR liposomes was 9.3± 2.8%, 12.4± 4.2%, 7.3±5.4% and 8.5± 5.7%, respectively. The results indicated that ~90% of the loaded pDNA remained encapsulated in the liposomes after storage at 4°C for two weeks. The pDNA release profile was determined after incubation of the liposomes at 37°C in the presence 10% FBS for 7 days. The results showed that approximately 70-80% of the pDNA remained encapsulated in the liposomes (Figure 2). The percent cumulative release was not significantly different ($p>0.05$) among the different liposomal formulations, however the release was observed to be slightly higher from the Tf-liposomes as compared to plain and Tf-PR-liposomes. Also, the Tf-CPP liposomes were assessed for doxorubicin encapsulation and leakage. The drug encapsulation efficiencies were observed to be 78±5.3%, 74.82±4.6%, 76.33±3.8%, and 77.98±4.3% for plain, TAT, Penetratin, and Mastoparan liposomes, respectively. The doxorubicin encapsulation efficiencies were 68.38±6.3%, 65.81±5.2%, and 66.73±5.8% for Tf-TAT, Tf-Penetratin and Tf-Mastoparan liposomes, respectively. The liposomes showed less than 31% of the doxorubicin leakage after 12 h of incubation in PBS (pH 7.4) in the presence of serum, at 37°C (Figure 3).

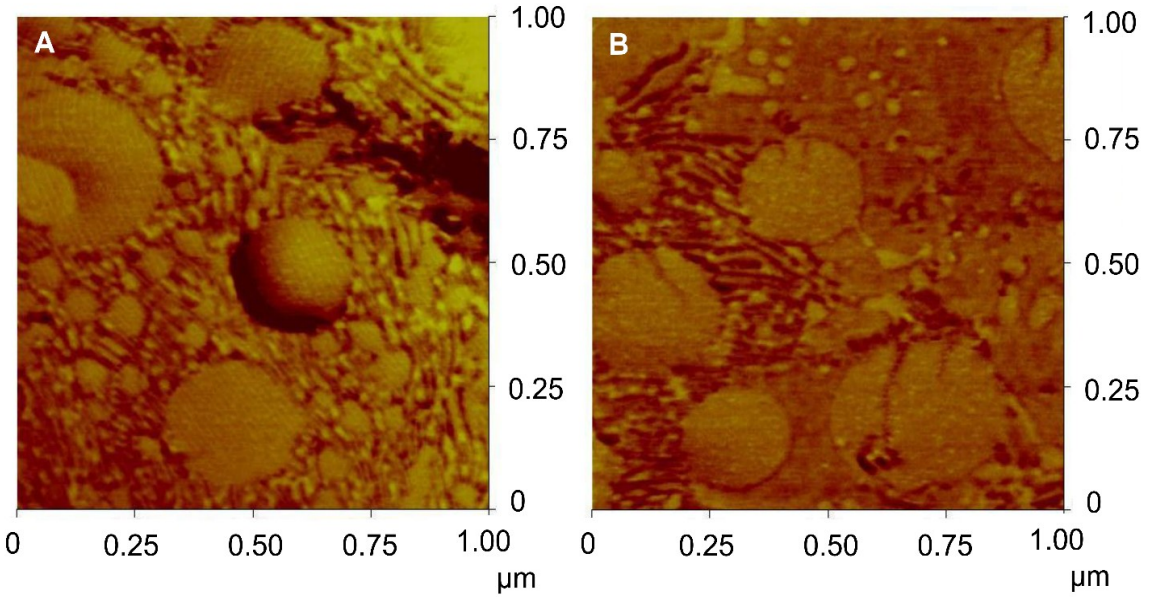

Figure 1. Morphological appearance of liposomes observed using atomic force microscope (A) Surface view of plain liposomes; (B) surface view of Tf–PR liposomes. Air-dried samples of the liposomal suspensions were observed under Veeco DI-3100 atomic force microscope in tapping contact mode at a scan size of 1 µm and at a scan rate of about 1 Hz. AFM images showed the formation of spherical liposome.

Table 4. Particle size and zeta potential measurements for liposomes

Liposomes	Physical property		
	Particle size (nm)	Zeta Potential (mV)	PDI*
Plain-liposomes	172.3±3.77	6.58 ± 3.27	0.258 ± 0.014
Tf-liposomes	185.6±8.40	-8.151±4.96	0.404 ± 0.037
PR-liposomes	188.3 ± 10.6	25.25 ± 3.6	0.275 ± 0.014
TAT-liposomes	176.7±4.70	19.07± 2.82	0.242 ± 0.008
Mast-liposomes	175.2±3.21	16.83 ± 2.82	0.231 ± 0212
Pen-liposomes	178.7±7.71	21.20± 2.471	0.218 ± 0.065
Tf -PR-liposomes	196.2±9.5	11.19 ± 2.7	0.290 ± 0.043
Tf-TAT-liposomes	183.0±6.41	13.16 ± 3.80	0.319 ± 0.038
Tf-Mast-liposomes	188.3±8.21	11.28 ± 5.73	0.212 ± 0.042
Tf-Pen-liposomes	186.82±9.21	15.28 ± 5.31	0.201 ± 0.073

Data are presented as mean ± SD from at least four different preparations.
*PDI: Poly Dispersity Index

Table 5. Particle size of different liposomes in the presence of serum at 37°C for 1h

Type of liposomes	Particle Size (nm)
Plain	175.5 ± 6.3
Tf	186.5 ± 7.3
PR	190 ± 9.9
Tf-PR	198 ± 7.9
Tf-TAT	184.2 ± 6.4
Tf-Pen	188.4 ± 7.2
Tf-Mast	190.8 ± 8.2
TAT	185.8 ± 5.9
Pen	190.6 ±6.8
Mast	188.2 ± 5.4

Data are presented as mean ± S.D, n=4. Polydispersity index (PDI) > 0.5 above 800 nmoles of phospholipids for all liposomal formulations.

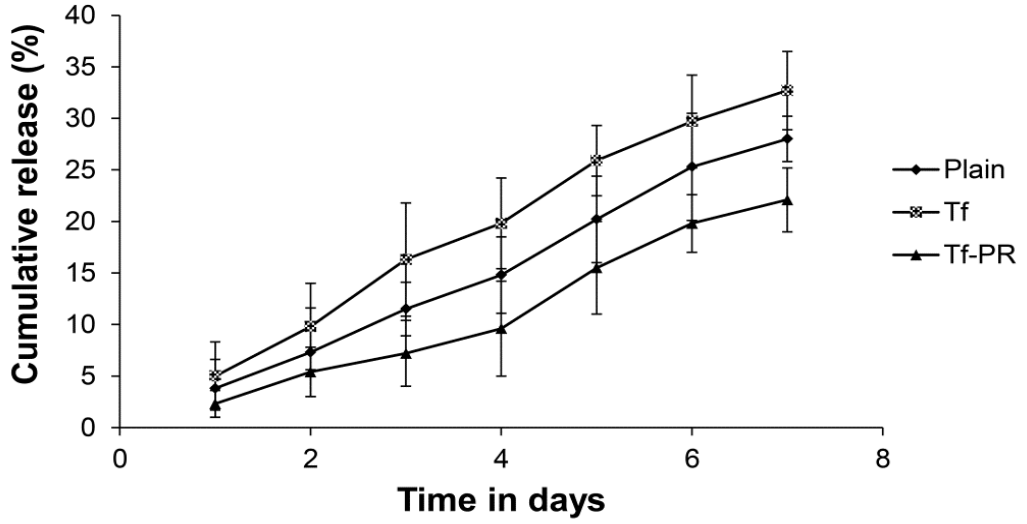

Figure 2. Graphical representation of the percent cumulative pDNA release profiles for Plain, Tf and Tf-PRliposomes. Data are presented as mean±SD from four different preparations.

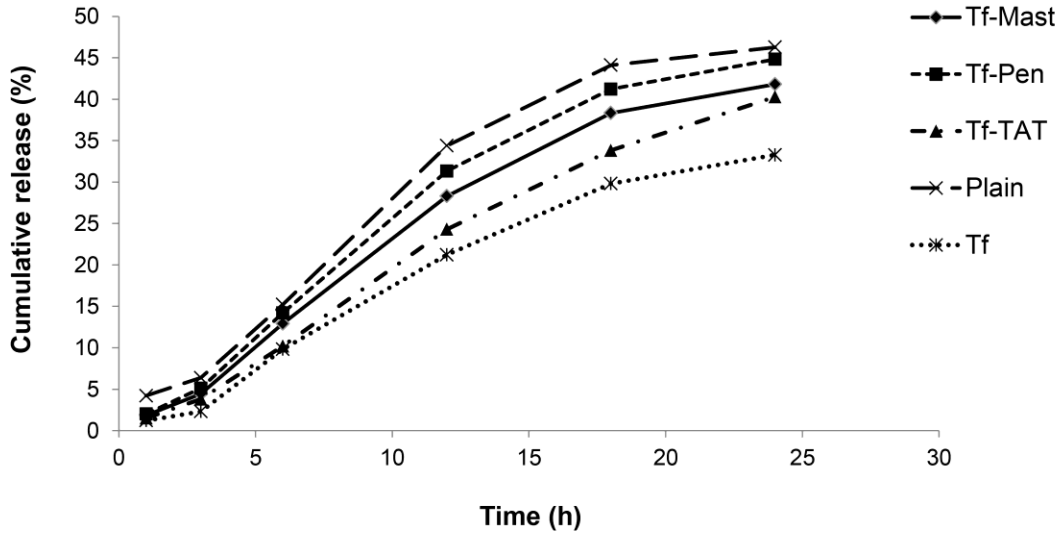

Figure 3. Graphical representation of the percent cumulative doxorubicin release profiles for Plain, Tf and Tf-CPP-liposomes. Data are presented as mean ± SD from at least four different preparations. The release studies were performed at 37°C in the presence of 10% FBS.

3.3. Transferrin receptor expression of brain endothelial cells

Brain capillary endothelial cells were stained with the endothelial marker, CD-31 antibody and counter stained with secondary antibody, Alexa fluor 594. Transferrin receptors, on the rat brain sections, were similarly stained with transferrin receptor antibody, OX26 and counterstained with secondary antibody, Alexa fluor 488. A strong overlap in the fluorescence regions of CD31 receptors on brain endothelial cells and transferrin receptors in brain provided a qualitative confirmation of the presence of high density of transferrin receptors on the brain capillary endothelial cells. The liposomal formulation in this study was designed to target these receptors on the brain capillary endothelial cells.

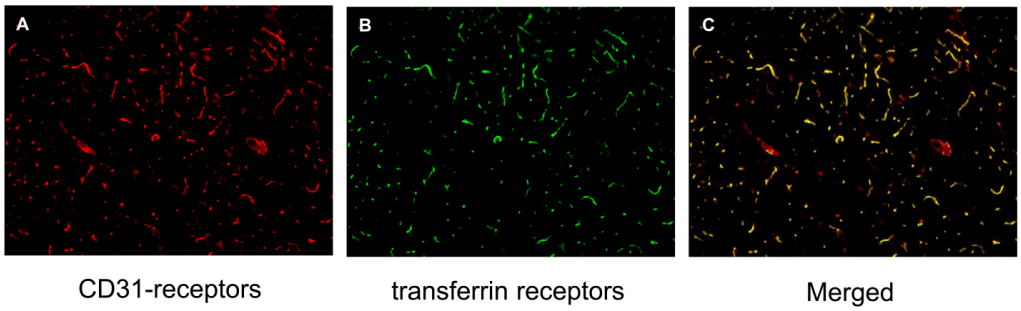

Figure 4. The brain capillary endothelial cells (red) were labeled with primary antibody (rabbit anti-CD31) and counterstained with secondary antibody (Alexa-Fluor 594 goat anti-rabbit IgG), transferrin receptors (green) were marked with mouse anti-transferrin receptor Ab (OX26) and counterstained with (Alexa-Fluor 488 goat anti-mouse IgG). Co-labeling of (A) CD31 and (B) transferrin receptors shown in the (C) merged image indicate the presence of high densities of transferrin receptors on brain capillary endothelium. Fluorescence images were taken at 10x magnification.

3.4. Biocompatibility of liposomes

3.4.1. Cytotoxicity assay

The results indicated a cell viability of about 90% in glial cells after exposure to plain liposomes (100nM) and about 80% after exposure to Tf-PR-liposomes (100nM) as depicted in Figure 5. Also, Figure 6 shows that the endothelial cell viabilities on exposure to plain liposomes

were close to the viabilities of unexposed endothelial cells and about 85% after exposure to Tf-PR-liposomes at the same concentration. The overall viabilities for endothelial cells were higher in comparison to the glial cells indicating greater sensitivity of glial cells on exposure to different liposomes. The cell viabilities were observed to increase with decreasing concentration of phospholipids. Consequently, cell uptake and transfection studies were performed at an optimized concentration of 100nM without compromising with cell viabilities (concentrations less than 100nM showed low transfection efficiencies).

The biocompatibilities of CPP and Tf-CPP liposomes were evaluated in bEnd3, U87 and Daoy cells. The liposomes, without doxorubicin, were observed to be non-toxic in all three cell lines and showed a cell viability of approximately 80–90% upto a phospholipid concentration of 200nM (Figure 10-12). The cell viabilities were observed to be lower with Tf-Mastoparan liposomes at higher concentrations in all three cell lines. The viabilities at 600 nM concentration were observed to be approximately 71.6%, 59.8% and 56.8% in Daoy, U87 and bEnd.3 cells, respectively. Furthermore, the viabilities were higher in the tumor cell lines (Daoy and U87) as compared to the brain endothelial (bEnd.3) cells. Also, U87 cells were found to be more sensitive to liposomal exposure as compared to the Daoy cells. In contrast, the negatively charged Tf-liposomes showed higher cell viabilities (approximately 90.23–95.48%), irrespective of the type of cells. The cell viabilities were observed to decrease significantly ($p < 0.05$) after encapsulation of doxorubicin (Figure 7-9). The cytotoxicity of Tf-TAT liposomes was least while Tf-Mastoparan liposomes showed maximum cytotoxic potential. In addition, a significant ($p < 0.05$) decrease in cell viability was observed at higher concentrations with all liposomes. Tf-Mastoparan liposomes showed a cell viability of approximately 13–18% at 600nMconcentration in all three cell lines. The cell viability of Tf-TAT liposomes decreased from approximately

75.7–35.6% with an increase in phospholipid concentration from 50nM to 600nM concentration in Daoy cells. The cell viabilities of the single ligand CPP-liposomes were lower as compared to the dual-functionalized, Tf-CPP or plain liposomes.

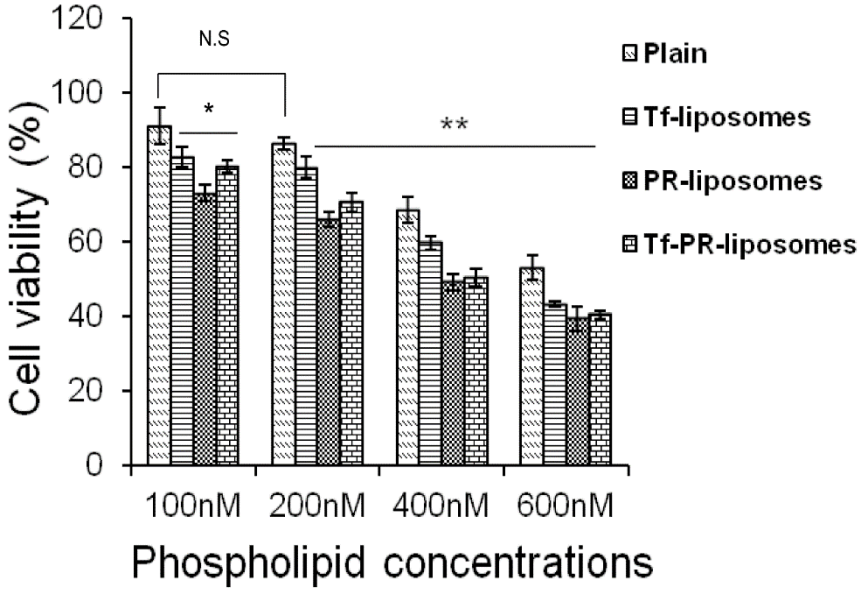

Figure 5. Bar graph representation of the viabilities of glial cells after exposure to varying concentrations of liposomes (plain, transferrin (Tf) coupled, poly-L-arginine (PR) coupled, and Tf–PR coupled). Results are expressed as mean ± SE (n = 4). $*p < 0.05$, $**p < 0.01$ against plain liposomes at 100 nM concentration.

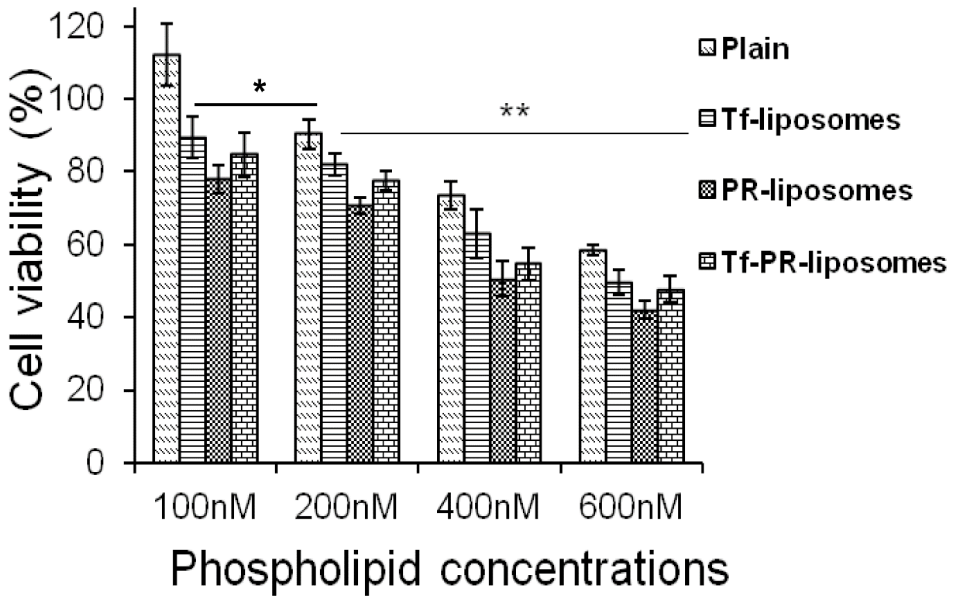

Figure 6. Bar graph representation of the viabilities of bEnd.3 cells after exposure to varying concentrations of liposomes (plain, transferrin (Tf) coupled, poly-L-arginine (PR) coupled, and Tf–PR coupled). Results are expressed as mean ± SE (n = 4). ∗p < 0.05, ∗∗p <0.01 against plain liposomes at 100 nM concentration.

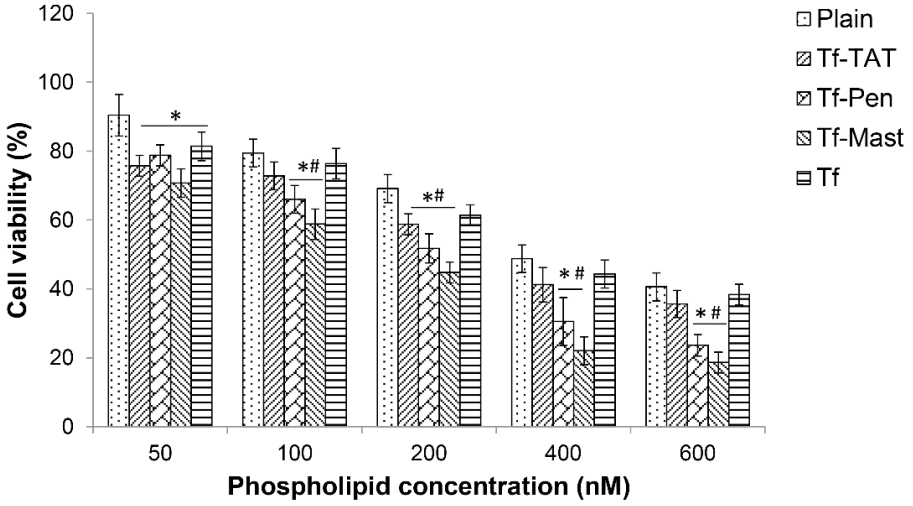

Figure 7. Bar graph depiction of the viabilities of Daoy cells after exposure to doxorubicin encapsulating plain and dual-functionalized liposomes. The data are presented as mean ± S.D. (n=4); Statistically significant ($p<0.05$) differences are indicated in comparison with (*) plain and (#) Tf-liposomes at the respective concentrations.

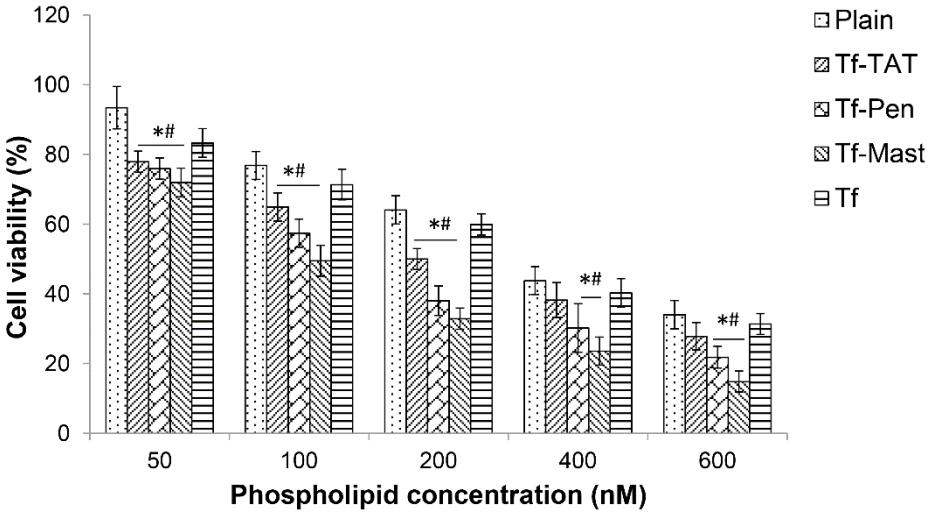

Figure 8. Bar graph depiction of the viabilities of U87cells after exposure to doxorubicin encapsulating plain and dual-functionalized liposomes. The data are presented as mean ± S.D. (n=4); Statistically significant ($p<0.05$) differences are indicated in comparison with (*) plain and (#) Tf-liposomes at the respective concentrations.

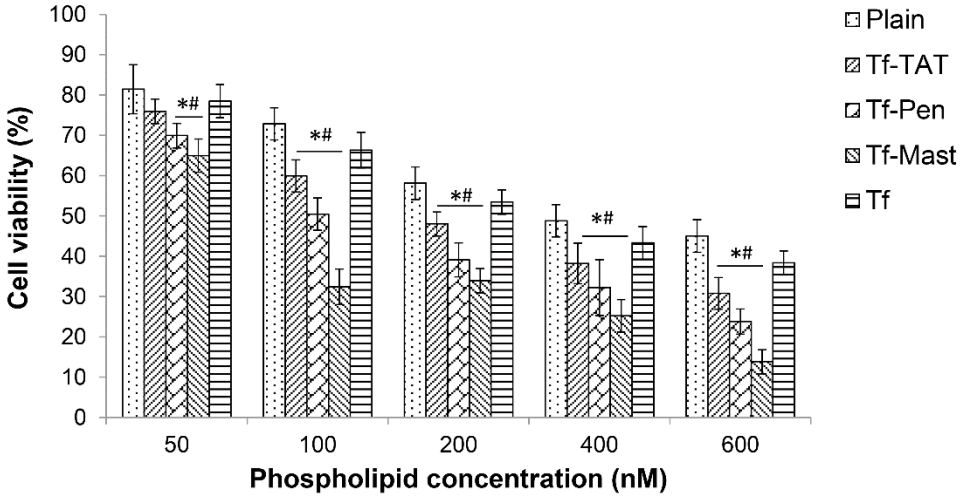

Figure 9. Bar graph depiction of the viabilities of bEnd3 cells after exposure to doxorubicin encapsulating plain and dual-functionalized liposomes. The data are presented as mean ± S.D. (n=4); Statistically significant ($p<0.05$) differences are indicated in comparison with (*) plain and (#) Tf-liposomes at the respective concentrations.

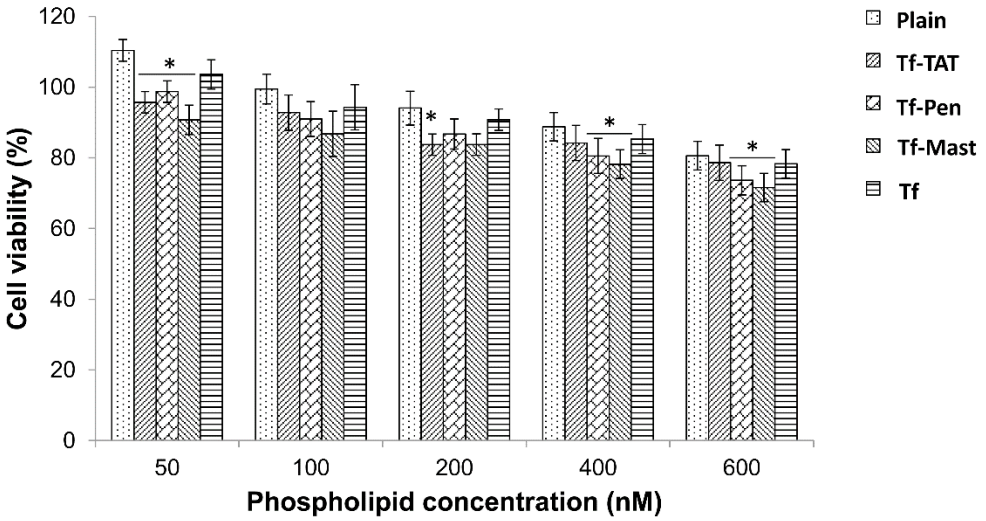

Figure 10. Graphical representation of the viabilities of Daoy cells after exposure to dual modified liposomes (without doxorubicin), at varying phospholipid concentrations. The results are expressed as mean ± S.D. (n=4); *p<0.05 against plain liposomes at respective concentrations.

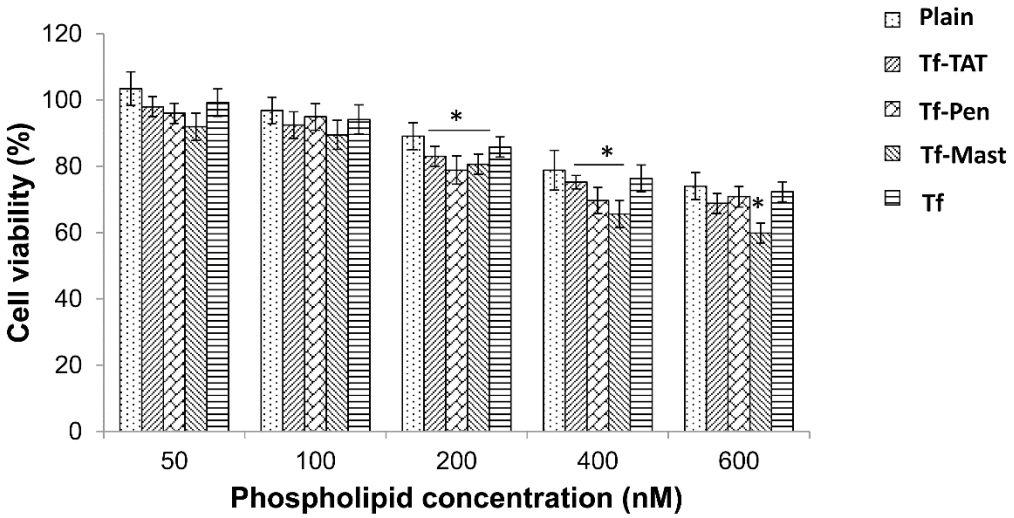

Figure 11. Graphical representation of the viabilities of U87 cells after exposure to dual modified liposomes (without doxorubicin), at varying phospholipid concentrations. The results are expressed as mean ± S.D. (n=4); *p<0.05 against plain liposomes at respective concentrations.

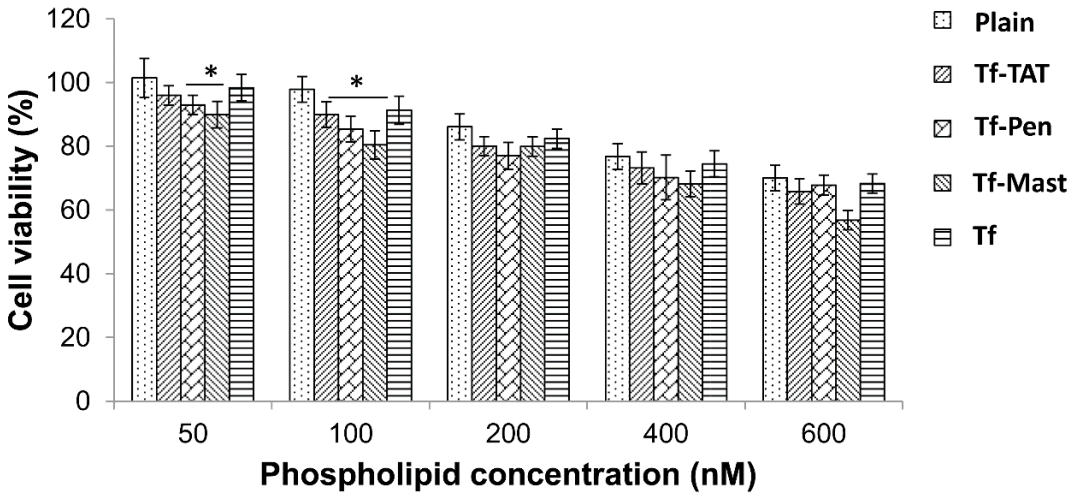

Figure 12. Graphical representation of the viabilities of bEnd3 after exposure to dual modified liposomes, at varying phospholipid concentrations. The results are expressed as mean ± S.D. (n=4); *$p<0.05$ against plain liposomes at respective concentration.

3.4.2. Hemolysis assay

The interaction of cationic polymers with the negatively charged membrane of the erythrocytes can cause cell lysis and release of hemoglobin (Antohi et al. 1984). Since the liposomes were designed to be injected intravenously into adult SD rats, we evaluated their interaction with the erythrocytes *in vitro* prior to the *in vivo* biodistribution analysis. Hemolysis assay of the liposomes demonstrated that the dual-modified liposomes did not show any significant ($p>0.05$)increase in the hemoglobin release up to 600 nmoles of phospholipids/$1.4x10^7$ erythrocytes (Figure 13-14) and were therefore, considered non-toxic. Slight hemolysis was observed with the Tf-PR-liposomes at 800 nmoles of phospholipids exposed to the same number of erythrocytes. The light microscopic observation of the erythrocytes did not reveal any disruption of cellular membrane or aggregation of the red blood cells with either Tf or Tf-PR-liposomes up to concentrations of 600 nmoles of phospholipids (Figure 15). Microscopic examination revealed changes in the structure of erythrocyte membrane and morphological appearance accompanied with slight aggregation after exposure to Tf-PR-

liposomes at 800 nmoles of phospholipids. PBS, pH 7.4, was used as a negative control and did not show any damage to erythrocyte membrane under microscopic examination or release of hemoglobin on spectrophotometric measurement. Triton X-100, used as a positive control, demonstrated maximum lysis of erythrocytes, as observed under the light microscope, and release of hemoglobin on spectrophotometric analysis.

Similar results were observed upon analyzing the hemolytic activity of Tf-CPP liposomes. The release of hemoglobin increased with increasing concentration of phospholipids (Figure 16). Lessthan 10% hemolysis was considered non-toxic (Sharma et al. 2013). Plain, Tf-Penetratin, and Tf-TAT liposomes were observed to be nontoxic upto a concentration of 600 nmol of phospholipids/1.5×10^7 erythrocytes. Slight hemolysis was observed withTf-Penetratin liposomes at concentration of 800 nmol ofphospholipids. However, Tf-Mastoparan liposomes showed a significantly higher ($p<0.05$) cytotoxicity at a concentration of 200 nmoles of phospholipids.

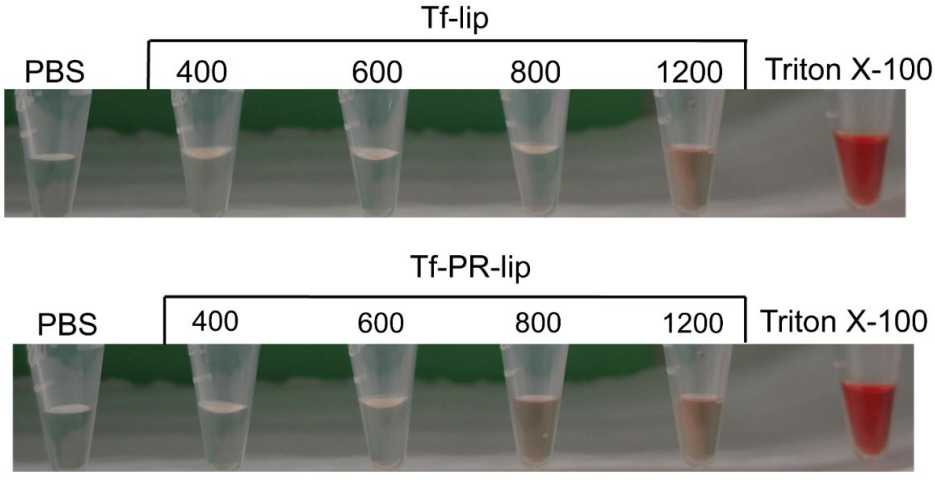

Figure 13. Photo images of ependorf-tubes containing supernatant from RBCs exposed to different liposomes at varying concentrations. PBS, pH 7.4 and triton X-100 were used as negative and positive controls, respectively.

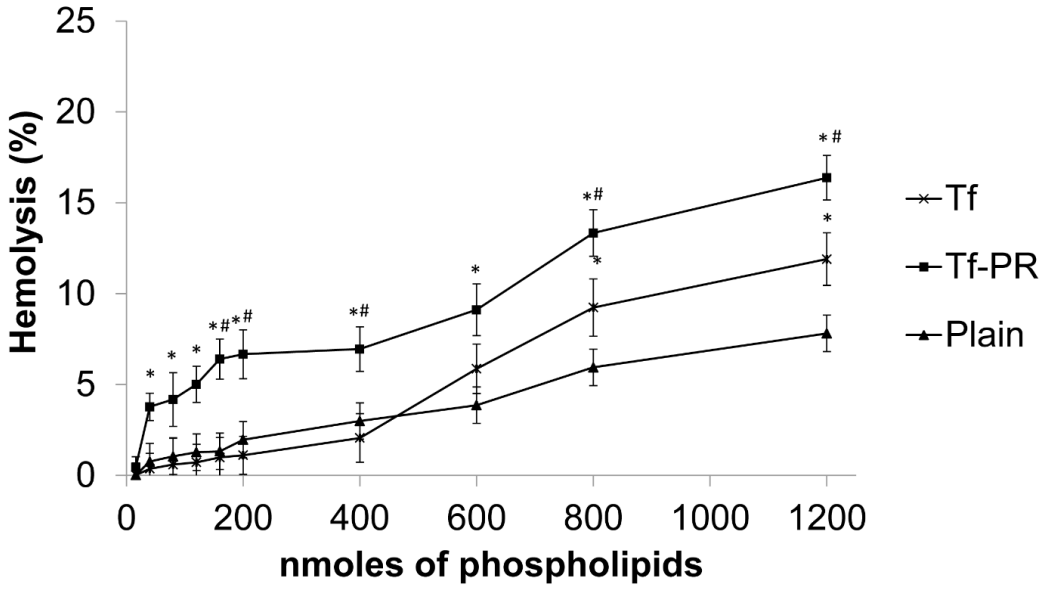

Figure 14. Graphical representation of percent hemolysis by different liposomes. Less than 10% hemolysis was considered non-toxic. *p<0.05 versus plain liposomes; #p<0.05 versus Tf-liposomes.

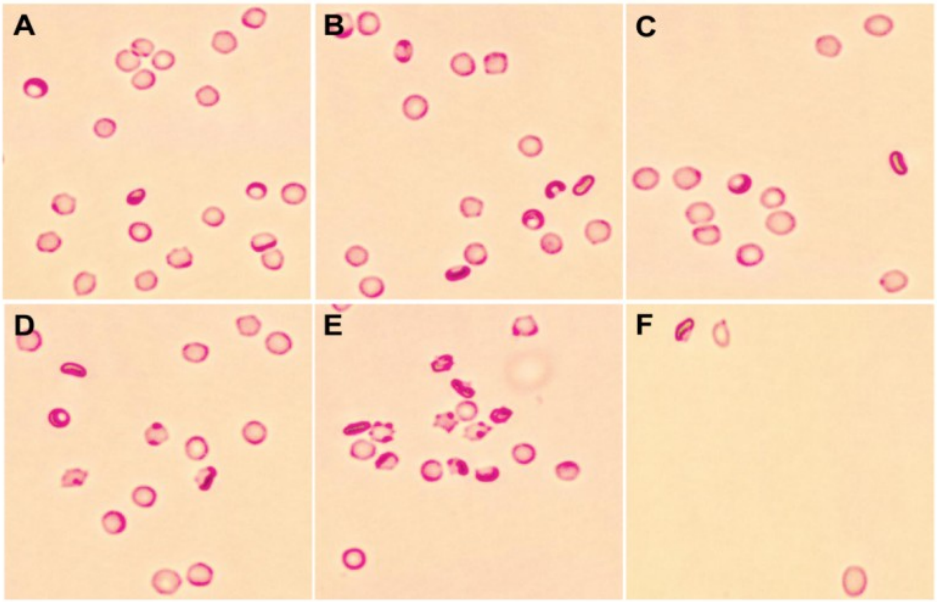

Figure 15. Microscopic images of RBCs exposed to (A) Plain (B) Tf (C) Tf-PR liposomes at 600 nmoles of lipids (D) PBS (E) Tf-PR-liposomes at 800 nmoles of lipids (F) Triton X 100.

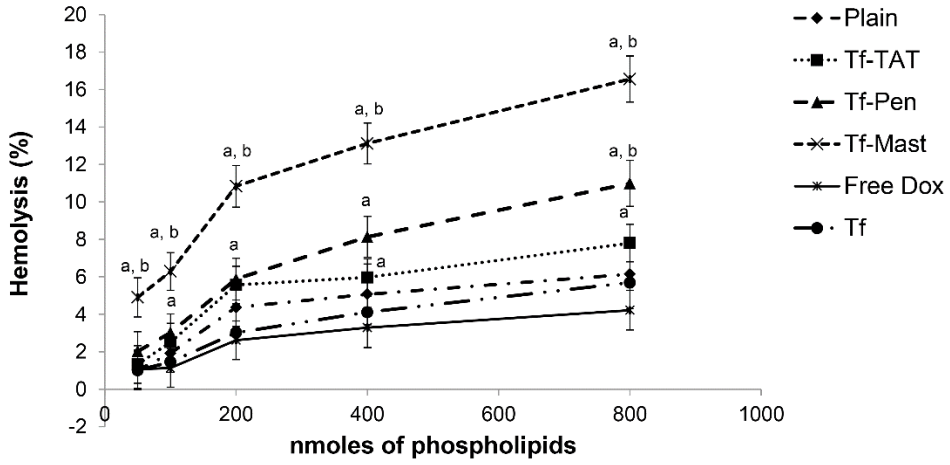

Figure 16. Graph showing the hemolytic activity (%) of various liposomal formulations. Red blood cells were exposed to PBS and triton X-100 for negative and positive controls, respectively. Less than 10% hemolysis was considered non-toxic. Statistically significant ($p<0.05$) differences are reported in comparison to free drug (a) and plain liposomes (b). Data are presented as mean ± S.D. (n=5).

3.5. Cellular uptake studies

3.5.1. Cell uptake of Tf-PR liposomes

The uptake of *DiI* labeled liposomes was investigated in bEnd.3 cells using confocal fluorescence microscopy. Figure 17 shows that the uptake of plain liposomes was lowest in the target cells while Tf-PR liposomes exhibited a clear and strong pattern of fluorescence throughout the cytoplasm and overlapping with the nuclei of the cells. The fluorescence of the cells was found to intensify with increase in the incubation time of cells with liposomes. The uptake of PR liposomes, facilitated by improved cellular binding and penetration alone, was lesser in comparison to the uptake of Tf-liposomes governed by receptor mediated endocytosis, indicating a higher uptake by receptor targeting mechanism in contrast to cell penetration. A combination of these two techniques resulted in substantial improvement in the uptake of fluorescently labeled liposomes by cells. Quantitative estimation of liposomal uptake was

performed by lysis of cells in PBS containing 0.1% triton X-100 followed by extraction of the fluorescent dye in methanol. Figure 18 shows that the fluorescence intensity of the samples increased with time. The uptake of Tf-liposomes was observed to increase from 35.9 ± 4.4% after 5 minutes to 82 ± 3.4% after 30 minutes. The increase in percent liposomal uptake was lowest for plain liposomes (from 18.4 ± 2.1% after 5 minutes to about 38.6 ± 5.8% after 30 minutes) followed by the uptake of PR-liposomes (from 29.2 ± 3.5% after 5 minutes to 58.9 ± 4.1% after 30 minutes). The extent of uptake was highest for Tf-PR-liposomes with an increase in percent liposomal uptake from 47.2 ± 4.2% after 5 minutes to 94.8± 3.4% after 30 minutes. Further, adding excess of free transferrin reduced the uptake of Tf-liposomes to 35.62± 6.4% (observed after 30 minutes) due to inhibition of transferrin receptors. Transport of Tf-PR-liposomes also decreased to 54.2 ± 5.8% after 30 minutes, however no significant alteration in the uptake behavior of plain and PR-liposomes was observed. Hence, the study demonstrated that uptake was mainly governed by receptor facilitated mechanism however, cell penetration significantly ($p<0.05$) improved the extent of liposomal delivery to cells.

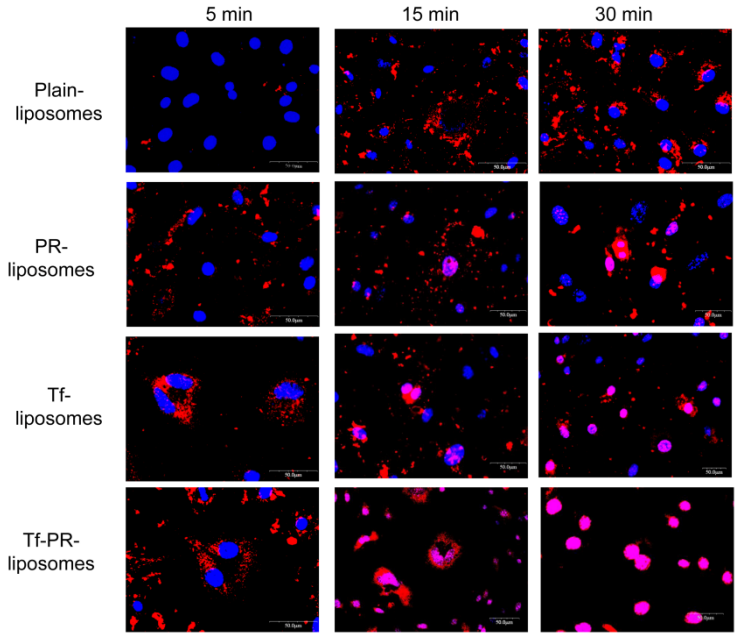

Figure 17. Confocal microscopic images of bEnd.3 cells after uptake of DiI (excitation 553 nm and emission 570 nm) labeled liposomes at different time intervals. The nuclei of the cells were stained with DAPI (excitation330-385 emission 420nm). The image shows an overlap of the nuclei (blue) and liposomes (red) after uptake of liposomes by the endothelial cells (bEnd3). (B) Quantitative assessment of liposomal uptake in bEnd.3 cells at different time intervals. The percent cellular uptake is expressed as mean ± S.E. (n=4). Statistically significant ($p<0.05$) in comparison to plain-lip (a), PR-lip (b), Tf-lip (c).

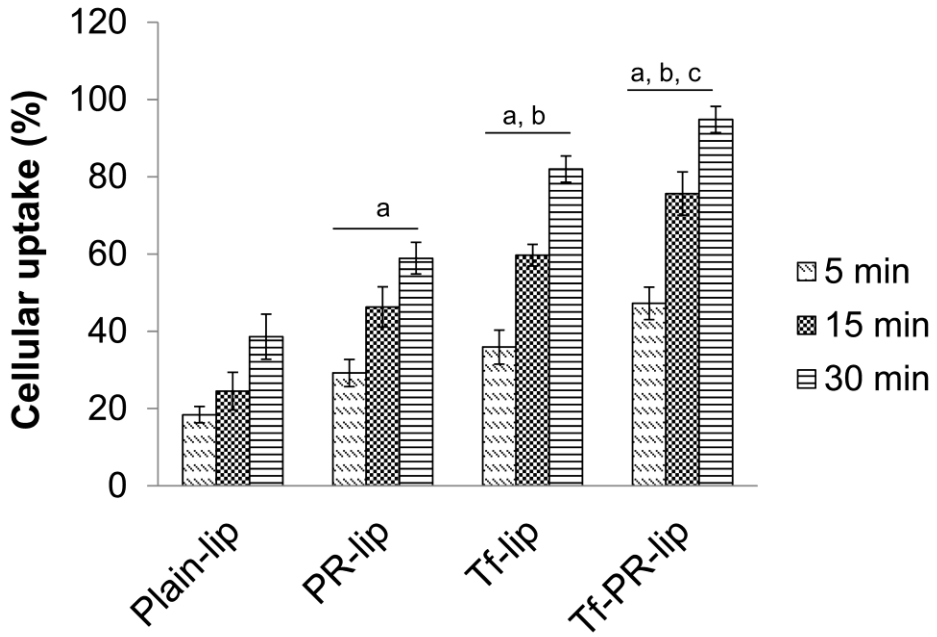

Figure 18. Quantitative assessment of liposomal uptake in bEnd.3 cells at different time intervals. The percent cellular uptake is expressed as mean ± S.E. (n=4). Statistically significant ($p<0.05$) differences are indicated in comparison to plain-lip (a), PR-lip (b), Tf-lip (c).

3.5.2. Cell uptake of Tf-CPP liposomes

We exploited the presence of transferrin receptors on the three cell lines (Daoy, U87 and bEnd.3) for delivery of Tf-CPP liposomes. Figures 19 and 20 illustrates the transport of different liposomes in the three cell lines following 1h of incubation. Free drug demonstrated negligible uptake after incubation with the cells (Figures 21 and 22). Plain liposomes, in the absence of any surface modification, showed the lowest transport in all types of cells while the dual-functionalized Tf-CPP liposomes showed maximum uptake and therefore, the strongest fluorescence pattern in all cells (Figure 19). Also, the uptake of Tf-liposomes was more than plain and CPP-liposomes. The uptake of liposomes was observed to increase with time (Figure 20, 23 and 24).

Quantitative estimation of liposomal uptake further confirmed the efficacy of dual-functionalized liposomes over single ligand and plain liposomes (Figure 20). Tf-TAT liposomes

showed an uptake of about 90%, 82% and 77% in U87, Daoy, and bEnd.3 cells, respectively. The uptake of Tf-Penetratin liposomes was about 98%, 96%, and 89% while the uptake of Tf-Mastoparan liposomes was about 97%, 90% and 87% in U87, Daoy, and bEnd.3 cells, respectively. The order of increasing fluorescence intensity for dual-functionalized liposomes was Tf-TAT<Tf-Mastoparan<Tf-Penetratin. The results emphasized the significance of dual-mechanism of uptake over receptor targeting or cell penetration alone.

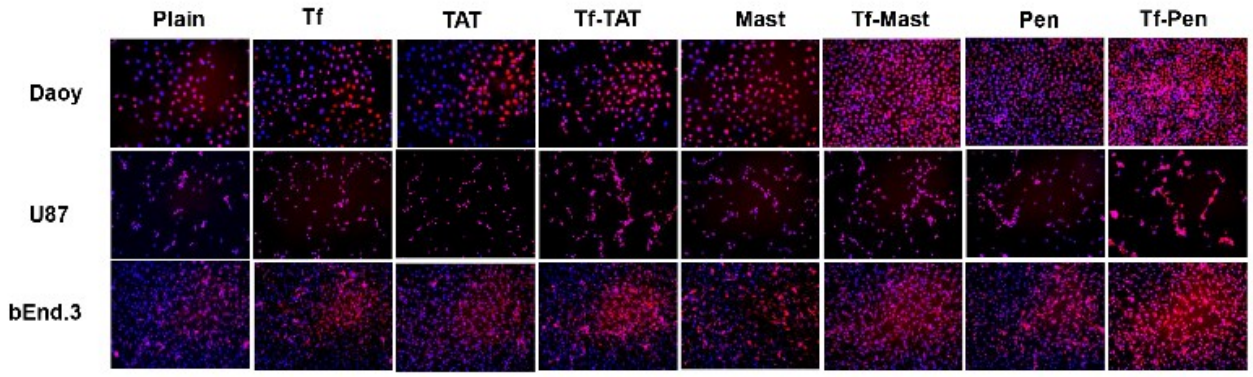

Figure 19. Fluorescence microscopic images (10x magnification) of different cells after uptake of doxorubicin encapsulating liposomes (excitation/emission wavelengths: 470/585 nm). The nuclei of the cells were stained with DAPI (excitation/emission: 330–385/420 nm). The image shows an overlap of the cells after uptake of doxorubicin liposomes (red) and the nuclei of the cells (blue).

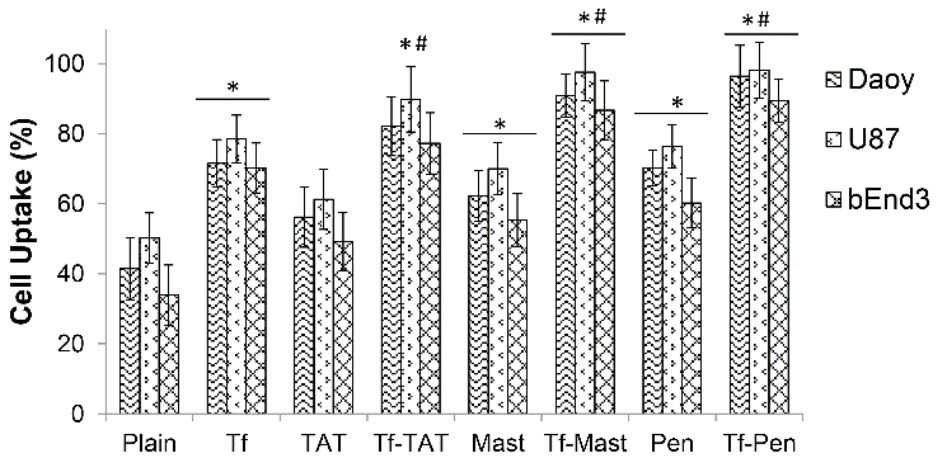

Figure 20. Bar graph representation of the uptake of doxorubicin liposomes after 1h of incubation with either Daoy, U87, or bEnd3 cells. Following uptake, the cells were lysed and the uptake of liposomes was determined using high performance liquid chromatography (HPLC) equipped with UV visible detector at 234nm. The results are expressed as mean ± S.D (n=5).Statistically significant ($p < 0.05$) differences are indicated versus plain liposomes (*) and Tf liposomes (#).

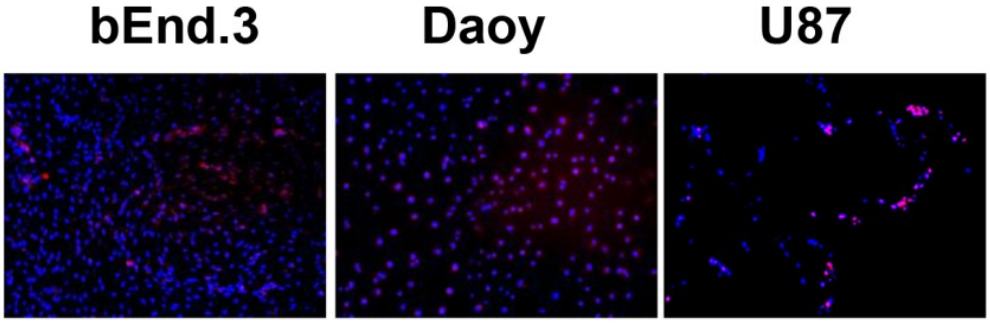

Figure 21. Fluorescence microscopic images (10x magnification) of bEnd.3, Daoy and U87 cells after exposure of these cells to free doxorubicin (1mg/ml in Hepes buffered saline, pH 7.4) (excitation/emission wavelengths: 470/585 nm) for 1h.

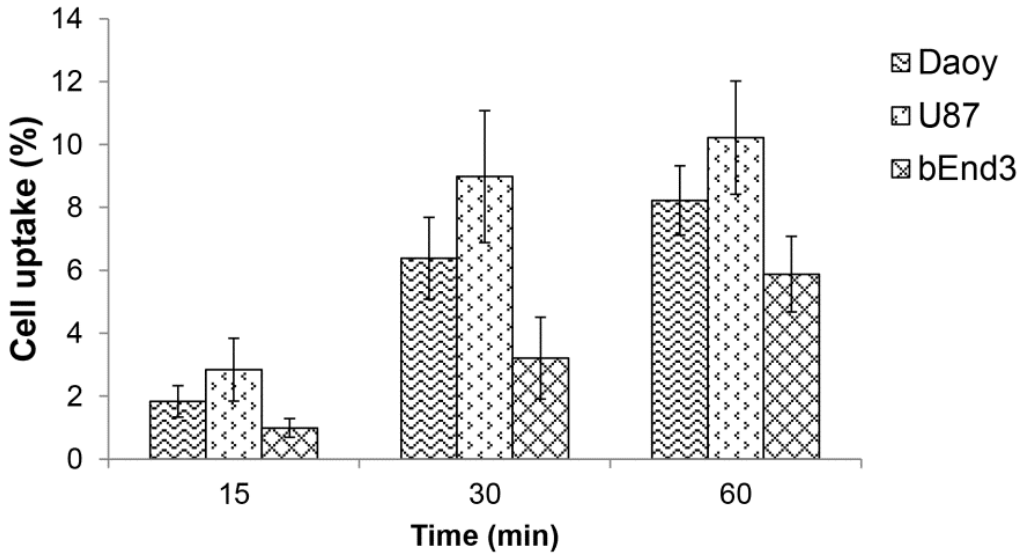

Figure 22. Bar graph representation of the quantitative assessment of the uptake of free doxorubicin in different cell lines after exposure of cells to the drug for 1h. The percent cell uptake is expressed as mean± S.D (n=4).

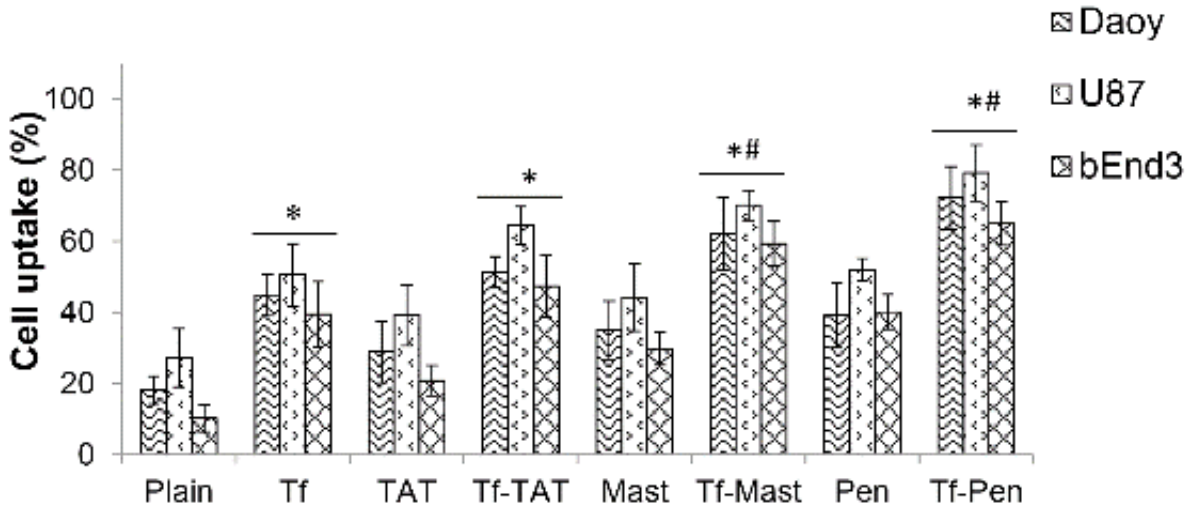

Figure 23. Quantitative assessment of the uptake of doxorubicin encapsulating liposomes after 15 minutes of incubation with the three cell lines. Following uptake, the cells were lysed and the uptake of liposomes was determined using high performance liquid chromatography (HPLC) equipped with UV-visible detector at 234nm. The results are expressed as mean ± S.D (n=5).

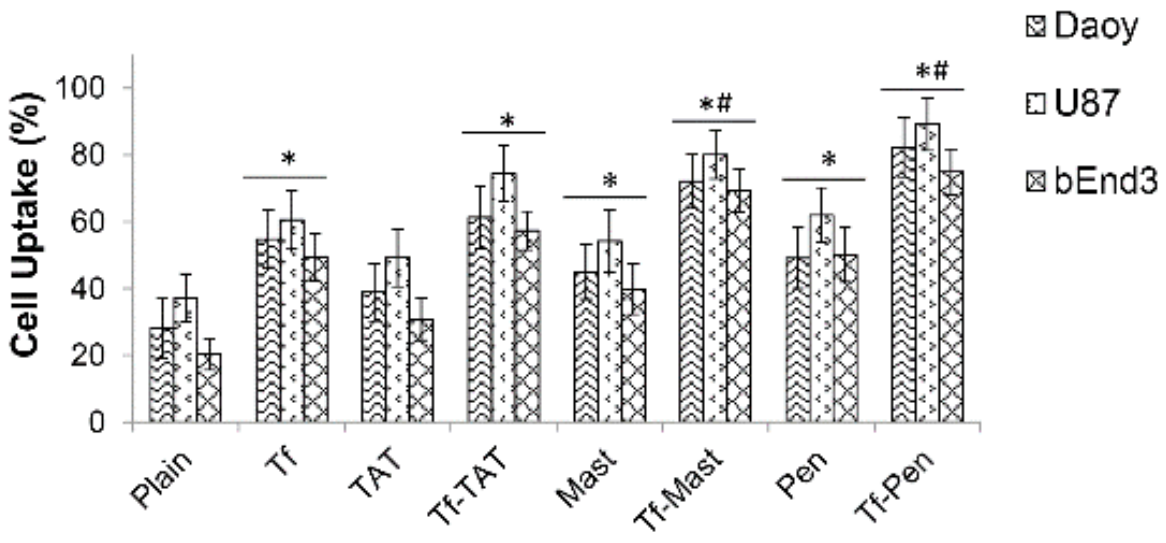

Figure 24. Quantitative assessment of the uptake of doxorubicin encapsulating liposomes after 30 minutes of incubation with the three cell lines. Following uptake, the cells were lysed and the uptake of liposomes was determined using high performance liquid chromatography (HPLC) equipped with UV-visible detector at 234nm. The results are expressed as mean ± S.D (n=5).

3.6. Mechanism of uptake

The uptake of all types of liposomes was almost completely inhibited at 4°C thus indicating an energy dependent uptake of the liposomes in all three cell lines (Figure 25-27). Colchicine, an inhibitor of caveolae formation, did not inhibit the uptake of plain, Tf, or Tf-CPP liposomes. Also, macropincytosis inhibitor amiloride did not significantly ($p>0.5$) inhibit the uptake of Tf-TAT, Tf-Penetratin, Tf, or plain liposomes. However, a significant ($p<0.05$) reduction in the uptake of Tf-Mastoparan liposomes was observed using amiloride, thereby indicating the contribution of Mastoparan in the macropinocytic uptake of the liposomes into all three cell lines. Some inhibition (non-significant) of other Tf-CPP liposomes was also observed in the presence of amiloride. However, plain and Tf-liposomes were not affected by the macropinocytic inhibitor thus eliminating macropinocytosis as the uptake pathway for these liposomes. In contrast, the uptake of single ligand CPP-liposomes was considerably affected by

the presence of amiloride and chlorpromazine (Figure 28-30). In addition, chlorpromazine reduced the uptake of all types of liposomes to approximately 30%-50% in all cell lines thereby illustrating clathrin-mediated uptake as the major pathway for uptake of liposomes. M-β-CD (methyl-β-cyclodextrin) depletes cholesterol, which is involved in the formation of invaginations leading to the development of clathrin-coated vesicles during the uptake of extracellular components (Rodal et al. 1999). A significant ($p<0.05$) reduction in the uptake of liposomes was observed using m-β-CD, thus re-confirming the participation of clathrin-coated vesicles in the uptake of liposomes. The results indicated clathrin-mediated uptake as the major pathway for the transport of plain, Tf and Tf-CPP liposomes. The uptake of free drug was only slightly inhibited at 4°C, thus indicating a non-energy dependent uptake as the major pathway for transport of free doxorubicin.

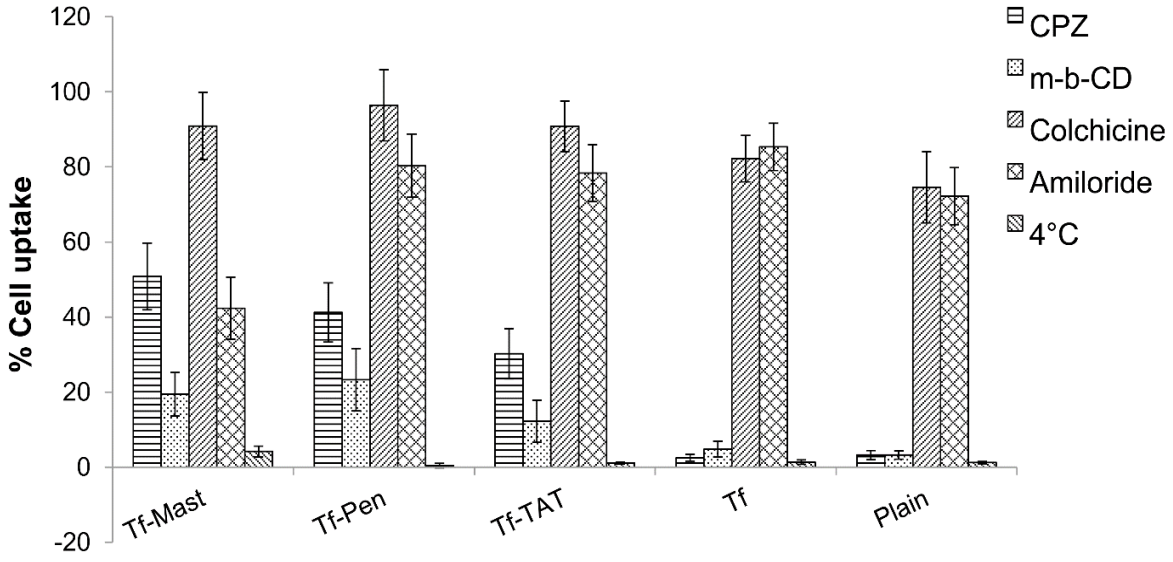

Figure 25. Graphical representation of effect of various inhibitors on the uptake of doxorubicin encapsulating Tf-CPP-liposomes in Daoy cells. The uptake of doxorubicin liposomes was quantified by lysis of the cells and measurement of the drug using HPLC system equipped with UV visible detector at 234 nm. The results are expressed as mean±S.D. (n=4).

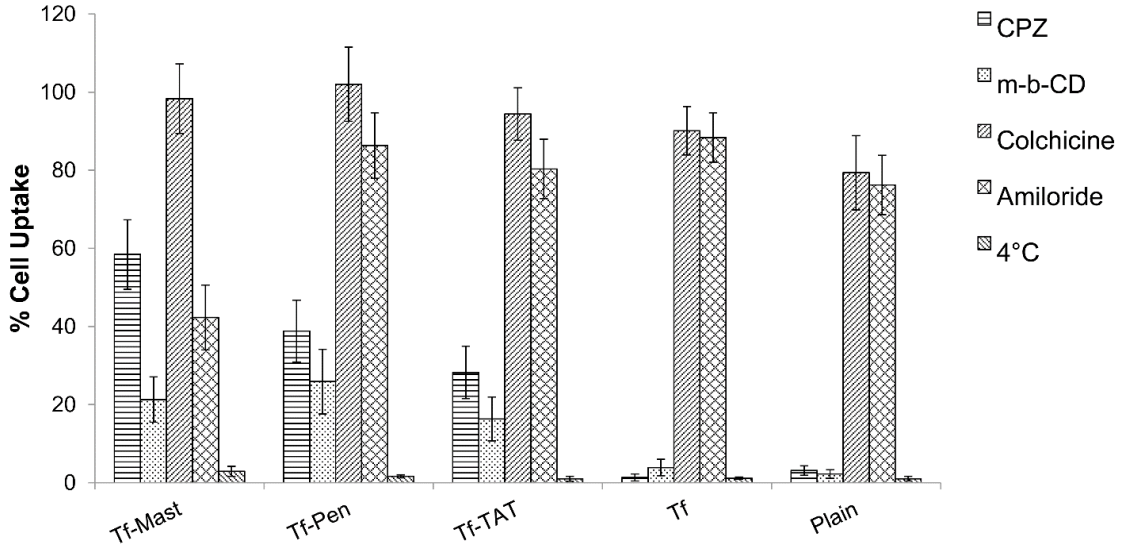

Figure 26. Effect of various inhibitors on the uptake of doxorubicin encapsulating Tf-CPP-liposomes in U87 cells.

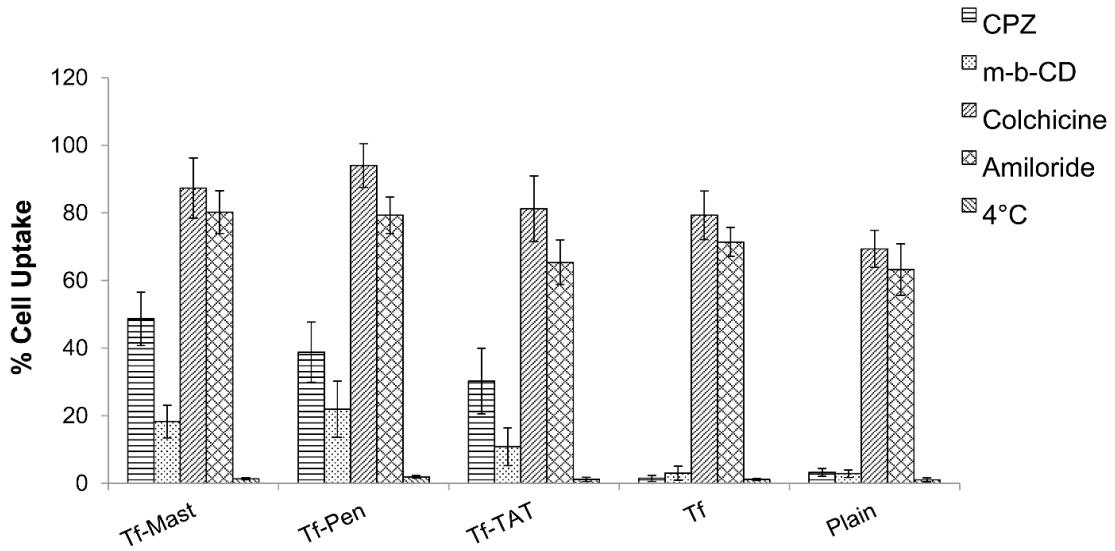

Figure 27. Effect of various inhibitors on the uptake of doxorubicin encapsulating Tf-CPP-liposomes in bEnd3 cells.

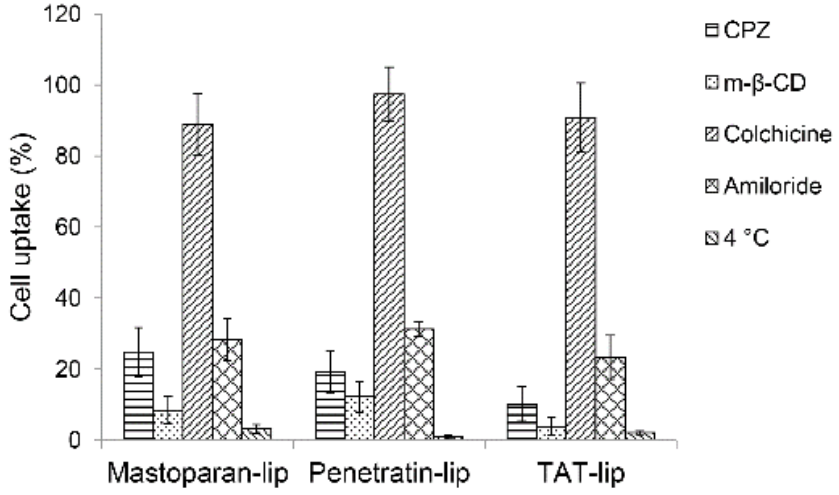

Figure 28. Effect of various inhibitors on the uptake of doxorubicin encapsulating CPP-liposomes in Daoy cells.

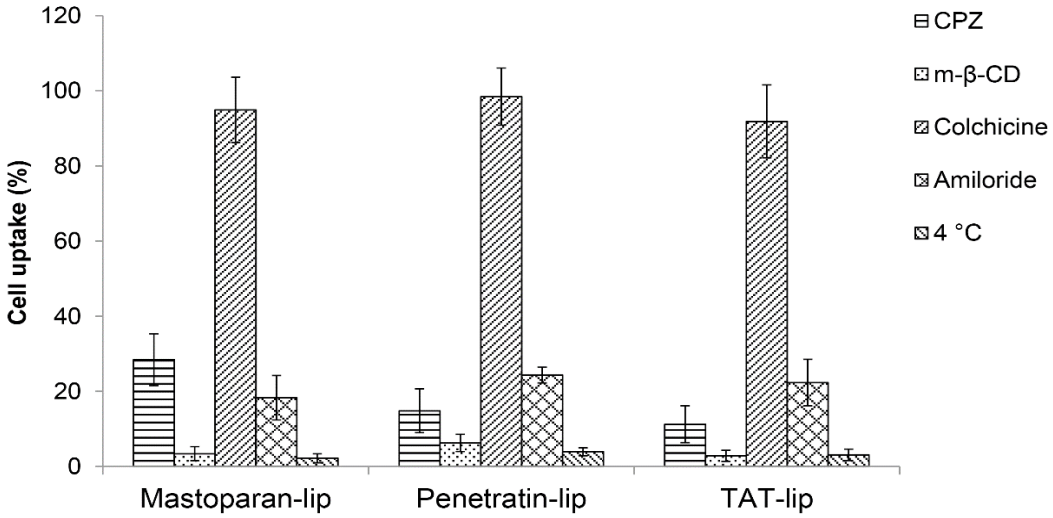

Figure 29. Effect of various inhibitors on the uptake of doxorubicin encapsulating CPP-liposomes in U87.

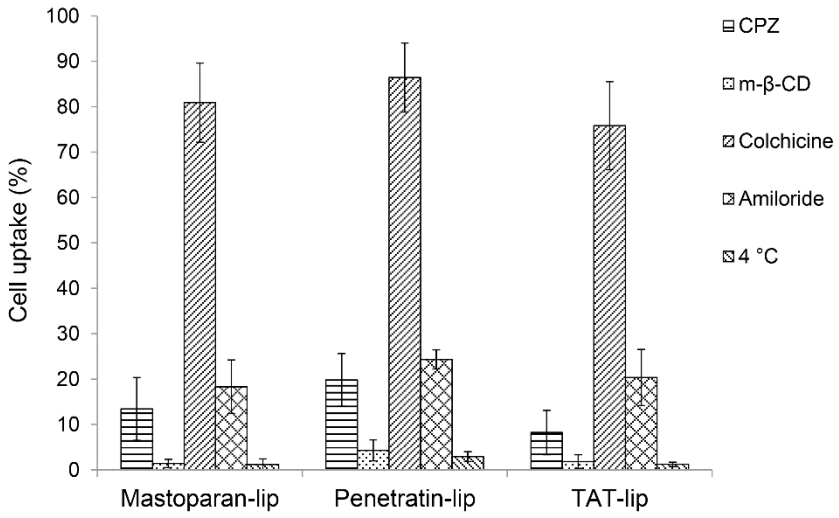

Figure 30. Effect of various inhibitors on the uptake of doxorubicin encapsulating CPP-liposomes in bEnd3.

3.7. *In vitro* transfection potential of liposomes

The designed liposomes were intended to target transferrin receptors, therefore, transfection efficiencies of only transferrin coupled (Tf and Tf-PR) liposomes were compared while plain liposomes were used as passive control. Confocal microscopic imaging showed the highest expression of green fluorescent protein in primary glial cells transfected with Tf-PR-liposomes (Figure 31a). Flow cytometeric evaluation indicated a transfection efficiency of 39.9% for Tf-PR-liposomes, as shown in Figure 31b, which was significantly ($p<0.05$) higher than the transfection efficiency of Tf- liposomes (5.89 %). The plain liposomes demonstrated higher transfection efficiency (11.9%) than Tf-liposomes in primary glial cells which can be explained by the higher zeta potential of plain liposomes in comparison to the Tf-liposomes.

In addition, the dual-functionalized liposomes also showed efficient gene expression in Daoy, U87, and bEnd.3 cells after transfection with liposomes encapsulating either green fluorescent protein or β-galactosidase expressing plasmid (Figure 32 and 33). Maximum transfection levels were obtained using Tf-Penetratin liposomes. The single ligand CPP

liposomes demonstrated lower transfection levels as compared to the Tf-CPP liposomes. Dual-modification increased the cellular translocation of plasmid carrying liposomes and therefore improved the cellular delivery of pDNA. The higher transfection levels of penetratin conjugated Tf-liposomes as compared to other CPP conjugated Tf-liposomes were attributed to the cationic charge and amphiphilicity of Penetratin as compared to the other CPPs.

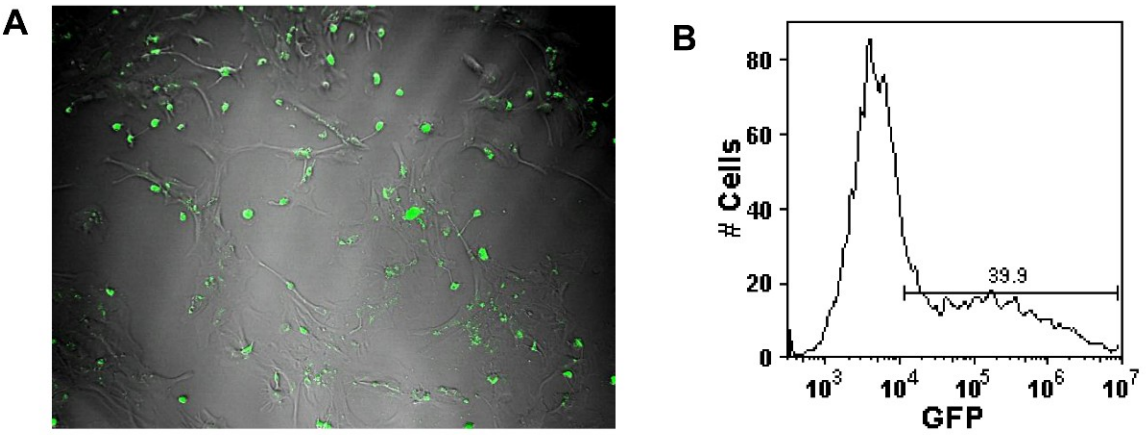

Figure 31. (A) Confocal microscopic images (10x magnification) of primary glial cells transfected with Tf-PR-liposomes encapsulating chitosan-GFP plasmid polyplexes (B) Quantitative evaluation performed using FACS analysis.

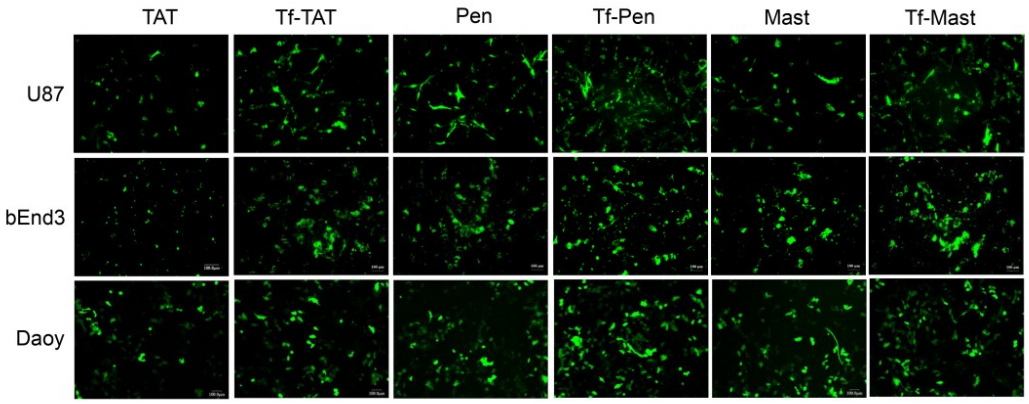

Figure 32. Fluorescence microscopic images of different cells transfected with either TAT, TAT-Tf, Penetratin, Penetratin-Tf, Mastoparan or Mastoparan-Tf liposomes encapsulating gWiz®GFP plasmid.

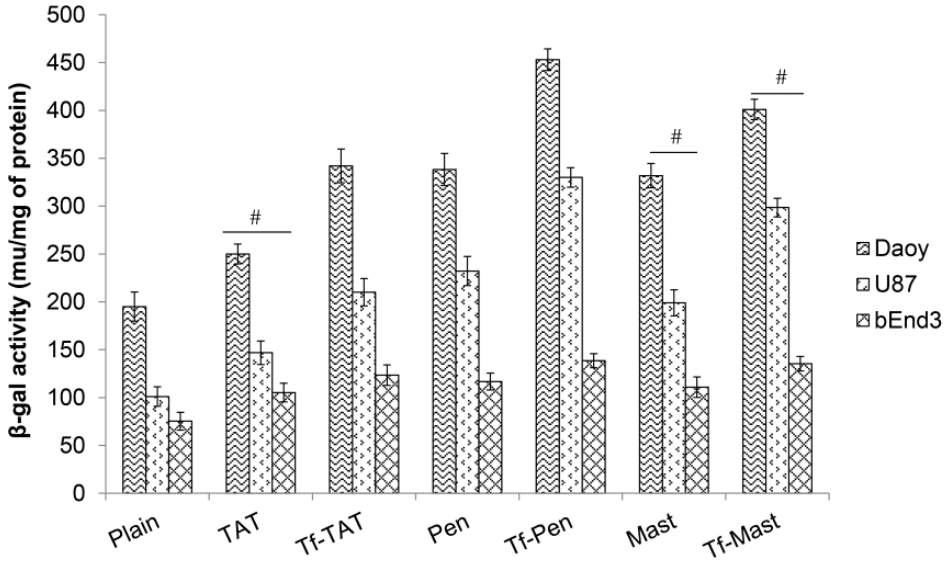

Figure 33. Transfection efficiencies of dual-modified, plain and single-ligand CPP-liposomes in three different cell lines; #p<0.05 versus plain liposomes.

3.8. Evaluation of *in vitro* BBB model

3.8.1. 2D *in vitro* BBB model

3.8.1.1. *In vitro* BBB integrity

The TEER of the both monolayer and co-culture models, was gauged every other day during the incubation period and was observed to increase with increase in the cell densities on the membrane. The TEER value for the co-culture model, as observed on the seventh day of incubation period, was found to be 315 ± 18 Ω cm^2 which was significantly ($p<0.05$) higher than the TEER of 198± 15 Ω cm^2 for the monolayer model. The paracellular permeability for both the models was also monitored correspondingly and the P_e value was found to be significantly ($p< 0.05$) less for the co-culture model as compared to the monolayer model for BBB as shown in Figure 34.

3.8.1.2. Transport of liposomes across *in vitro* BBB

Tf-liposomes and Tf-PR-liposomes showed significantly ($p<0.05$) higher permeability across the barrier layer in comparison to the plain unconjugated and PR-liposomes as shown in Figure 35. Also, permeability of Tf-PR-liposomes (P_e 4.79) was observed to be higher as compared to the Tf-liposomes, thereby validating the incorporation of poly-L-arginine to the liposomes. Assessment of the percent liposomal transport across *in vitro* BBB model, illustrated a similar pattern as observed with the permeability data. The percentage of liposomes transported increased from about 5.4% for plain unconjugated liposomes to approximately 18.9% for Tf-PR-liposomes. Also, transport of Tf-liposomes and PR-liposomes was lesser as compared to Tf-PR-liposomes as shown in Figure 36. Therefore, maximum transport across the barrier layer was achieved using liposomal delivery vector conjugated to both poly-L-arginine and transferrin.

3.8.2. 3D *in vitro* BBB model

3.8.2.1. Evaluation of barrier properties

The scanning electron microscopic (SEM) images confirmed the formation of a porous scaffold and the growth of tumor spheroids inside the pores after approximately 35 days of culture in high serum containing media (Figure 37). The scaffold showed excellent cellular biocompatibility and a considerable improvement in cell growth with time as observed with hematoxylin-eosin staining. Dense growth of overlapping tumor cells was observed on 20μm thick sections of the scaffold on day 35 (Figure 38). The 3D tumor culture was combined with the inserts (0.4μm pore size) carrying brain endothelial cells cultured on the luminal side of the membrane. For 2D BBB model (described above), we observed a significantly lower ($p<0.05$) paracellular transport of Na-F across the *in vitro* BBB model constructed using both bEnd.3 cells and primary glial cells as compared to the model without glial cells. In this study, we observed a

significant reduction in the paracellular transport of Na-F across the bEnd.3 cells on culture inserts combined with glioblastoma tumor scaffolds (P_e = 3.96 x 10^{-6}) as compared to the transport of the fluorescent molecule across the inserts with bEnd.3 cells alone (P_e= 7.93 x 10^{-6}) (Figure 39). However, the paracellular transport across the *in vitro* 3D tumor model was greater than the *in vitro* BBB model with primary glial cells on the underside of the membrane (P_e = 1.98 x 10^{-6}). In addition, the TEER value of the endothelial cell layer cultured with the 3D tumor (226 ± 14 Ωcm^2) was higher than the TEER across the endothelial cell layer cultured alone (192 ± 23 Ωcm^2) but was lower than the TEER across the *in vitro* BBB model with endothelial cells on the upper side and the glial cells on the underside of the membrane (323 ± 16 Ωcm^2).

3.8.2.2. Transport of liposomes across 3D brain tumor model

The transport of dual-functionalized Tf-CPP liposomes was observed to be significantly ($p<0.05$) higher in comparison to the single ligand Tf or CPP liposomes. The transport of plain liposomes was the lowest and was comparable to that of the free drug. Tf-Penetratin liposomes showed the highest endothelial permeability coefficient (P_e = 5.52 x 10^{-6}) which was not significantly different ($p>0.05$) from the Tf-Mastoparan liposomes (P_e= 4.89 x 10^{-6}) (Fig 40). The percentage of liposomes transported increased from approximately 4.2% for TAT to 10.6 % for Tf-TAT liposomes, from 5.4% for Mastoparan to 13.9% of Tf-Mastoparan liposomes, and from 6.5% for Penetratin to 14.9 % for Tf-Penetratin liposomes (Figure 41). Therefore, dual modification considerably improved the transport across the *in vitro* brain tumor model. Additionally, the scaffolds were embedded into Tissue Tek OCT™ compound (Sakura Finetek USA, Inc., Torrance, CA) and sectioned on a cryostat to evaluate the uptake of doxorubicin liposomes by tumor cells growing in a 3D microenvironment (Figure 42). Maximum fluorescence was observed in tumor scaffolds exposed to Tf-Penetratin liposomes. The results

further justified the incorporation of CPP to Tf liposomes and triggering of the dual mechanism of transport via both receptor-mediated transcytosis and improved cell penetration.

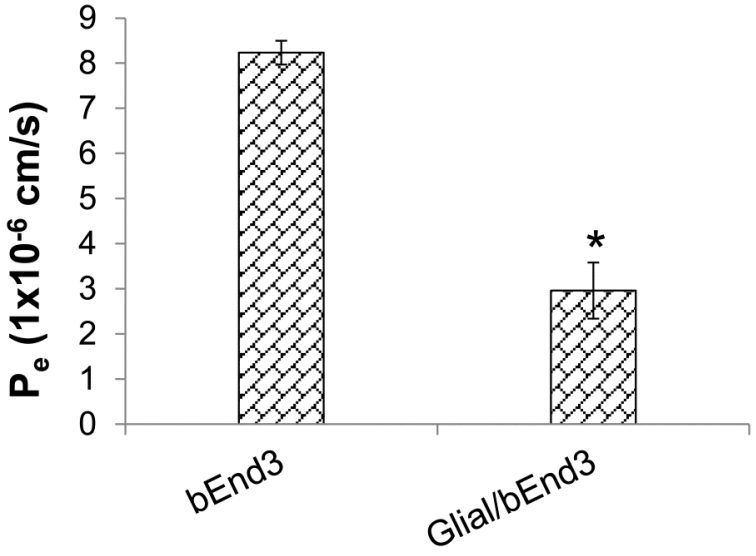

Figure 34. Endothelial permeability coefficient for sodium fluorescein (Na-F P_e, expressed in 10^{-6} cm/s) of blood-brain barrier models.

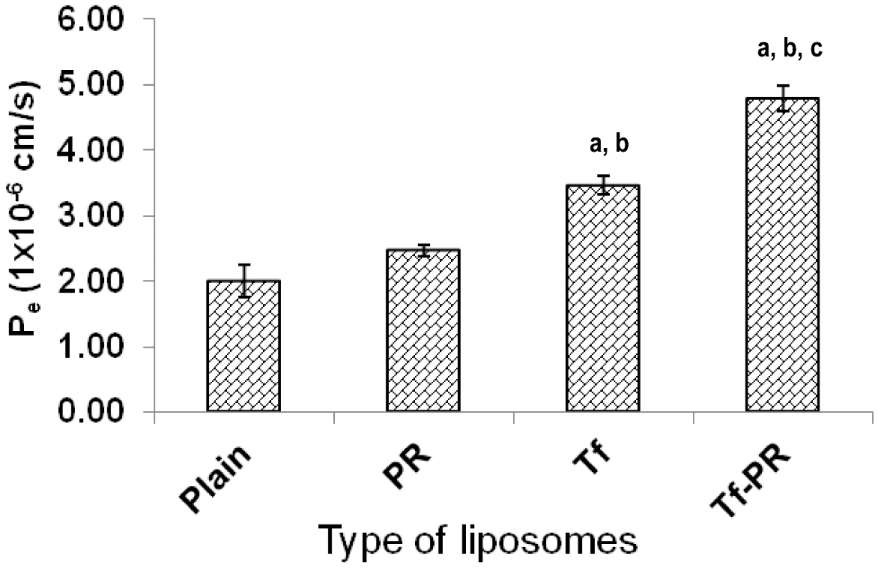

Figure 35. Endothelial cell permeability (Pe, expressed in 10^{-6} cm/s) coefficient for different liposomal formulations; $p<0.05$ versus (a) plain liposomes (b) PR liposomes (c) and Tf-liposomes.

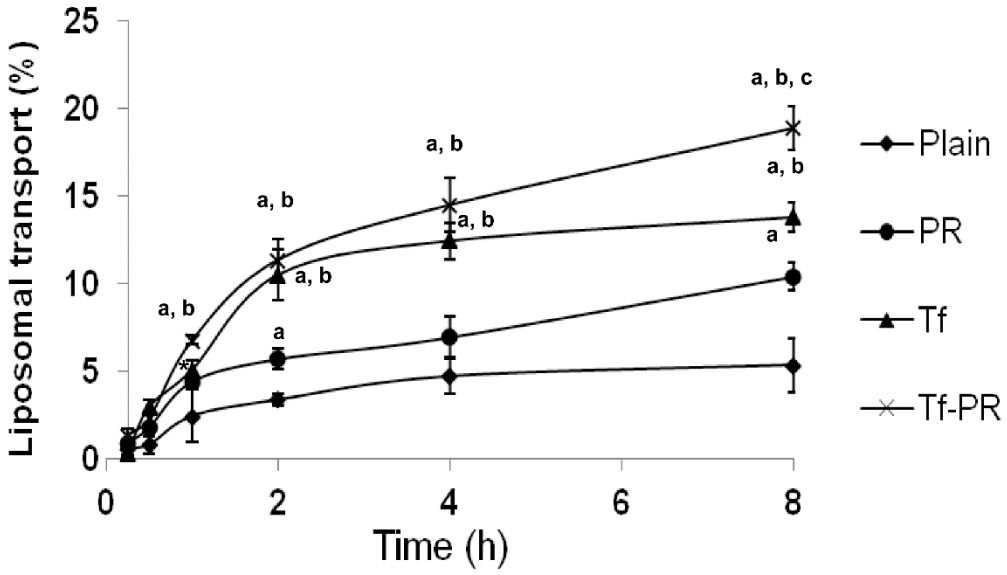

Figure 36. Flux of different liposomes evaluated across *in vitro* BBB model, over 8h; $p<0.05$ versus (a) plain liposomes (b) PR liposomes and (c) Tf-liposome.

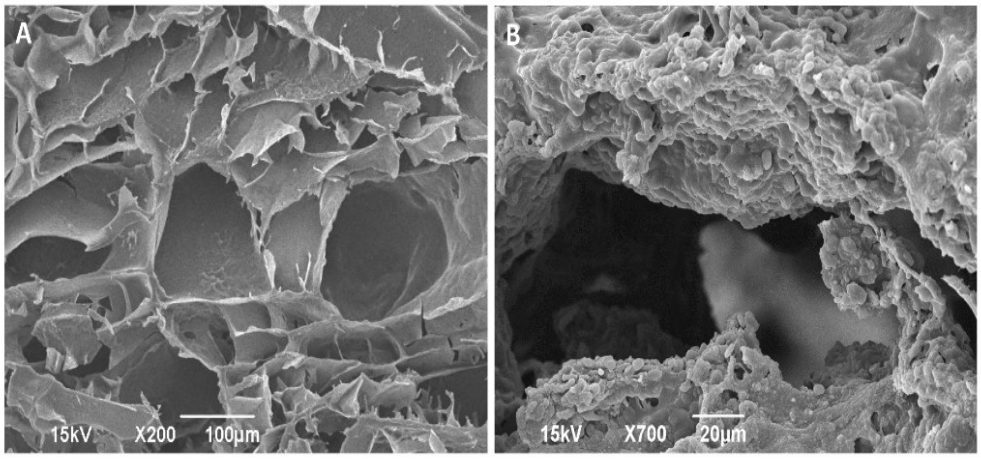

Figure 37. SEM images showing (A) porous structure chitosan-PLGA scaffold and (B) tumor cells growing in a 3 dimensional environment within the pores of the scaffold.

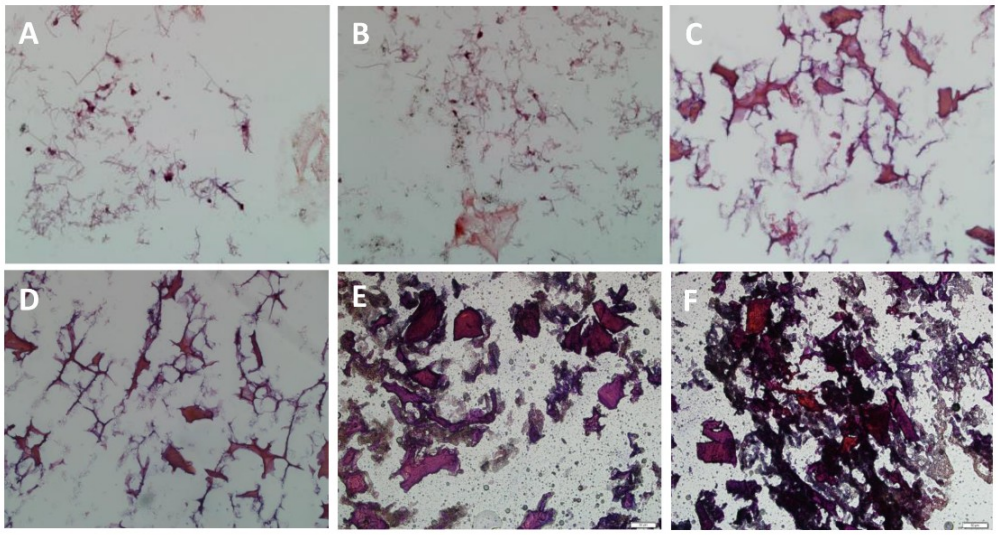

Figure 38. Hematoxylin-eosin staining of 20μm thick sections of scaffolds with tumor cells growing in 3 dimensional environment in the porous scaffold.

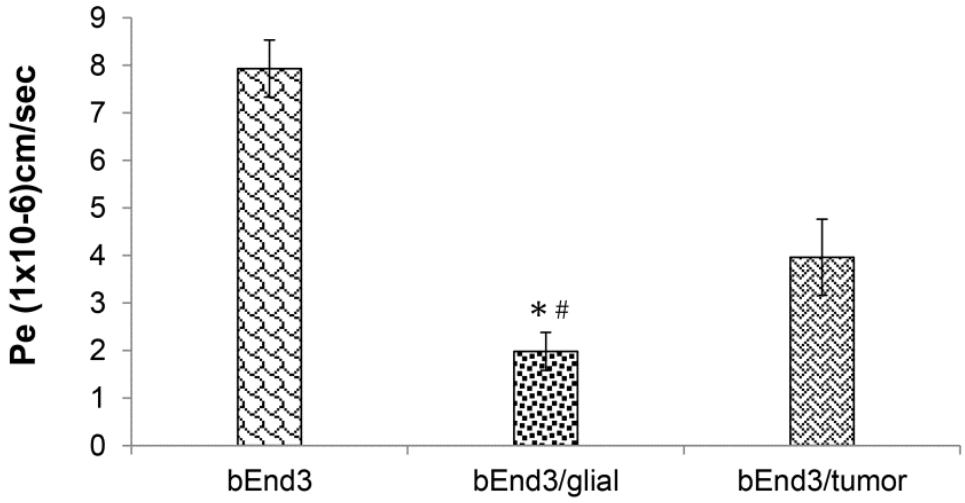

Figure 39. Endothelial cell permeability coefficient for sodium fluorescein (Na–F Pe, expressed in 10^{-6} cm/s) for brain tumor model; $p < 0.05$ versus (*) only bEnd.3 cells and (#) bEnd3/tumor cells on 3D scaffolds.

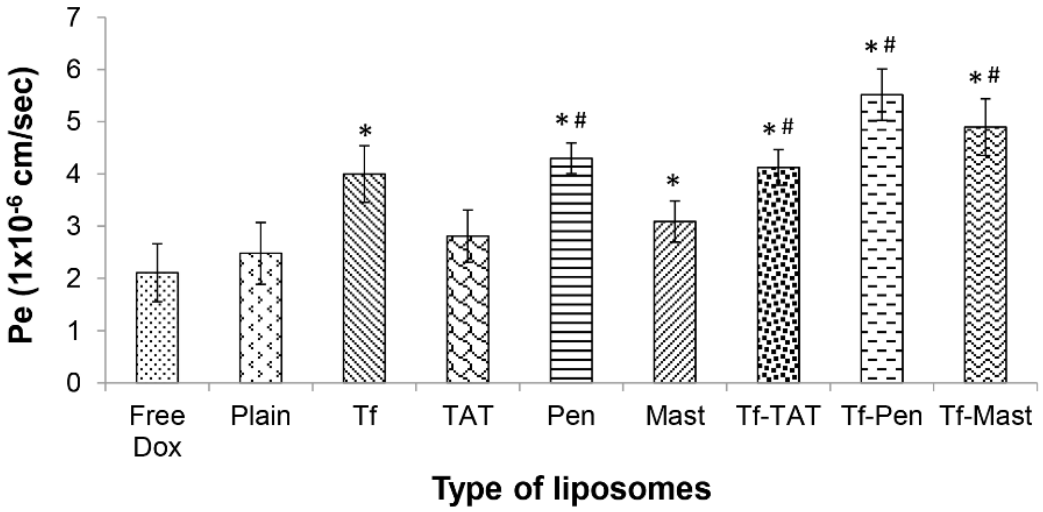

Figure 40. Endothelial cell permeability (Pe, expressed in $1x10^{-6}$ cm/s) coefficient for different liposomal formulations; $p<0.05$ versus free doxorubicin (*) and plain liposomes (#).

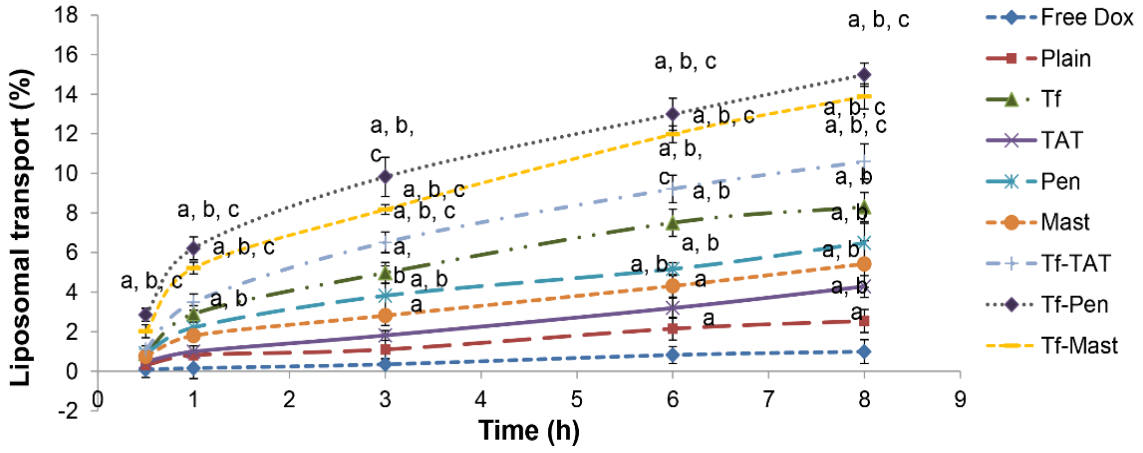

Figure 41. Percent transport of different doxorubicin encapsulating liposomes across *in vitro* brain tumor model, over a period of 8 h; $p<0.05$ versus (a) free drug, (b) plain, (c) Tf.

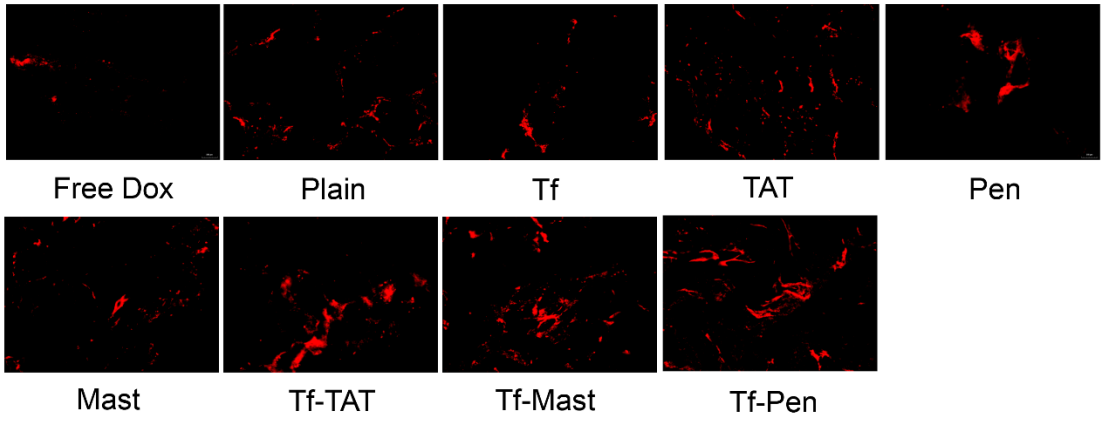

Figure 42. The images show 20µm thick sections of the scaffolds with tumor cells after 8h of liposomal transport

3.9. *In vivo* evaluation of liposomes

3.9.1. Evaluation of Tf-PR-liposomes

3.9.1.1. Biodistribution

The biodistribution of DiR-labeled liposomes was tracked using NIR imaging of various organs at different time points. Considering the previous report demonstrating poor transport of PR-liposomes across *in vitro* BBB model (Sharma et al. 2012) and due to the absence of the targeting ligand, transferrin, PR-liposomes were not evaluated for distribution *in vivo*. Plain liposomes were used as passive control for evaluating the biodistribution of DiR-labeled phospholipid liposomes. Quantitative estimation of liposomal distribution (Figure 43a-f) showed maximum accumulation of fluorescently labeled liposomes in the spleen and liver, 12h post intravenous injection. The amount of liposomes (%ID/ gram of tissue) in different organs decreased at increasing time intervals. A more rapid decrease in fluorescence intensity of plain liposomes was observed, in different tissues, with time as compared to the Tf and dual-modified liposomes thus indicating a higher clearance of plain liposomes from circulation. The decrease in the concentration of Tf-liposomes was less in liver, spleen and kidneys as compared to the plain and dual-modified liposomes thus indicating increased circulation and lower elimination of Tf-

liposomes by the macrophage system. The dual-modified liposomes accumulated more in lungs and heart as compared to other liposomes. The liposomes were transported to lungs and were gradually eliminated with time. Presumably, the cationic charge of Tf-PR-liposomes also increased their penetration in the highly perfused heart. Also, the occurrence of a cell penetrating peptide on the transferrin receptor targeted liposomes resulted in eight fold greater penetration of Tf-PR-liposomes into brain in comparison to plain liposomes and two fold greater than the Tf-liposomes. The results from *ex vivo* imaging of organs (Figure 44) showed that the fluorescence intensity of dual modified liposomes in the brain was stronger as compared to either plain or Tf-liposomes and maximum fluorescence was observed after 24h of liposomal administration. Also, the fluorescence decreased 72h post intravenous injection. The decrease in fluorescence in various organs with time might be explained by increased elimination of liposomes from the body with time (MacKaya et al. 2005).

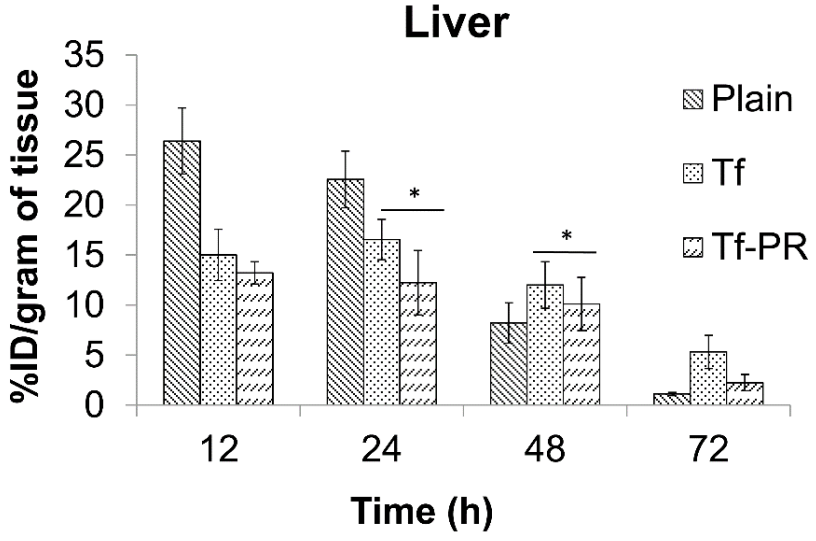

Figure 43. Distribution of liposomes in liver at different time points, expressed as percent injected dose (ID)/gram body weight; *$p<0.05$ versus plain liposomes.

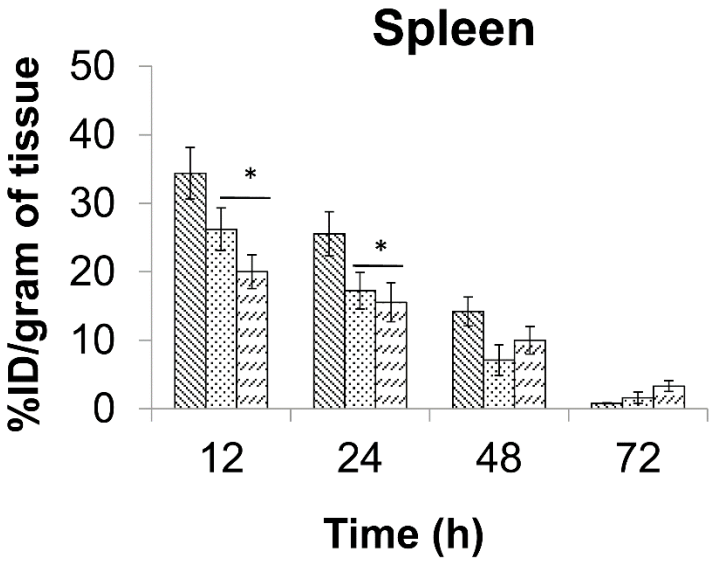

Figure 44. Distribution of liposomes in spleen at different time points, expressed as percent injected dose (ID)/gram body weight; *p<0.05 versus plain liposomes.

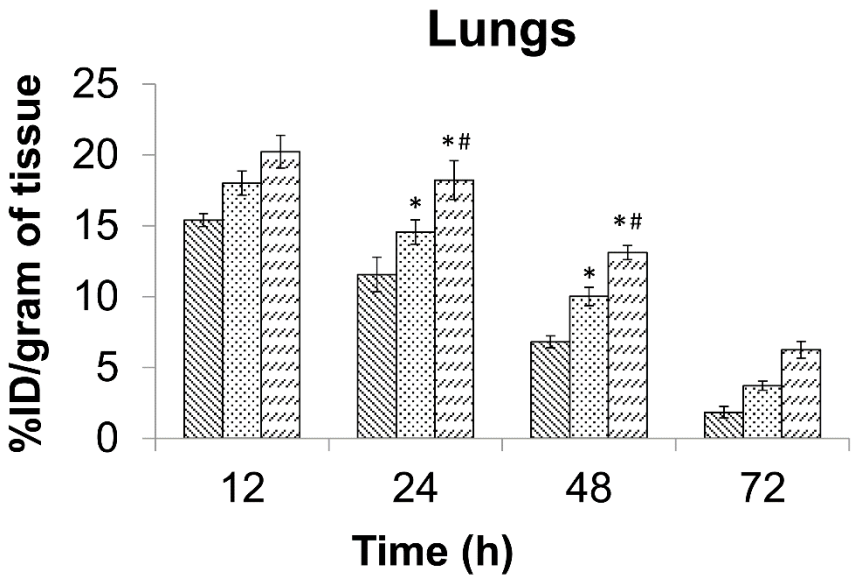

Figure 45. Distribution of liposomes in lungs at different time points, expressed as percent injected dose (ID)/gram body weight; p<0.05 versus (*) plain and (#) Tf-liposomes.

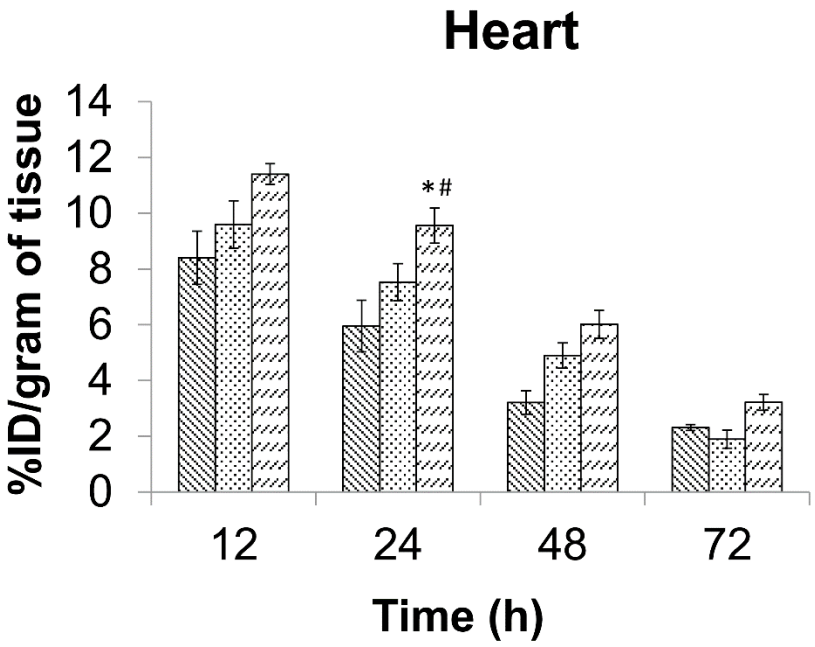

Figure 46. Ddistribution of liposomes in heart at different time points, expressed as percent injected dose (ID)/gram body weight; $p<0.05$ versus (*) plain and (#) Tf-liposomes.

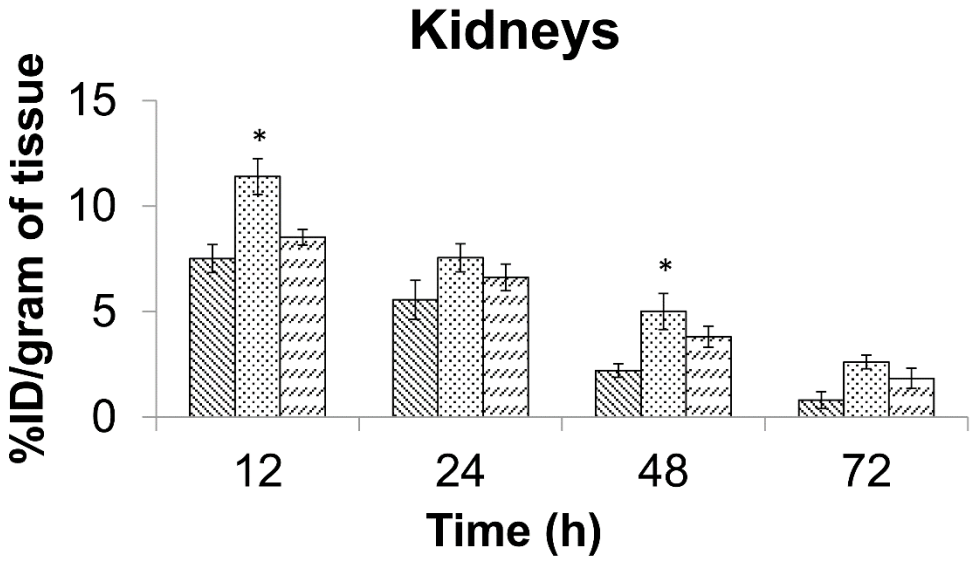

Figure 47. Distribution of liposomes in kidneys at different time points, expressed as percent injected dose (ID)/gram body weight; *$p<0.05$ versus plain liposomes.

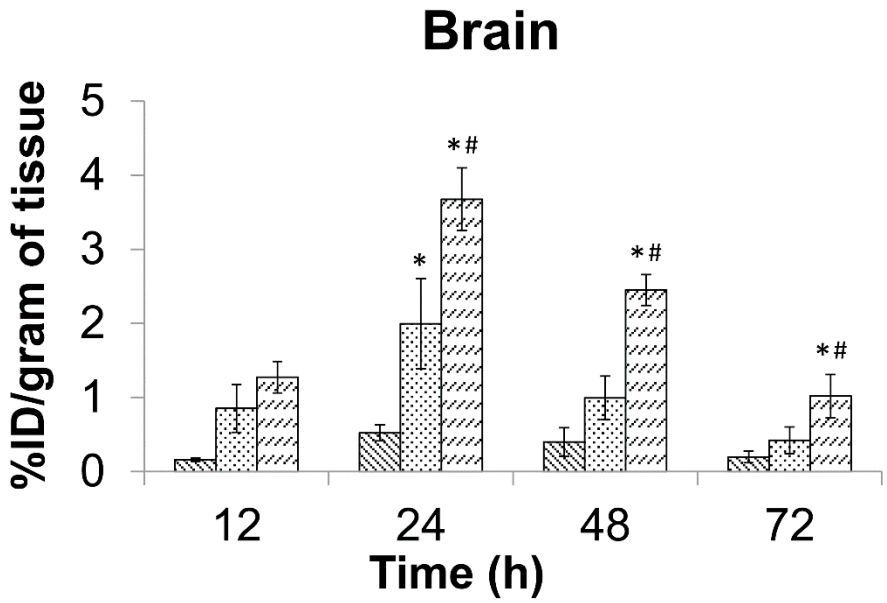

Figure 48. Distribution Distribution of liposomes in brain at different time points, expressed as percent injected dose (ID)/gram body weight; $p<0.05$ versus (*) plain and (#) Tf-liposomes.

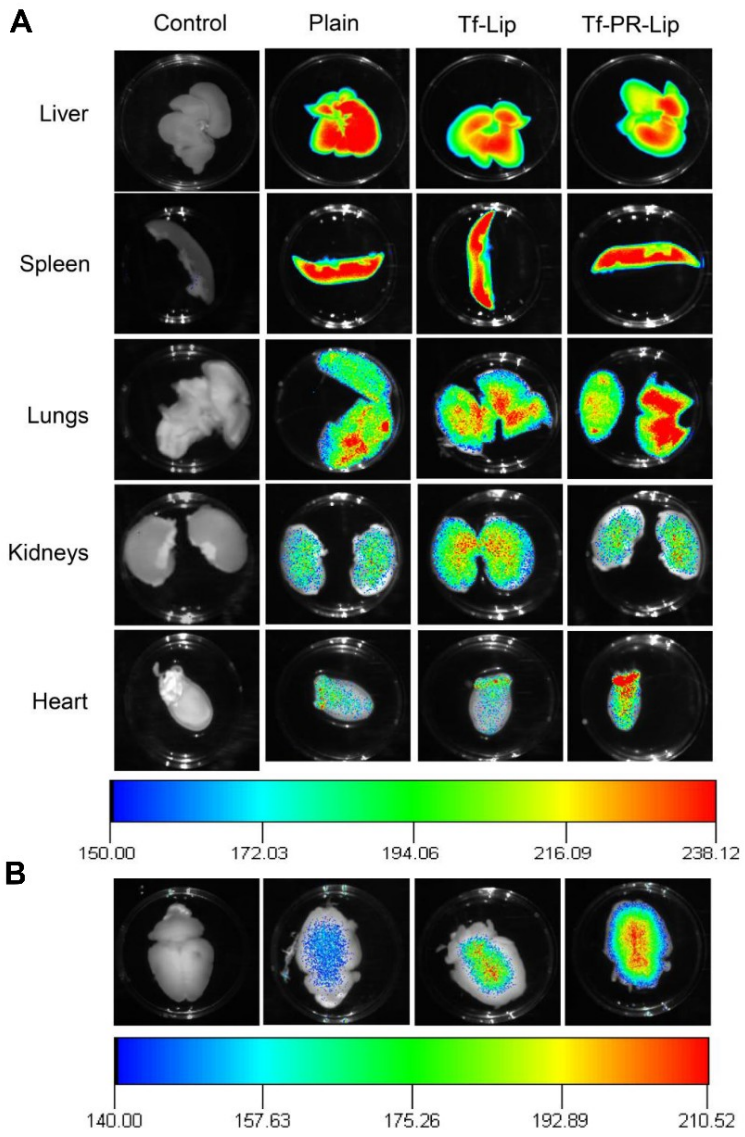

Figure 49. (A) *Ex vivo* imaging of different organs isolated from rats at 24h post intravenous injection (exposure time 2 min). (B) *ex vivo* imaging of brains isolated from rats at 24h time point (exposure time 8 minutes).

3.9.1.2. Transfection potential

The β-gal activity of the tissues was determined using the β-gal assay kit. The dual-modified liposomes demonstrated significantly ($p<0.05$) higher levels of enzyme activity in brain (1.49± 0.22mU/mg of protein) as compared to the single-ligand liposomes (0.90± 0.21mU/mg of protein) or naked DNA (0.65 ± 0.13 mU/mg of protein) (Figure 45). The Tf-PR-liposomes also

showed higher levels of enzyme activity in different organs (Figure 46) e.g. liver and spleen. The enzymatic activity varied from 23.38 ± 2.58 mU/mg of protein in spleen, 12.67±2.98 mU/mg of protein in liver, 9.73±1.9 mU/mg of protein in lungs, 6.43± 1.91 mU/mg of protein in kidneys to 4.54 ±1.3 mU/mg of protein in heart using the dual-modified liposomes. The levels of enzyme activity in these organs were observed to be comparatively low with the Tf-liposomes varying from 16.9 ± 1.98 mU/mg of protein in spleen, 9.29 ±2.33 mU/mg of protein in liver, 4.43 ±1.99 mU/mg of protein in lungs, 4.48 ± 1.76 mU/mg of protein in kidneys to 2.32 ± 0.81 mU/mg of protein in heart. In addition, the enzyme activity induced by naked DNA in different tissues was close to the endogenous activity of the corresponding tissue thereby indicating practically no transfection with plasmid DNA alone.

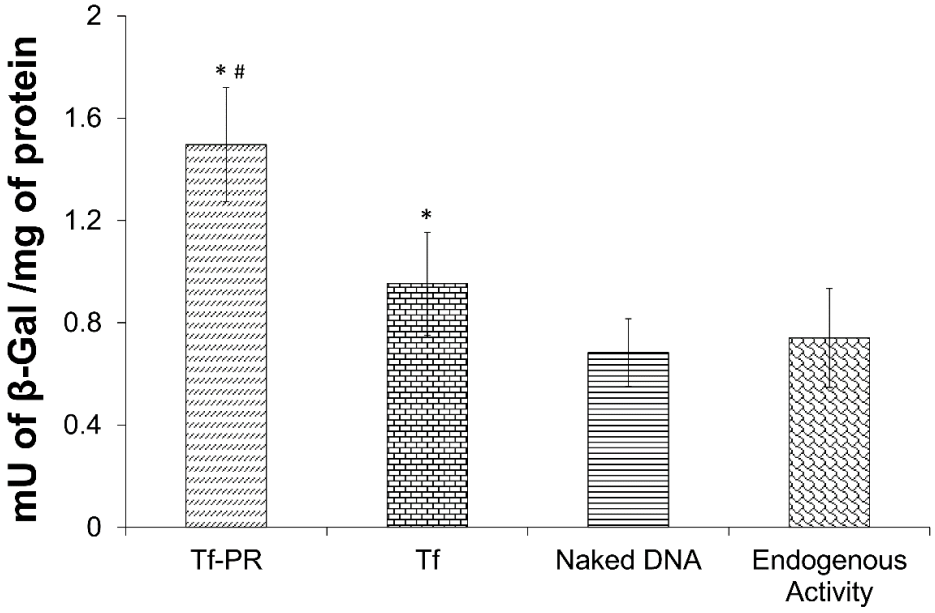

Figure 50. Comparison of transfection efficiencies of dual-modified and conventional Tf-liposomes in brain after intravenous injection of β-gal plasmid encapsulating liposomes; $p<0.05$ versus (*) naked DNA, (#) Tf-liposomes.

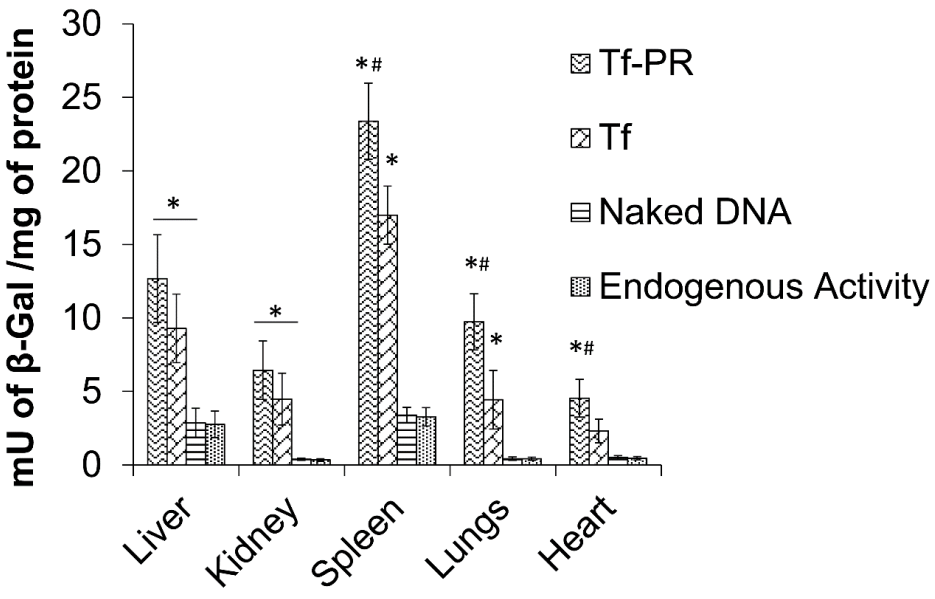

Figure 51. Comparison of transfection efficiencies of dual-modified and conventional Tf-liposomes, in different organs after intravenous injection of β-gal plasmid encapsulating liposomes; $p<0.05$ versus (*) naked DNA, (#) Tf-liposomes.

3.9.1.3. Tissue biocompatibility

Cell penetrating peptides have been reported to cause toxicity in highly perfused organs like lungs, heart, kidneys and liver due to their non-specific interaction and higher penetration in tissues (Ramana et al. 2010).The histological examination of transfected tissues facilitated the evaluation of *in vivo* biocompatibility of liposomal formulations. The tissue sections from the animals administered with PBS were used as control. Hematoxylin-eosin staining of the transfected tissue sections revealed no alterations in the morphological appearance of the tissues. Tissue sections from different organs did not show any necrosis, inflammation or enlargement of nuclei (Figure 47) and were comparable to the tissue sections obtained from control animals. Since the biodistribution studies demonstrated higher accumulation of liposomes in liver and spleen, these organs were carefully examined for any histological changes. No ballooning of hepatocytes or signs of inflammation were observed in the liver sections and no signs of necrosis

were evident in the tissue sections obtained from spleen at the administered dose of liposomes (15.2 μmoles of phospholipids/kg body weight). There were no signs of toxicity in the tissue sections up to a dose of 20 μmoles of phospholipids/kg body weight. Also, in our pilot studies, we evaluated the transfection efficiency and tissue histology after 48 h (based on *in vitro* transfection studies) of the intravenous administration of liposomes. No inflammation or tissue necrosis was observed at this time point or later.

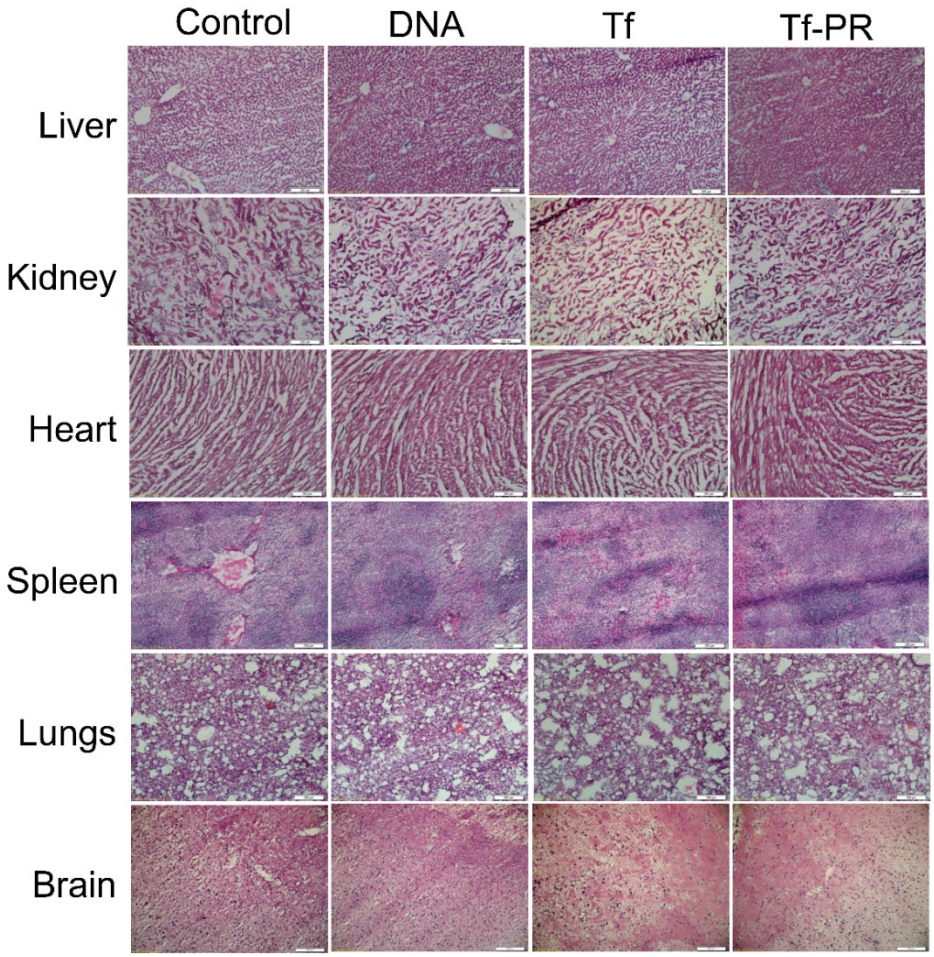

Figure 52. Histological examination of different tissues after transfection with β-gal plasmid encapsulating liposomes.

3.9.2. Biodistribution of Tf-CPP liposomes

Considering the poor transport of CPP-liposomes across the *in vitro* brain tumor model, these liposomes were not evaluated for *in vivo* transport to brain. Doxorubicin loaded plain liposomes were used as a passive control. HPLC analysis of tissue samples indicated maximum accumulation of Tf conjugated liposomes in the spleen and liver 12h post intravenous administration (Figure 48a-g). The %ID (percent injected dose) of the liposomes per gram of tissue decreased with increasing time intervals in all organs. Free doxorubicin and plain liposomes were eliminated more rapidly from the liver and spleen as compared to the Tf-CPP liposomes. Tf-Mastoparan liposomes showed a higher elimination from the major macrophage organs including the liver and spleen as compared to Tf-TAT or Tf-Penetratin liposomes. Tf-Penetratin liposomes were transported more to the heart and their elimination from heart was slower as compared to the other liposomes. The transport of Tf-Mastoparan liposomes to the lungs was slightly higher as compared to the Tf-Penetratin liposomes, nevertheless, the elimination of Tf-Mastoparan liposomes was more rapid than the Tf-Penetratin liposomes. Previous studies reported greater interaction of cationic polymers and CPPs with the blood cells and their subsequent accumulation in lungs (Sharma et al. 2013; Kibria et al. 2011). In this study, approximately 10-15% of the dual-functionalized liposomes were transported to the lungs after 24h. The elimination of negatively charged Tf-liposomes was slower from liver, spleen and kidneys as compared to plain or dual-functionalized liposomes. The dual-functionalized, Tf-Penetratin liposomes showed maximum brain penetration after 24h (~3.67% ID/gram of tissue) followed by the Tf-TAT liposomes (~2.89% ID/gram of tissue). The accumulation of Tf-Mastoparan liposomes was lower as compared to the other Tf-CPP liposomes in brain.

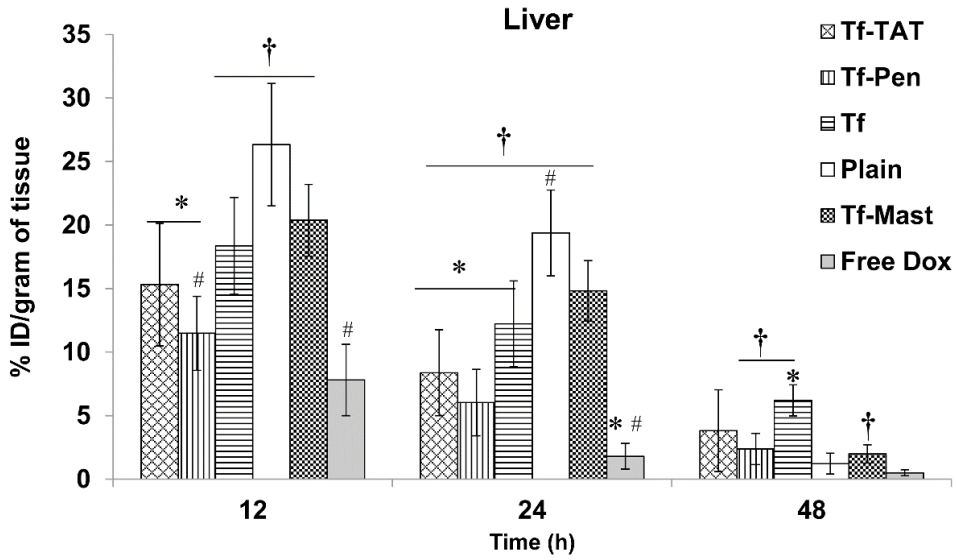

Figure 53. Distribution of doxorubicin containing liposomes in liver at various time points; $p<0.05$ versus (†) free doxorubicin, (*) plain and (#) Tf liposomes.

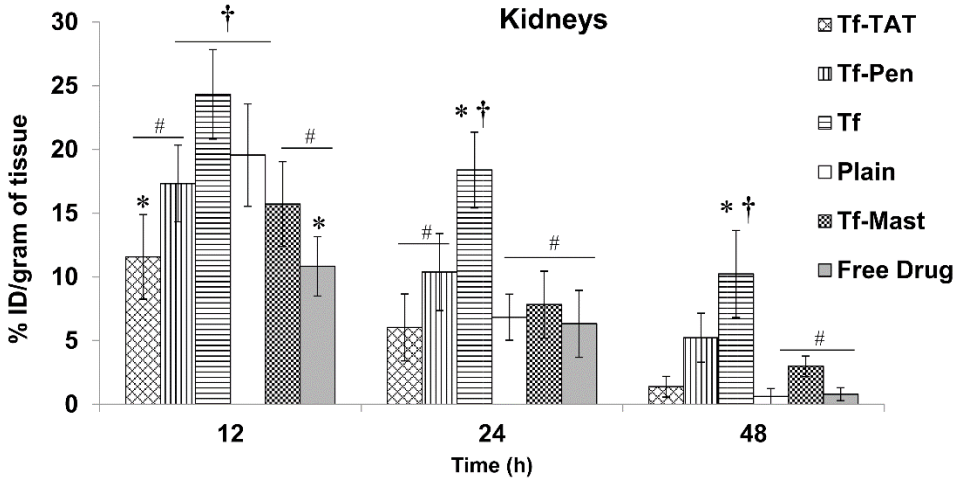

Figure 54. Distribution of doxorubicin containing liposomes in kidneys at various time points; $p<0.05$ versus (†) free doxorubicin, (*) plain and (#) Tf-liposomes.

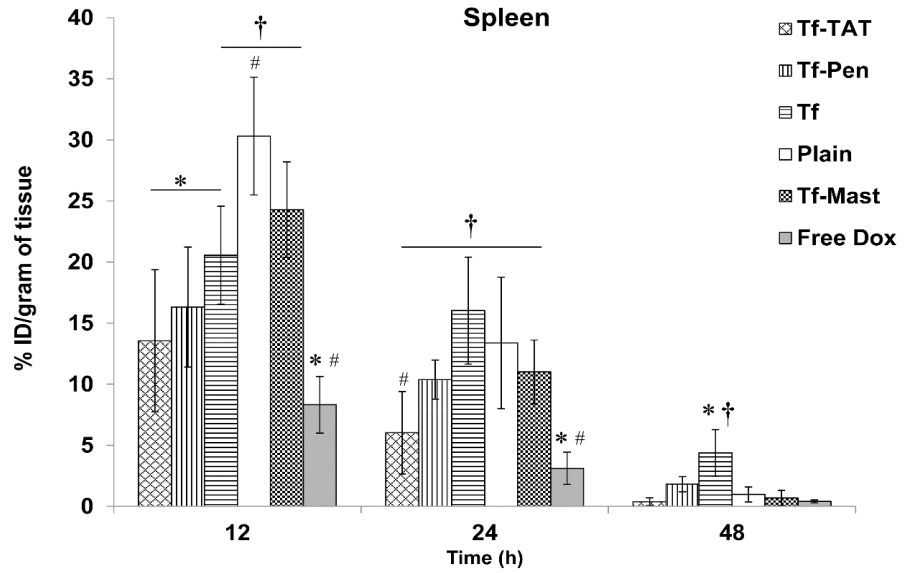

Figure 55. Distribution of doxorubicin containing liposomes in spleen at various time points; $p<0.05$ versus (†) free doxorubicin, (*) plain and (#) Tf-liposomes.

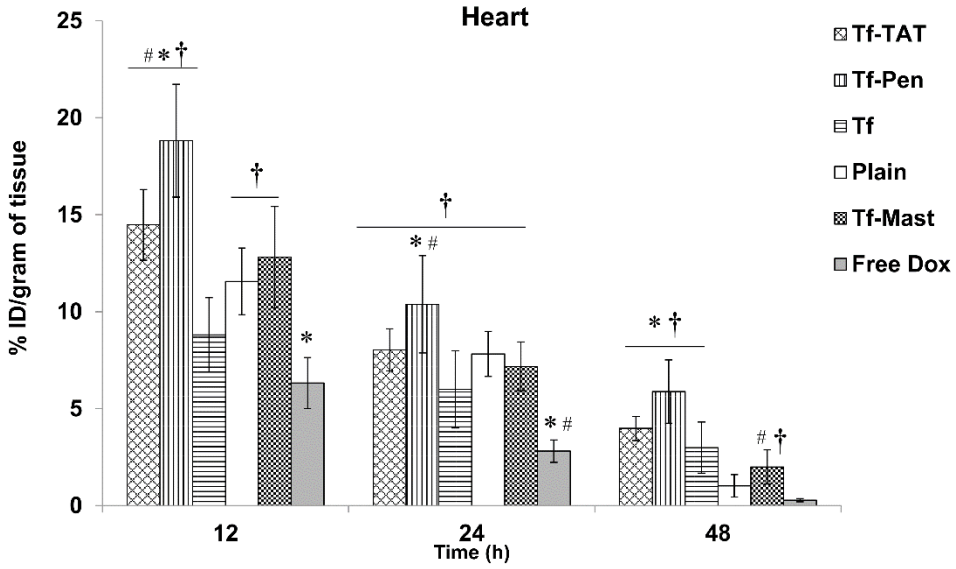

Figure 56. Distribution of doxorubicin containing liposomes in heart at various time points; $p<0.05$ versus (†) free doxorubicin, (*) plain and (#) Tf-liposomes.

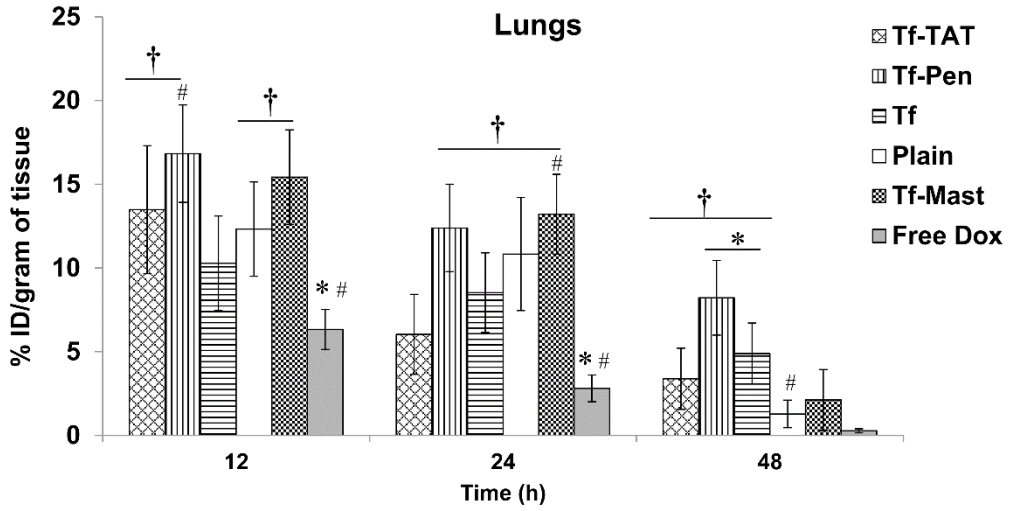

Figure 57. Distribution of doxorubicin containing liposomes in lungs at various time points; $p<0.05$ versus (†) free doxorubicin, (*) plain and (#) Tf-liposomes.

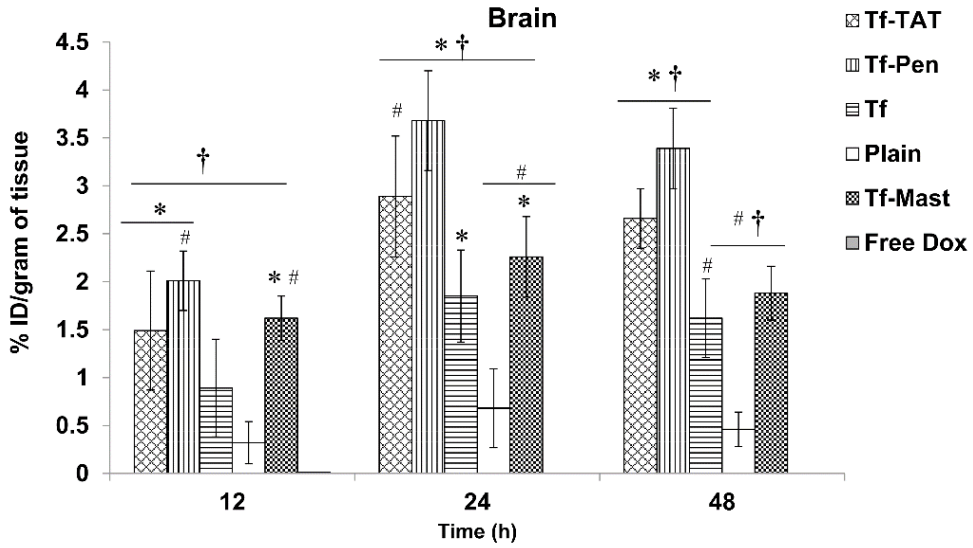

Figure 58. Distribution of doxorubicin containing liposomes in brain at various time points; $p<0.05$ versus (†) free doxorubicin, (*) plain and (#) Tf-liposomes.

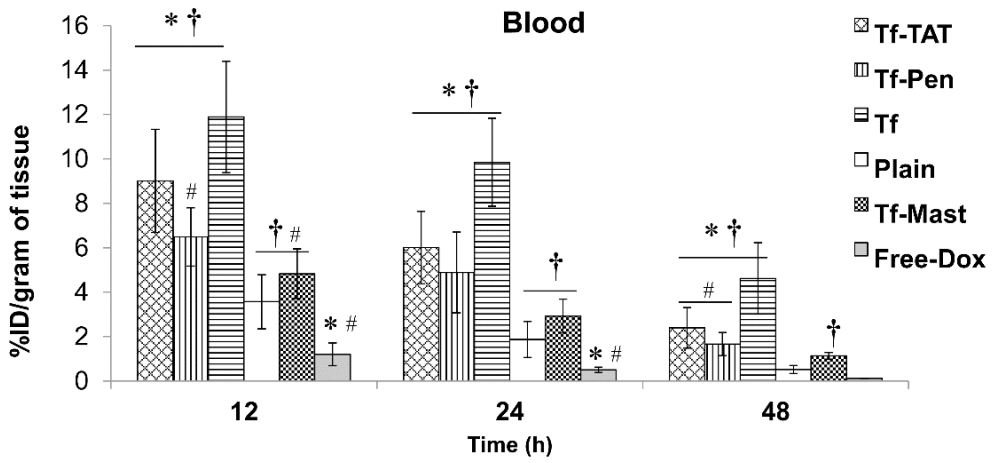

Figure 59. Distribution of doxorubicin containing liposomes in blood at various time points; $p<0.05$ versus (†) free doxorubicin, (*) plain and (#) Tf-liposomes.

CHAPTER IV. DISCUSSION

Targeted delivery vectors can be administered systemically without causing physiological disruption of the BBB (Huwyler et al. 1996; Pardridge et al. 1985). The application of sterically stabilized Tf receptor targeted nanoparticles, for delivery to the brain, after parenteral administration has become well established over the past years (Sharma et al. 2013; Zhong et al. 2002; Cheng et al. 2004).However, receptor saturation has been identified as the major challenging factor that limits the transport of molecules via receptor targeted systems (Sharma et al. 2012; Kibria et al. 2011). In addition, the endocytic uptake of these nanoparticulate drug carriers eventually leads to lysosomal degradation (Varga et al. 2000; Gupta et al. 2005). This research work is focused on developing novel dual-modified delivery systems for therapeutic agents (small molecule drugs and genes). The liposomes were conjugated to transferrin protein for targeting the transferrin receptors on BBB. In addition, the liposomes were conjugated to various cell penetrating peptides to improve the penetration of molecules into the targeted tissue. Surface modification of liposomes with CPPs facilitates endosomal escape and increases their cellular delivery (Bolhassani 2011). The mechanism of internalization of these peptides is greatly dependent on the CPP used, the concentration, the type of cell line, and cargo carried. Although it is now known that the uptake of CPPs is mediated both via endocytic and non-endocytic pathways, the exact mechanism of cellular uptake still remains controversial. We investigated the influence of various cell penetrating peptides on internalization of transferrin receptor targeted liposomes and their mechanism of uptake by different cell lines. The rationale for using these peptides was based on the difference in proportion of hydrophilic, amphiphilic, and hydrophobic amino acid residues in these three CPPs. Poly-L-arginine consists of all hydrophilic arginine acid residues, TAT peptide consists of more hydrophilic amino acids as compared to hydrophobic

amino acids, Penetratin has almost an equal proportion of hydrophilic and hydrophobic amino acids while Mastoparan consists of more hydrophobic amino acid residues.

4.1. Physical characterization of liposomes

We designed novel liposomal vectors combining the effects of receptor targeting and improved cell penetration. Using the AFM technique, we visualized the spherical shape of evenly dispersed nanosized liposomes clearly, both with and without conjugation of Tf and PR. The existence of PEG chains on the surface of the liposomes inhibited aggregation of the vesicles in spite of the near-neutral zeta potential values. Tf was conjugated to the liposomes via post-insertion technique. This simple, effective, and flexible method for preparing ligand-conjugated liposomes allows insertion of biologically active ligand proteins into preformed drug or gene-loaded liposomes (Iden and Allen 2001). The conventional method of incorporating a functional lipid to the liposomal bilayer followed by coupling of a protein is accompanied with the possibility of leaving untreated functional groups or traces of coupling reagents on the inside of the bilayer, thus exposing the encapsulated agent to chemical reagents (Moreira 2002). In this study, PEG–lipid–Tf was inserted into preformed PR liposomes encapsulating the desired gene using simple stirring at room temperature. The coupling efficiency of Tf with PR or CPP liposomes was observed to be slightly (non-significantly) less than with the plain liposomes. This was attributed to the presence of PEG-conjugated PR/CPPs in the preformed liposomes that resulted in a decrease in the equilibrium shift of PEGylated Tf from the micellar phase to the liposomal bilayer.

Liposomes, being uniformly dispersed nano-sized vesicles, can be classified as colloidal suspensions. The size and charge of a colloidal suspension are important factors controlling its stability during storage. Large sized colloidal suspensions with neutral charge tend to become

unstable and gradually agglomerate (duPlessis et al. 1996). As previously discussed, the liposomal vesicles were synthesized to possess near neutral charge (Sharma et al. 2012)which emphasizes the significance of monitoring the stability of liposomes during storage and under simulated *in vivo* conditions. The stability of the liposomes was examined at 4°C for 30 days and in the presence of serum (10% FBS) at 37°C for 60 min. The occurrence of a stearic stabilizer, polyethylene glycol (PEG), reduced aggregation and improved the stability of near neutral liposomes during prolonged storage and in the presence of serum at 37°C. In addition, the presence of a negatively charged protein, transferrin balanced the cationic charge of CPP and further reduced the destabilization of liposomes by decreasing the non-specific binding of serum proteins with the cationic peptide. The liposomes were observed to be stable and showed no significant change ($p>0.05$) in size and zeta potential values under the tested conditions (Table 5). Since the liposomes were intended to deliver the desired gene to the target tissue, therefore we evaluated the pDNA encapsulation and release profile of the liposomes under storage at 4°C and under biologically relevant conditions, in the presence of 10% serum at 37°C. The liposomes demonstrated stable encapsulation of the pDNA at 4 °C for 30 days. Also, approximately 20% of the DNA was released from the dual-modified and plain liposomes after incubation at 37 °C for 7 days in the presence of serum. The release of pDNA from Tf-liposomes was about 30% and was not significantly different ($p>0.05$) from the percent DNA release from plain and Tf-PR liposomes. However, since the encapsulation efficiencies were not significantly different for different liposomes, therefore the slight increase in the release of pDNA from the negatively charged Tf-liposomes can be attributed to greater displacement of the released DNA from Tf-liposomes by serum proteins (Xu et al. 1996). The PR-liposomes showed a release of about 18% after incubation at 37°C for 7 days. No significant ($p>0.05$) difference in the Doxorubicin

encapsulation efficiencies of dual-functionalized liposomes was observed, however, the loading of plain and CPP modified liposomes was slightly higher (non-significantly) than the dual-functionalized liposomes. This might be due to the interference in the transport of drug molecules into preformed liposomes, via pH gradient loading, due to the presence of transferrin protein on the surface. In addition, the Tf-CPP liposomes showed less than 31% of the drug leakage after 12 h of incubation in PBS (pH 7.4) in the presence of serum, at 37°C (Figure 3). The percent cumulative release of the drug was greater with plain liposomes as compared to the Tf and Tf-CPP liposomes. This was due to the presence of negatively charged protein, transferrin, which reduced the interaction of the Tf and Tf-CPP liposomes with serum proteins. Also, the higher positive charge of Penetratin contributed to greater interactions of the Tf-Penetratin liposomes with the serum proteins and therefore, a greater release (non-significant) of the encapsulated drug as compared to the other Tf-CPP liposomes.

4.2. *In vitro* biocompatibility of liposomes

The efficiency of the delivery vector lies not only in its ability to carry the encapsulated agent intothe desired cells but also in its biocompatibility atthe concentrations used. The cytotoxic potential of liposomes, at varying concentrations, was evaluated *in vitro*. BBB is composed of tightly packed endothelial cells supported by the surrounding glial cells that aid in the induction and maintenance of tight junction barrier (Malina et al. 2009; Tontsch et al. 1991). Since, the liposomes were intended for delivery across BBB; hence, we initially evaluated the biocompatibility of Tf-PR-liposomes in both glial and brain endothelial cells for finding an optimized concentration for further assessment of cellular uptake and transfection efficiency. In addition, we assessed the cytotoxicity of Tf-CPP-liposomes, using MTT assay in Daoy, U87, and bEnd.3 cells. The rationale for selecting these tumor cell lines was based on the incidence and

severity of these tumors in the human population which directly relates to the need for establishing a successful treatment strategy for these tumors. Glioblastoma multiforme is the highest grade of astrocytic tumors and is associated with very low survival rates (Krex et al. 2007). Also, medulloblastoma is a rapidly growing high grade tumor and is the most common type of embryonal tumors (McNeil et al. 2002).

Tf-PR liposomes showed a cell viability of about 84% in endothelial cells and 81%in primary glial cells (Figures 5 and 6). The PR liposomes demonstrated lowest biocompatibility, which was attributed to the positive charge of PR. A decrease in the viability was observed with increasing concentration of phospholipids, which was ascribed to the presence of cationic lipids forming liposomes and positively charged peptide on the liposomal surface. An acceptable balance between transfection efficiency and biocompatibility of bifunctional liposomes was achieved at a concentration of 100 nM. The liposomes showed low transfection efficiencies at concentration below 100 nM. The liposomes were, therefore, used at 100 nM concentration for further *in vitro* studies. Also, the dual-functionalized Tf-CPP-liposomes were highly biocompatible, however, the liposomes considerably increased the cytotoxic potential of the anticancer drug, doxorubicin. The Tf-PR liposomes showed efficient biocompatibility in bEnd.3 and glial cells up to 100nMphospholipid concentration.

However, the short chain CPPs (TAT, Penetratin and Mastoparan) demonstrated an improved cellular biocompatibility up to 200nM phospholipid concentration. The Tf-TAT and Tf-Penetratin liposomes showed higher cell viability as compared to the Tf-Mastoparan liposomes. The cell viabilities of the dual-functionalized liposomes without doxorubicin were approximately 85–98%, however, incorporation of the drug reduced the viability of tumor cells to approximately 30–40%indicating efficient translocation of the anticancer drug intothe tumor

cells. The greater cytotoxic effect of Tf-Mastoparan liposomes could be partially attributed to the membrane disruptive potential of Mastoparan via binding to intracellular targets (Saar et al. 2005). The single ligand CPP-liposomes were observed be more cytotoxic as compared to the dual modified Tf-CPP liposomes. The greater cytotoxicity of the CPPliposomes was due to the higher cationic charge of the CPP modified liposomes as compared to the dual functionalized (Tf-CPP) or plain liposomes. In contrast, the negative charge of transferrin protein resulted in greater cell viabilities of Tf-liposomes as compared to the Tf-CPP liposomes.

The Dual-modified liposomes were intended for delivery into systemic circulation. Cationic macromolecules have been reported to trigger thrombosis, embolization and hemolysis, *in vivo* (Antohi and Brumfeld 1984; Zhu et al. 2007). The presence of cationic peptides on the liposomal surface can therefore, induce interactions with the erythrocyte membrane causing cell lysis and release of hemoglobin. Therefore, we performed a hemolysis assay to afford additional information regarding *in vivo* biocompatibility of the proposed liposomes. Both dual-modified and Tf-liposomes were biocompatible at elevated phospholipid concentrations. However, at extremely high concentrations of liposomes (~800 nmoles of phospholipids/1.4×10^6 erythrocytes), hemolysis was evident. This can be explained by the increasing interactions of the liposomes at higher phospholipid concentrations, with the same number of erythrocytes. The *in vitro* assay for hemolysis was performed by exposing ~10^7 erythrocytes to varying phospholipid concentrations. Both Tf and Tf-PR-liposomes were observed to be safe up to 600nmoles of phospholipids in a volume of 0.5 ml of PBS. Therefore, the concentration of the phospholipids was 1.2 mM. We can estimate the total blood volume of an adult SD rat using Lee and Blaufox equation (Lee and Blaufox 1985): BV=0.06 X BW+0.77. Therefore, the blood volume will range from 15.7 to 21.7 ml for adult rats (250–350 g).The dose of liposomes injected was 15.2

μmoles/kg body weight i.e.~3.8–5.32 μmoles for rats weighing 250–350g blood volume~20 ml). Therefore, the concentration of phospholipids used is ~228μM, which is much below the hemolytic concentration of phospholipids. The dose of the liposomes (15.2μmoles of phospholipids/kg body weight) was obtained by initial optimization during the preliminary pilot studies. The hemolytic activity of the plain liposomes was observed to be significantly ($p<0.05$) lower than Tf-PR-liposomes. This can be explained by absence of cationic poly-L-arginine and the shielding effect of the PEG molecules on the surface of plain liposomes. Tf-liposomes demonstrated minimal hemolytic activity at low phospholipid concentrations which can be attributed to the presence of negatively charged proteins molecules on the liposomal surface, thereby reducing interactions with the erythrocyte membrane. However, at higher concentrations the Tf-liposomes demonstrated greater hemolysis as compared to the plain liposomes. This can be attributed to the aggregation of protein conjugated Tf-liposomes at elevated concentrations, thus initiating non-specific interactions and destabilization of erythrocyte membrane. To confirm the aggregation of Tf-liposomes, we performed additional studies relating the effect of phospholipid concentrations to the particle size and zeta potential values of the liposomes (Sharma et al. 2013). Tf-liposomes showed significant ($p<0.05$) increase in size above 500 nmoles of phospholipids/40 μl of suspension, exposed to erythrocytes. The Tf-PR-liposomes did not shown any significant aggregation up to 750 nmoles of phospholipids, nonetheless, the cationic charge of CPP caused greater interactions with the erythrocyte membrane as compared to the Tf-liposomes. The shielding effect of PEG on the plain liposomes averted any significant changes in particle size distribution of these liposomes. Nevertheless, such high amounts of phospholipids in small buffer volumes, exposed to a fixed number of erythrocytes, were not

physiologically relevant and were only evaluated to study the interaction behavior of liposomes with erythrocytes at higher lipid concentrations.

The interaction of Tf-CPP liposomes with the erythrocytes showed that the liposomes with short chain CPPs were more biocompatible as compared to Tf-PR liposomes. Both Tf-TAT and Tf-penetratin were observed to be non-toxic up to concentrations as high as 800 nmoles of phospholipids. However, Tf-Mastoparan liposomes demonstrated significantly higher ($p < 0.05$) hemolytic activity as compared to other Tf-CPP liposomes. This could be due to the cytolytic nature of the Mastoparan peptide (Cardozo et al. 2007). In addition, we anticipate that the presence of more hydrophobic amino acids in Mastoparan might increase the interaction of this peptide with the lipophilic erythrocyte membrane.

4.3. Cellular uptake and transfection studies for liposomes

The presence of high concentrations of protein, caveolin-1, in brain capillary endothelial cells assists transcytosis of essential nutrients from blood to brain (Frank et al. 2009). An efficient transport to brain would require effectual uptake of nutrients by brain capillary endothelial cells followed by transfer to other brain cells, for example, astrocytes, pericytes, and neurons. Cellular uptake of *DiI*-labeled Tf-PR liposomes was, therefore, evaluated in brain endothelial cells. The uptake of dual-modified liposomes was significantly ($p<0.05$) higher than the plain and single-ligand liposomes (Figure 17). The binding and internalization of PR liposomes was facilitated by the cationic charge of the peptide. Previous studies report the initial electrostatic binding of CPPs to heparan sulfate proetoglycans on the cell surface that promote subsequent interactions responsible for internalization of the peptides via endocytic mechanisms (Trabulo et al. 2010). Cell uptake of PR liposomes facilitated by these electrostatic interactions was observed to be lesser in comparison with the uptake of Tf liposomes mediated by receptor

uptake, indicating that receptor-mediated uptake leads to greater internalization of the associated vector. A combination of cell penetration and receptor targeting, however, involved both initial binding of the liposome followed by receptor-mediated endocytosis, leading to considerable improvement in the uptake of liposomes. The dual functionalized liposomes were transported across the cell membranes more efficiently as compared to the single ligand, Tf or CPP-liposomes.

The celluptake of Tf-CPP (TAT, Penetratin or Mastoparan) liposomes (approximately 77–89% in bEnd.3 cells and approximately 90–98% in tumor cells after 1 h) was slower in comparison to the previously reported Tf-PR-liposomes (approximately 95% in bEnd.3 cells after 30 min) (Sharma et al. 2012). This was ascribed to the presence of greater number of basic arginine residues in long chain poly-L-arginine as compared to the short chain CPPs used in this study. However, as mentioned above, the lower cationic charge of the CPPs used in this study considerably improved the biocompatibility of the liposomes. Binding and internalization of CPP-liposomes were driven by the cationic charge of CPPs and interaction of CPP-liposomes with heparan sulfate proteoglycans (Sharma et al. 2012). In comparison, the translocation of dual-modified Tf-CPP liposomes was facilitated via specific receptor targeting and improved penetration effect of CPPs. Since doxorubicin, acts by nuclear localization, the uptake of doxorubicin encapsulating liposomes resulted in an intense overlap in the fluorescence regions of the drug and nuclei. Furthermore, the rate of liposomal uptake was dependent on the type of cells. A more rapid and greater uptake was observed in the tumor cell lines, Daoy and U87, while the bEnd.3 cells showed less and slower uptake. In entirety, the results emphasized the significance of dual-mechanism of uptake over receptor targeting or cell penetration alone. The analysis of the uptake pathways performed using various inhibitors indicated that the transferrin

conjugated (Tf and Tf-CPP) liposomes were primarily transported into the cells via clathrin mediated endocyotis, irrespective of the type of cells, while the uptake of CPP-liposomes was controlled by both macropinocytosis and clathrin coated vesicles (Figures 28-30).

We also evaluated the ability of Tf–CPP liposomes to efficiently deliver the desired gene to the primary culture of glial cells, bEnd3, Daoy and U87 cells and compared the transfection efficiency of CPP modified Tf-liposomes with single ligand, Tf liposomes. Single-ligand modification with only Tf was not able to produce efficient transfection. The incorporation of cell-penetrating cationic peptide to the Tf-conjugated liposomes significantly ($p<0.05$) increased their transfection efficiency. The increase can be explained by the positive charge of Tf–CPP liposomes due to incorporation of CPPs, whereas the zeta potential of Tf liposomes was observed to be negative. Also, Tf liposomes showed lower transfection *in vitro* as compared with plain liposomes; however, the transport of plain liposomes across the endothelial barrier was observed to be significantly ($p<0.05$) less than the Tf liposomes, thereby delivering less liposomes for transfection of cells.

4.4. 2D and 3D *in vitro* BBB models

The results cannot directly predict *in vivo* performance of liposomes, which depends on their transport across the BBB. The studies were, therefore, scaled to the evaluation of liposomal transport across the *in vitro* BBB model. We initially designed an *in vitro* BBB model to evaluate the ability of liposomes to cross the barrier layer. Glial cells were seeded on the bottom side of PET membrane of transwell inserts, and endothelial cells were seeded on the upper side of these inserts. The lower density of glial cells in comparison with endothelial cells was maintained to simulate *in vivo* barrier conditions and to avoid any redundant entrapment of liposomes in the glial cell layer. *In vitro* models, both with glial and endothelial and only endothelial cells, were

assessed for barrier tightness by measuring the TEER and flux of Na–F across the barrier layer. The TEER of the coculture model with both glial and endothelial cells was significantly ($p<0.05$) higher than that of the monolayer model with only endothelial cells. Also, the permeability of Na-F across the co culture barrier layer was lesser as compared with the monolayer. Decreased permeability in the presence of glial cells could be ascribed to the improvement of junctional properties along with the additional physical barrier provided by the glial cell layer. These findings were in accordance with previous studies reporting the significance of glial cells in induction and maintenance of BBB composed of closely packed endothelial cells (Deli et al. 2005; Arthur et al. 1987; Janzer and Raff 1987); therefore, a co-culture of glial and endothelial cells was used to establish the 2D *in vitro* model for evaluating the transport of liposomes.

Further, we followed an innovative approach in designing a simple and robust 3D *in vitro* brain tumor model. The model was constructed by culturing the glioblastoma cells in the porous chitosan-PLGA scaffolds and combining it with the tightly packed endothelial cell layer to simulate the *in vivo* tumor environment. The porous structure of the scaffold supported the growth of tumor cells in 3-dimensional milieu (Kim 2005). Reportedly, the cells attach to the intertwined scaffold fibers and fill the spaces/pores within the scaffold to forma 3D tumor (Sourla et al. 1996; Bell 1995). The tightness of the tumor associated endothelial barrier was compared with the intactness of the endothelial barrier without the tumor scaffold and with glial cells on the abluminal side of the membrane. The lower transport of sodium fluorescein across the tumor associated endothelium versus the endothelial cells alone was partially ascribed to the physical contact of endothelial cells with scaffold in the *in vitro* brain tumor model versus the presence of only endothelial cells on the luminal surface of culture inserts (bEnd.3 model). Also, since the transport was based on the lysis of cells and release of fluorescent molecule, incomplete

lysis of the tumor could also contribute to lower fluorescence intensity. However, significant reduction ($p<0.05$) in the transport of Na-F was observed across the *in vitro* BBB model, where primary glial cells were grown on the abluminal surface of the membrane with the endothelial cells inside the culture inserts (Sharma et al. 2012). This was similar to the *in vivo* condition where the occurrence of tumor is associated with the increased permeability of the BBB (Provenzale et al. 2005). The paracellular transport of Na-F increased (non-significantly) after the transport of liposomes which could be due to the increased permeability of the barrier after interaction with the cationic peptide conjugated liposomes. However, the tightness of the endothelial barrier (decreased permeability of Na-F) was restored after incubation of the endothelial cell culture inserts with the 3D tumor in the presence of 20–30% serum. The TEER across the endothelial cell layer of the BBB model with bEnd.3 cells and glial cells was considerably higher as compared to the TEER across the endothelial cell layer of the tumor model and across the endothelial cell layer cultured alone. This was ascribed to the down regulation of tight junction proteins like occludin and claudin in the tumor associated endothelial barrier (Ishihara et al. 2008). Also, the absence of any glial cells, in the model with the endothelial cell culture alone, contributed to the formation of leakier barrier due to the lack of the induction and maintenance of barrier properties (Janzer and Raff 1987). The dual-functionalized liposomes showed higher transport across the barrier layer with Tf-Penetratin liposomes demonstrating the maximum permeability. The cationic charge of penetratin and the presence of amphiphilic amino acids contributed to increased interaction of Tf-Penetratin liposomes with the endothelial membrane as compared to the Tf-TAT liposomes. The presence of transferrin triggered receptor mediated transcytosis across the endothelial membrane. In contrast, the lower cationic charge of the mastoparan peptide reduced the endothelial transcytosis of Tf-Mastoparan

liposomes (non-significantly) as compared to the Tf-Penetratin liposomes. In addition, the transport of CPP and plain liposomes was lower in comparison to the Tf-CPP liposomes which could be attributed to the absence of dual-mechanism of cell uptake and greater entrapment of these liposomes in the endothelial cell layer.

4.5. *In vivo* evaluation of liposomes

4.5.1. *In vivo* evaluation of Tf-PR-liposomes

Considering the complexity of *in vivo* environment, we examined the ability of Tf-PR-liposomes to target brain after administration into systemic circulation. The distribution of the liposomes *in vivo* was tracked by fluorescent labeling of the liposomes with DiR followed by NIR imaging of different organs (spleen, liver, heart, kidneys, lungs and brain) at specific time points. The preliminary results from whole animal imaging indicated significant accumulation of the DiR labeled liposomes in brain after 24 h. Very less fluorescence was observed in the brain at 6 h time point. As expected, a strong fluorescence signal was observed in the liver immediately after injection and the signal intensity decreased gradually with time resulting in very low fluorescence after 48 h. Individual organs were therefore isolated and examined by NIR imaging at 12, 24, 48, and 72 h time points (Figure 44). Considering the lower accumulation of DiR labeled liposomes in brain as compared to other organs, the exposure time was adjusted to 8 min for brain while 2 min for other organs (i.e., liver, spleen, kidneys, heart and lungs) to avoid a large background signal while imaging the brain. This was followed by quantification of liposomal accumulation using organ homogenization and extraction of the fluorescent dye in chloroform: methanol. The results showed that incorporation of cell penetrating peptide, poly-L-arginine, significantly increased ($p<0.05$) liposomal accumulation in lungs, heart, and brain 24 h post intravenous injection. This indicates that the dual-modified liposomes pass into circulation,

penetrate the highly perfused organs and reach brain more rapidly than other liposomal formulations. Previous studies have reported a large uptake of intravenously administered liposomes by the highly perfused organs like heart, lungs, liver and spleen and very low transport of the liposomes to brain (Awasthi et al. 2003; Afergan et al. 2008). The presence of transferrin receptors in liver, spleen and kidneys can trigger the non-specific uptake of transferrin receptor targeted liposomes by these organs (Deaglio et al. 2002, Jefferies et al. 1984). Also, Liver and spleen are the major macrophage organs and therefore, a large portion of the intravenously administered liposomes is eliminated by these organs. In addition, it has been previously reported the poly-arginine modified liposomes can interact with blood cells and are transported to the lung capillaries (Awasthi et al. 2003, Audouyet al. 2002). Nano particulate systems have also been reported to passively accumulate in heart (Ishiwata et al. 2000). In this study, about 20% and 10% of the injected dose was transported to the lungs and heart, respectively. The liposomes were eliminated from these organs with time. The transport of liposomes to brain was ~4% of the injected dose. The percentage of liposomes transported to brain versus those transported to other organs is comparatively higher than the percent transport of liposomes to brain in previous reports (Awasthi et al. 2003; Afergan et al. 2008). Presumably, the combination of a targeting ligand and CPP improved the transport of liposomes to brain. Plain liposomes accumulated largely in liver and spleen and exhibited very low transport across BBB. Also, plain liposomes showed a more rapid elimination from the organs as compared to the Tf- or dual-modified liposomes. In contrast, the initial uptake of Tf-liposomes was lower in liver and spleen and their accumulation in these organs continued at 72 h indicating longer circulation time of Tf-liposomes as compared to other liposomes (Figure 43). Also, the transport of Tf-liposomes to kidneys was more as compared to other liposomes, however the elimination of Tf-liposomes

from kidneys was slower. The presence of negatively charged transferrin molecules, on the surface of Tf-liposomes, reduced their non-specific interactions in circulation thereby, decreasing their elimination by macrophage system as compared to the plain or Tf-PR-liposomes. The accumulation of all liposomal formulations was observed to be least in heart as compared to other highly perfused organs. However, comparison of the distribution of different liposomal formulations indicates that the Tf-PR-liposomes showed higher penetration in heart and lungs as compared to other liposomes which can be ascribed to the occurrence of cell penetrating peptide on dual-modified liposomes (Mudhakir et al. 2005; Hayashi et al. 2011). Furthermore, the cell penetrating peptide conjugated liposomes showed the highest penetration across BBB. Approximately 4% of the injected dose of Tf-PR-liposomes/gram of tissue was transported to brain, 24 h post intravenous injection. The accumulation of Tf-PR-liposomes in brain was significantly ($p<0.05$) higher than the accumulation of Tf-liposomes. The cell penetrating property of the dual-modified liposomes, in combination with the receptor targeting effect of transferrin protein resulted in higher accumulation of Tf-PR-liposomes in the brain as compared to the single-ligand transferrin receptor targeted, Tf-liposomes.

Therapeutically active genes can be delivered to brain via receptor mediated transcytosis (Qian et al. 2002). *In vivo* evaluation of transfection potential is important from the standpoint of generating preliminary data for clinical translation. The β-gal expressing plasmid has been previously used for evaluating the transfection efficiency of polymeric delivery vectors, *in vivo* (Kim et al. 2007; Guliyeva et al. 2006).With the aim of evaluating the transfection potential of dual-modified liposomes *in vivo*, we encapsulated β-gal plasmid polyplexes in the aqueous core of the liposomes, followed by intravenous injection of the formulation via tail vein at a dose of 50 μg of DNA/rat. The results illustrated significantly higher potential of dual-modified

liposomes to cross the BBB (~4% of the ID/gram) and deliver the desired gene to brain as compared to plain or Tf-liposomes. However, the expression of transferrin receptors in peripheral organs can result in non-specific gene expression in organs other than brain (Deaglio et al. 2002; Zhao et al. 2010; Shi et al. 2001). Maximum gene expression was observed in spleen which corresponds to greater transport of liposomes to this organ. The gene expression of Tf-PR-liposomes in lungs, heart and kidneys was also higher as compared to other liposomes. Also, the transport of Tf-PR liposomes to liver was lower as compared to Tf or plain liposomes, however, the gene expression in liver and lungs was observed to be comparable. This can be explained by the higher positive charge of Tf-PR-liposomes which increased their transfection efficiency over Tf or plain liposomes. The non-specific gene expression in the peripheral organs can be reduced by incorporating an organ specific promoter to allow the expression of the therapeutic gene in specific tissues (Zhao et al. 2010) Measurably improved brain-specific gene expression can be achieved by incorporating a brain specific promoter (e.g. GFAP promoter) with the desired therapeutic gene (Lee et al. 2008). The results from *in vivo* transfection studies further emphasized the significance of dual-mechanism of liposomal transport that resulted in a higher penetration across BBB and improved the expression of the encapsulated gene in brain (Prabhakara et al. 2011, Bolhassani 2011). The liposomes were primarily transported across the BBB via receptor mediated transcytosis, nevertheless the presence of poly-L-arginine on the surface of receptor targeted liposomes further improved their penetration into brain. In addition, the cationic charge of CPP improved gene expression in the targeted cells and tissues.

The cationic charge of CPP conjugates can induce tissue necrosis and inflammation (Jones et al. 2005).The biocompatibility of the liposomes was therefore, evaluated by histological examination of the transfected tissues (Guo et al. 2011). The transfected tissues from

different organs were sectioned and stained with hematoxylin-eosin followed by examination under light microscope. Liver and spleen were exposed to highest load of the liposomes and were therefore, considered as primary organs for evaluation of toxicity. The histological examination confirmed absence of inflammation, ballooning of hepatocytes or enlargement of nuclei in liver and necrosis in spleen. Other organs such as brain, kidneys, heart and lungs were also examined for tissue necrosis or lesions. No toxicity was observed in any of the tissues isolated from the animals that were administered with liposomes at dose of 15.2 μmoles of phospholipids/kg body weight. The poly-ethylene-glycol chains and transferrin protein counterbalanced the cationic charge of poly-L-arginine peptides and reduced the negative effects of this cell penetrating peptide.

4.5.2. *In vivo* evaluation of Tf-CPP-liposomes

The evaluation of *in vivo* biodistribution of doxorubicin encapsulating Tf-CPP liposomes (Tf-TAT, Tf-Penetratin and Tf-Mastoparan) showed more rapid uptake of doxorubicin encapsulating Tf-Mastoparan liposomes in liver and spleen as compared to the Tf and the other Tf-CPP liposomes. The greater hydrophobicity of the mastoparan peptide and its potential to trigger non-specific interactions was considered to affect its uptake by the major macrophage organs. Also, the decrease in the concentration of the drug transported to the macrophage organs via Tf- Mastoparan liposomes was greater as compared to that transported via Tf-Penetratin and Tf-TAT liposomes, thus, indicating a more rapid clearance of Tf-Mastoparan liposomes from the system. Tf-Penetratin liposomes showed maximum transport of doxorubicin into brain (approximately 4% ID/g) *in vivo* followed by Tf-TAT liposomes (approximately 2.9% ID/g). The lower transport using Tf-Mastoparan liposomes, into brain, was attributed to the greater uptake of these liposomes by liver, spleen and lungs and therefore, lesser availability for

transport to brain. The drug encapsulated in the negatively charged Tf-liposomes remained in circulation for long however, the penetration of drug into brain using Tf-liposomes was lesser as compared to the Tf-CPP liposomes. Apparently, the combination of Tf and CPP in dual-modified liposomes increased their penetration into brain. Plain liposomes were transported largely to liver and spleen and showed negligible transport of drug across BBB. The occurrence of Tf receptors in the major macrophage organs (liver, spleen and kidneys) can result in non-specific uptake of the transferrin conjugated liposomes by these organs (Deaglio et al. 2002, Jefferies et al. 1984). Also, a major portion of the intravenously administered delivery systems is eliminated via liver and spleen therefore, a large portion of these liposomes was transported to these organs. In addition, previous studies indicate increased interaction of cationic polymers and CPPs with the blood cells and their subsequent accumulation in lungs (Fueyo et al. 1999, Audouy et al. 2002). The transport of drug encapsulated in the Tf-Mastoparan was more to the lungs than Tf-Penetratin or Tf-TAT liposomes. This was due to the greater interaction of these liposomes with the erythrocytes (Figure 48). Since, the transport of drug encapsulated into the non-targeted CPP-liposomes, across the *in vitro* brain tumor model, was lower as compared to the transferrin receptor targeted Tf and Tf-CPP liposomes, these liposomes were not considered for *in vivo* evaluation of biodistribution. Evaluation of biodistribution of the water soluble drug encapsulated in the Tf-CPP liposomes, provides an insight into the *in vivo* fate and brain transport of the encapsulated agent in these liposomes. The enhanced permeability of the tumor associated brain endothelial barrier is anticipated to further increase the translocation of the targeted Tf-CPP liposomes into brain, *in vivo*.

CHAPTER V. SUMMARY AND CONCLUSION

In view of the compelling need for the development of an efficient delivery vehicle that can transport the desired therapeutic agents (small molecules, genes etc.) across the formidable BBB, we focused our efforts in designing a novel vector that can overcome the limitations of conventional delivery agents like receptor targeted polymeric and lipid based carriers. In our study, we developed and evaluated dual-modified liposomes that possessed the ability to serve as promising vectors for site-specific delivery of desired therapeutic molecules. The liposomes were surface conjugated with transferrin protein to achieve targeting of desired receptors on brain endothelial cells. In addition, these liposomes were conferred with enhanced permeation properties of various cell penetrating peptides. The contribution is significant because this is the first step in the continuum of research that is expected to illustrate the influence of grafting the targeted liposomal delivery vector to cell penetrating peptide and forming near neutral vesicles for improving the delivery of therapeutics across BBB.

We illustrated the influence of different CPPs on the cell uptake, *in vitro* tumor penetration, cytotoxic potential of Tf-receptor targeted liposomes and *in vivo* distribution and biocompatibility. The dual-modified liposomes showed significantly ($p<0.05$) higher accumulation *in vitro* in different cell lines (brain endothelial, Daoy, U87) and *in vivo* rat brain as compared to transferrin-liposomes. The results indicated that the incorporation of amphiphilic CPPs, TAT and Penetratin, on the surface of Tf-liposomes resulted in biocompatible formulations leading to efficient translocation of doxorubicin and genes (pβ-gal and pGFP) across cellular and brain endothelial barriers both *in vitro* and *in vivo*. The conjugation of hydrophobic CPP, Mastoparan, also resulted in improved cellular uptake of Tf-liposomes, however, the higher cytotoxicity and hemolytic activity of this peptide provided a strong

evidence for restricting its use *in vivo*. The Tf-Penetratin liposomes showed maximum cell uptake and transport of the encapsulated drug, across the *in vitro* endothelial barrier, followed by the transport of Tf- Mastoparan liposomes. However, increased hemolytic activity of Tf-Mastoparan liposomes resulted in greater clearance of these liposomes by the macrophage system and therefore, less availability for penetration into the brain, *in vivo*. Also, the β-gal activity of brain tissue transfected using dual-modified liposomes was higher than the single ligand, Tf-liposomes or naked DNA. Also, Histological examination of the transfected tissue demonstrated excellent biocompatibility of dual-modified liposomes. The single-ligand liposomes showed lower uptake by liver and spleen and greater uptake by kidneys, whereas, the Tf-CPP liposomes showed higher penetration in highly perfused tissues like lungs and heart along with greater transport across the targeted BBB. Incorporation of CPP to the Tf-receptor-targeted liposomes caused a considerable improvement in cellular uptake, transfection, transport across *in vitro* BBB models and *in vivo* in adult SD rats, as compared with the plain and single ligand, Tf liposomes.

In conclusion, this work demonstrates the development and characterization of dual-modified liposomes for delivery of small molecule drugs and genes to brain. The dual-modified liposomes bear the potential to serve as safe and efficient non-viral gene delivery vectors for the transport of desired therapeutic molecules across the BBB. We anticipate that this research work will contribute towards the development of high efficiency and low toxicity delivery systems and subsequently help to find new treatment strategies for CNS diseases (e.g., tumors, Alzheimer's disease and certain neuropsychiatric disorders).

5.1. Future directions

The study illustrates that the dual-modified liposomes can serve as promising platform for the design of novel drug and gene delivery vectors involving the combination of targeting ligand and cell penetrating peptide into single delivery system. In this study we combined the receptor targeting properties of transferrin protein with various CPPs and illustrated improved penetration into the targeted organ. It would be interesting to employ different targeting ligands, specifically the receptor binding amino acid sequences of antibodies and proteins, in the liposomal formulations, for delivery to desired cells. These specific receptor binding sequences, in combination with short chain CPP sequences, are anticipated to augment the targeting and cellular delivery of lipid based nanocarriers across different cellular barriers. This approach could therefore, be used to target numerous receptors like insulin, neuronal nicotinic Acetyl choline, vascular endothelial growth factor receptors etc. for the treatment of diseases like diabetes, Alzheimer's disease, schizophrenia and tumors. Also, this work involved the investigation of 3D *in vitro* BBB model, where the porous structure of polymeric scaffold supported the 3-dimensional growth of tumor cells. The process involved construction of scaffold using the polymers PLGA and chitosan. It would be valuable to explore other polymers like poly ethylinimine (PEI) or poly-L-lysine in combination with PLGA for improving the cellular adherence on scaffolds. Both PEI and poly-L-lysine are cationic polymers with basic amine groups (pKa 10-11) and stronger bases as compared to chitosan (pKa 6.8). Replacing chitosan with these cationic polymers might further improve the interaction of negatively charged cell membranes with the polymer coated scaffold, thus increasing the cellular adherence and facilitating tumor growth on scaffold. Additionally, the influence of cross linking these polymers (using reagents like EDC/NHS) on the stability and rigidity of the scaffold would be

another interesting aspect to investigate. Further, since the scaffolds have demonstrated the efficient tumor growth, various anticancer drugs and drug delivery vehicles can be evaluated, using this model, by monitoring the growth or regression of tumor spheroids in the porous structure.

LITERATURE CITED

Abbott, N.J., 2005. Dynamics of CNS barriers: evolution, differentiation, and modulation, Cell. Mol. Neurobiol., 25, 5–23.

Abbott, N.J., Ronnback, L., Hansson, E., 2006. Astrocyte-endothelial interactions at the blood–brain barrier, Nat. Rev. Neurosci., 7, 41–53.

Abdelhalim, M.A.K., 2011. Exposure to gold nanoparticles produces cardiac tissue damage that depends on the size and duration of exposure, Lipids Health Dis., 10, 205.

Adenot, M., Merida, P., Lahana, R., 2007.Applications of a blood–brain barrier technology platform to predict CNS penetration of various chemotherapeutic agents. Cationic peptide vectors for brain delivery. Chemotherapy, 53, 73–76.

Afergan, E., Epstein, H., Dahan, R., Koroukhov, N., Rohekar, K., Danenberg, H.D., Golom, G., 2008. Delivery of serotonin to the brain by monocytes following phagocytosis of liposomes, J.Control. Rel., 132: 84–90.

Allen, T.M., Cullis, P.R., 2004. Drug delivery systems: entering the mainstream, Science, 303, 1818–1822.

Alyautdin, R.N., Gothier, D., Petrov, V., Kharkevich, D.A., Kreuter, J., 1995. Analgesic activity of the hexapeptide dalargin adsorbed on the surface of polysorbate 80-coated poly(butyl cyanoacrylate) nanoparticles, Eur. J. Pharm. Biopharm., 41, 44–48.

Alyautdin, R.N., Tezikov, E.B., Ramge, P., Kharkevich, D.A., Begley, D.J., Kreuter, J., 1998. Significant entry of tubocurarine into the brain of rats by absorption to polysorbate 80-coated polybutylcyanoacrylate nanoparticles: an in situ brain perfusion study, J. Microencapsul., 15, 67–74.

Anabousi, S., Laue, M., Lehr, C.M., Bakowsky, U., Ehrhardt, C., 2000. Assessing transferrin modification of liposomes by atomic force microscopy and transmission electron microscopy, Eur. J. Pharm. Sci., 11, S81–S91.

Anderson, P., 1983. Antibody responses to Haemophilusinfluenzae type b and diphtheriatoxin induced by conjugates of oligosaccharides of the type b capsulewith the nontoxic protein CRM197. Infect. Immun., 39: 233–238.

Antohi, S., Brumfeld, V., 1984. Polycation-cell surface interactions and plasma membrane compartments in mammals. Interference of oligocation with polycationic condensation. Z Naturforsch C., 39, 767–75.

Arunothayanun, P., Bernard, M.S., Craig, D.Q., Uchegbu, I.F., Florence, A.T., 2000. The effectof processing variables on the physical characteristics of non-ionic surfactantvesicles (niosomes) formed from a hexadecyldiglycerol ether. Int. J. Pharm. 201: 7–14.

Arthur, F.E., Shivers, R.R., Bowman, P.D., 1987. Astrocyte mediated induction of tight junctions in brain capillary endothelium: An efficient *in vitro* model, Brain Res., 433, 155–159.

Audouy, S.A.L., de Leiji, L.F.M.H., Hoekstra, D., Molema, G., 2002. *In vivo* characteristics of cationic liposomes as delivery vectors for gene therapy, Pharm. Res., 19, 1599–1605.

Awasthi, V.D., Garcia, D., Goins, B.A., Phillips, W.T., 2003. Circulation and biodistribution profiles of long circulating PEG-liposomes of various sizes in rabbits, Int. J. Pharm., 253, 121–132.

Banks, W.A., 2012. Drug delivery to the brain in Alzheimer's disease: Consideration of the blood–brain barrier. Adv. Drug Deliver Rev., 64, 629–639.

Béduneau, A., Saulnier, P., Benoit, J.P., 2007. Active targeting of brain tumors using nanocarriers, Biomaterials, 28, 4947–4967.

Blasi, P., Giovagnoli, S., Schoubben, A., Ricci, M., Rossi, C., 2007.Solid lipid nanoparticlesfor targeted brain drug delivery.Adv. Drug Deliv. Rev., 59, 454–477.

Bartsch, M., Weeke-Klimp, A.H., Meijer, D.K.,Scherphof, G.L., Kamps, J.A., 2005. Cellspecifictargeting of lipid-based carriers for ODN and DNA, J. Liposome Res., 15, 59–92.

Batrakova, E.V., Miller, D.W., Li, S., Alakhov, V.Y., Kabanov, A.V., Elmquist, W.F., 2001. Pluronic P85 enhances the delivery of digoxin to the brain: *in vitro* and *in vivo* studies, J. Pharmacol. Exp. Ther., 296, 551–557.

Batrakova, E.V., Li, S., Miller, D.W., Kabanov, A.V., 1999. Pluronic P85 increases permeabilityof a broad spectrum of drugs in polarized BBMEC and Caco-2 cell monolayers,Pharm. Res., 16, 1366–1372.

Batrakova, E.V., Li, S., Alakhov, V.Y., Miller, D.W., Kabanov, A.V., 2003. Optimal structure requirementsforpluronic block copolymers inmodifying P-glycoprotein drug effluxtransporter activity in bovine brainmicrovessel endothelial cells, J. Pharmacol. Exp.Ther., 304, 845–854.

Begley, D., 1996. The blood-brain barrier: Principles for targeting peptides and drugs to the central nervous system, J. Pharm. Pharmacol., 48, 136–146.

Bell, E., 1995. Strategy for the selection of scaffolds for tissue engineering.Tissue Eng., 1, 163–79.

Bhaskar, S.,Tian, F., Stoeger, T., Kreyling, W., de la Fuente, J.M.,Grazu, V., Borm, P., Estrada, G., Ntziachristos, V., Razansky, D., 2010. Multifunctional Nanocarriers for diagnostics,drug delivery and targeted treatment across blood–brain barrier: perspectiveson tracking and neuroimaging, Part. FibreToxicol.7: 3.

Blasi, P., Giovagnoli, S., Schoubben, A., Ricci, M., Rossi, C., 2007.Solid lipid nanoparticles for targeted brain drug delivery.Adv. Drug Deliv. Rev. 59, 454–477.

Bolhassani, A., 2011. Potential efficacy of cell-penetrating peptides for nucleic acid and drug delivery in cancer, Biochim. Biophys. Acta., 1816, 232–246.

Borchard, G., Audus, K.L., Shi, F., Kreuter, J., 1983. Uptake of surfactant-coated poly(methyl methacrylate)-nanoparticles by bovine brain microvessel endothelial cell monolayers, Int. J. targeting, and use, Pharm. ActaHelv., 58, 242–250.

Boviatsis, E.J., Park, J.S., Sena-Esteves, M., Kramm, C.M., Chase, M., Efird, J.T., Wei, M.X., Breakefield, X.O., Chiocca, E.A., 1994. Long-term survival of rats harboring brain neoplasms treated with ganciclovir and a herpes simplex virus vector that retains an intact thymidine kinase gene, Cancer Res., 54, 5745–5751.

Bowers, W., Howard, D., Federoff, H., 1997.Gene therapeutic strategies for neuroprotection: implications for Parkinson's disease, Exp. Neurol. 144 (1997) 58–68.

Bradbury, M., 1979. The Concept of a Blood–Brain Barrier, John Wiley and Sons Ltd, New York.

Buckley, R.H., 2002. Gene therapy for SCID — a complication after remarkable progress,Lancet, 360, 1185–1186.

Buzzi, S., Rubboli, D., Buzzi, G., Buzzi, A.M., Morisi, C., Pironi, F., 2004.CRM197 (nontoxicdiphtheria toxin): effects on advanced cancer patients.CancerImmunol.Immunother. 53: 1041–1048.

Carter, B.S., Zervas, N.T., Chiocca, E.A., 1999. Neurogenetic surgery: current limitations and the promise of gene- and virus-based therapies, Clin. Neurosurg., 45, 226–246.

Calvo, P., Gouritin, B., Chacun, H., Desmaele, D.,D'Angelo, J., Noel, J.P., Georgin, D.,Fattal, E., Andreux, J.P., Couvreur, P., 2001. Long-circulating PEGylated polycyanoacrylate nanoparticles as new drug carrier for brain delivery, Pharm. Res., 18: 1157–1166.

Calvo, M.C., Bey, S.H., Yates, F., de Villartay, J.P., Deist, F.L., Fischer, A., 2001.Gene therapy of severe combined immunodeficiencies, J. Gene Med., 3, 201–206.

Calvo, M.C., Bey, S.H.., de Saint Basile, G., Gross, F., Yvon, E., Nusbaum, P., Selz, F., Hue,C., Certain, S., Casanova, J.L., Bousso, P., Deist, F.L., Fischer, A., 2000. Gene therapy of human severe combined immunodeficiency (SCID)-X1 disease, Science, 288, 669–672.

Calvo, M.C., Fischer, A., 2007. Gene therapy for severe combined immunodeficiency: are we there yet? J. Clin. Invest., 117, 1456–1465.

Cardozo, A.K., Buchillier, V., Mathieu, M., Chen, J., Ortis, F., Ladrire, L., Allaman-Pillet, N., Poirot, O., Kellenberger, S., Beckmann, J.S., Eizirik, D.L., Bonny, C., Maurer, F., 2007.Cell-permeable peptides induce dose- and length-dependent cytotoxic effects,Biochim. Biophys. Acta(BBA) –Biomembranes, 1768, 2222–2234.

Carlmark, A., Hawker, C.J., Hult, A., Malkoch, M., 2009. New methodologies in the construction of dendritic materials, Chem. Soc. Rev., 38, 352–362.

Chen, Y., Dalwadi, G., Benson, H., 2004. Drug delivery across the blood–brain barrier,Curr. Drug Deliv., 1, 361–376.

Chen, Y., Liu, L., 2012. Modern methods for delivery of drugs across the blood–brain barrier. Adv. Drug Deliver Reviews, 64, 640–665.

Chen, H., Qin, Y., Zhang, Q., Jiang, W., Tang, L., Liu, J., He, Q., 2011. Lactoferrin modified doxorubicin-loaded procationic liposomes for the treatment of gliomas. Eur. J.Pharm. Sci. 44, 164–173.

Chen, H., Tang, L., Qin, Y., Yin, Y., Tang, J., Tang, W., Sun, X., Zhang, Z., Liu, J., He, Q., 2010. Lactoferrin modified procationic liposomes as a novel drug carrier for brain delivery, Eur. J. Pharm. Sci., 40, 94–102.

Cheng, J., Teply, B.A., Sherifi, I., Sung, J., Luther, G., Gu, F.X., Nissenbaum, E., Moreno, A.F., Langer, R., Farokhzad, O.C., 2007. Formulation of functionalized PLGA-PEG nanoparticles for *in vivo* targeted drug delivery, Biomaterials, 28, 869–876.

Cheng, Y., Zak, O., Alsen, P., Harrison, S.C., Watz, T., 2004. Structure of the human transferrin receptor-transferrin complex. Cell, 116, 565–76.

Christiaens, B., Dubruel, P., Grooten, J., Goethals, M., Vandekerckhove, J., Schacht, E., Rosseneu, M., 2005.Enhancement of polymethacrylate-mediated gene delivery by Penetratin. Eur. J. Pharm. Sci. 24, 525–537.

Clinicaltrials.gov, Pegylated Liposomal Doxorubicin and Prolonged Temozolomidein Addition to Radiotherapy in Newly Diagnosed Glioblastoma. http://clinicaltrials.gov/ct2/show/NCT00944801, Last access 21st July 2011.

Cole, A.J., David, A.E., Wang, J., Galbán, C.J., Yang, V.C., 2011, Magnetic brain tumor targeting and biodistribution of long-circulating PEG-modified, cross-linked starch-coated iron oxide nanoparticles, Biomaterials, 32, 6291–6301.

Coombes, A.G.A., Scholes, P.D., Davies, M.C.,Illum, L., Davis, S.S., 1994. Resorbable polymericmicrospheres for drug delivery – production and simultaneous surface modification using PEO-PPO surfactants, Biomaterials 15, 673–680.

Costantini, L.C., Bakowska, J.C., Breakefield X.O., Isacson, O., 2000. Gene therapy in the CNS, Gene Ther., 7, 93–109.

Couvreur, P., Grislain, L., Lenaerts, V., Brasseur, F., Guiot, P., Biernacki, A., 1986.Biodegradable polymeric nanoparticles and drug carriers for antitumor agents, in: P. Guoit, P. Couvreur (Eds.), Polymeric Nanoparticles and Microspheres, CRC Press, Boca Raton, FL, 27–93.

Crone, C., Olesen, S.P.,1982. Electrical resistance of brain microvascular endothelium, Brain Res, 241, 49–55.

Crone, C., Cristensen, O., 1981.Electrical resistance of capillary endothelium. J. Gen. Physiol., 77, 349–371.

Cserr, H.F., Knopf, P.M., 1992. Cervical lymphatics, the blood–brain barrier and the immunoreactivity of the brain: a new view. Immunol. Today, 13, 507–512.

da Cruz, M.T., Simoes, S., de Lima, M.C., 2004. Improving lipoplex-mediated gene transferrin to C6 glioma cells and primary neurons. Exp. Neurol., 187, 65–75.

Daneman, R., Rescigno, M., 2009. The gut immune barrier and the blood–brain barrier: are they so different? Immunity, 31, 722–735.

Davson, H., Segal, M.B., 1996. Blood–brain barrier, Physiology of the CSF and Blood– brain Barriers. CRC Press, Boca Raton, 49–91.

Dakwar, G.R., Hammad, I.A., Popov, M., Linder, C., Grinberg, S., Heldman, E., Stepensky, D., 2012.Delivery of proteins to the brain by bolaamphiphilic nano-sized vesicles,J. Control. Release, 160, 315–321.

de Boer, A.G., Gaillard, P.J., 2007. Drug targeting to the brain, Annu. Rev. Pharmacol.Toxicol., 47, 323–355.

De Jong, W.H., Hagens, W.I., Krystek, P., Burger, M.C., Sips, A.J., Geertsma, R.E., 2008. Particle size-dependent organ distribution of gold nanoparticles after intravenous administration, Biomaterials, 29, 1912–1919.

Deli, M.A., Abraham, C.S., Kataoka, Y., Niwa, M., 2005. Permeability studies on *in vitro* blood–brain barrier models: Physiology, pathology and pharmacology, Cell. Mol. Neurobiol., 25, 59–127.

Demeule, M., Poirier, J., Jodoin, J., Bertrand, Y., Desrosiers, R.R., Dagenais, C., Nguyen, T., Lanthier, J., Gabathuler, R., Kennard, M., Jefferies, W.A., Karkan, D., Tsai, S.,Fenart, L., Cecchelli, R., Beliveau, R., 2002.High transcytosis of melanotransferrin(P97) across the blood–brain barrier, J. Neurochem., 83, 924–933.

Deshayes, S., Morris, M.C., Divita, G., Heitz, F., 2005. Cell-penetrating peptides: tools for intracellular delivery of therapeutics, Cell. Mol. Life Sci., 62 (2005) 1839–1849.

Discher, D.E., Ahmed, F., 2006. Polymersomes, Annu. Rev. Biomed., Eng. 8: 323–341.

Disalvo, E.A., Bouchet, A.M., 2012. Electrophoretic mobility and zeta potential of liposomes due to arginine and polyarginine adsorption, Colloids and Surfaces A: Physicochem. Eng. Aspects, http://dx.doi.org/10.1016/j.colsurfa.2012.09.012.

Deaglio, S., Capobianco, A., Cali, A., Bellora, F., Alberti, F., Righi, L., Sapino, A., Camaschella, C., Malavasi, F., 2002. Structural, functional, and tissue distribution analysis of human transferrin receptor-2 by murine monoclonal antibodies and a polyclonal antiserum, Blood 100, 3782–3789.

Demeule, M., Regina, A., Che, C., Poirier, J., Nguyen, T., Gabathuler, R., Castaigne, J.P., Beliveau, R., 2008.Identification and design of peptides as a new drug delivery system for the brain. J. Pharmacol. Exp. Ther., 324, 1064–1072.

Demeule, M., Currie, J.C., Bertrand, Y., Che, C., Nguyen, T., Regina, A., Gabathuler, R., Castaigne, J.P., Beliveau, R., 2008.Involvement of the low-density lipoprotein receptor-relatedprotein in the transcytosis of the brain delivery vector angiopep-2. J. Neurochem.106, 1534–1544.

Deshayes, S., Morris, M.C., Divita, G., Heitz, F., 2005. Cell-penetrating peptides: tools forintracellular delivery of therapeutics. Cell. Mol. Life Sci. 62, 1839–1849.

Dohgu, S.,Takata, F., Yamauchi, A., Nakagawa, S., Egawa, T., Naito, M., Tsuruo, T., Sawada, Y., Niwa, M., Kataoka, Y., 2005.Brain pericytes contribute to the induction and upregulation of blood–brain barrier functions through transforming growth factorbeta production. Brain Res. 1038, 208–215.

Dom, G., Jackson, C.S., Matis, C., Bouffioux, O., Picard, J.J., Prochiantz, A., Paule, M., Leclercq, M., Brasseur, R., Rezsohazy R., 2003. Cellular uptake of Antennapedia Penetratin peptides is a two-step process in which phase transfer precedes a tryptophan-dependent translocation. Nucleic Acids Res., 31, 556-561.

Drin, G., Cottin, S., Blanc, E., Rees, A.R., Temsamani, J., 2003. Studies on the internalization mechanism of cationic cell-penetrating peptides. J. Biol. Chem., 278, 31192–31201.

Drin,G., Mazel,M., Clair,P., Mathieu,D., Kaczorek,M. and Temsamani,J. (2001) Physico-chemical requirements for cellular uptake of pAntp peptide: Role of lipid-binding affinity. Eur. J. Biochem., 268, 1304–1314.

Drin, G., Rousselle, C., Scherrmann, J.M., Rees, A.R., Temsamani, J., 2002. Peptide Delivery to the Brain via Adsorptive-Mediated Endocytosis: Advances WithSynB Vectors. AAPS Pharm Sci., 4, 1-7.

du Plessis, J., Ramachandran, C., Weiner, N., Oiler, D.G.M., 1996. The influence of lipid composition and lamellarity of liposomes on the physical stability of liposomes upon storage, Int. J. Pharm., 127, 273–278.

Dufes, C., Schatzlein, A.G., Tetley, L., Gray, A.I., Watson, D.G., Olivier, J.C., Couet, W., Uchegbu, I.F., 2000. Niosomes and polymeric chitosan based vesicles bearing transferrinand glucose ligands for drug targeting. Pharm. Res. 17: 1250–1258.

Edmondson, J.M., Armstrong, L.S., Martinez, A.O., 1998. A rapid and simple MTT-based spectrophotometric assay for determining drug sensitivity in monolayer cultures. Methods Cell. Sci., 11, 15–17.

Ekambaram, P., Sathali, A.A.H., Priyanka, K.,2012. Solid lipid nanoparticles: a review. Sci. Revs. Chem. Commun., 2, 80-102.

Erben, M., Decker, S., Franke, H., Galla, H.J., 1995. Electrical resistance measurements on cerebral capillary endothelial cells—a new technique to study small surface areas, J. Biochem. Biophys. Methods, 30, 227–38.

Etame, A.B., Diaz, R.J., O'Reilly, M.A., Smith, C.A., Mainprize, T.G., Hynynen, K., Rutka, J.T., 2012.Enhanced delivery of gold nanoparticles with therapeutic potential into the brain using MRI-guided focused ultrasound, Nanomed. Nanotech., Biol. Med., 8, 1133–1142.

Fenke, H., Galla, H.J., Beuckmann, C.T., 2000. Primary cultures of brain microvessel endothelial cells: a valid and flexible model to study drug transport through the blood–brain barrier *in vitro*, Brain Res. Brain Res. Protoc., 5, 248–56.

Feng, B., Tomizawa, K., Michiue, H., Miyatake, S., Han, X.J., Fujimur, A., Seno, M., Kirihata, M., Matsui, H., 2009. Delivery of sodium borocaptate to glioma cells using immunoliposome conjugated with anti-EGFR antibodies by ZZ-His, Biomaterials, 1746-55.

Fillebeen, C., Descamps, L., Dehouck, M.P., Fenart, L., Benaissa, M., Spik, G., Cecchelli, R., Pierce, A., 1999. Receptor-mediated transcytosis of lactoferrin through the blood–brain barrier. J.Biol.Chem. 274, 7011–7017.

Fischer, D., Li, Y., Ahlemeyer, B., Krieglstein, J., Kissel, T., 2003. *In vitro* cytotoxicity testing of polycations: influence of polymer structure on cell viability and hemolysis, Biomaterials, 24, 1121–31.

Fishman, JB., Rubin, JB., Handrahan JV., Connor JR., Fine RE., 1987. Receptor mediated transcytosis of transferrin across the blood-brain barrier, J. Neurosci. Res., 18, 299-304.

Foust, K.D., Nurre, E., Montgomery, C.L., Hernandez, A., Chan, C.M., Kaspar, B.K., 2009. Intravscular AAV9 preferentially targets neonatal neurons and adult astrocytes. Nat.biotechnol., 27, 59-65.

Fueyo, J., Gomez-Manzano, C.., Yung, W.K., Kyritsis, A.P., 1999. Targeting in gene therapy for gliomas, Arch. Neurol., 56, 445–448.

Furrer, E., Hulmann, V., Urech, D.M., 2009.Intranasal delivery of ESBA105, a TNF-alpha-inhibitory scFv antibody fragment tothe brain, J. Neuroimmunol., 2009, 65-72.

Frank, P.G., Pavlides, S., Lisanti, M.P., 2009. Caveolae and transcytosis in endothelial cells: Role in atherosclerosis, Cell Tissue Res., 335, 41–47.

Frolich, L., Blum-Degen, D., Bernstein, H.G., Engelsberger, S., Humrich, J., Laufer, S., Muschner, D., Thalheimer, A., Turk, A., Hoyer, S., Zochling, R., Boissl, K.W., Jellinger, K.,

Riederer, P., 1998. Brain insulin and insulin receptors in aging and sporadic Alzheimer'sdisease, J. Neural Transm., 105, 423–438.

Fromm, M.F., 2000. P-glycoprotein: a defense mechanism limiting oral bioavailabilityand CNS accumulation of drugs, Int. J. Clin. Pharmacol.Ther., 38, 69–74.

Gabathuler, R., 2010. Approaches to transport therapeutic drugs across the blood–brain barrier to treat brain diseases. Neurobiol. Dis., 37, 48–57.

Gabathuler, R., Arthur, G., Kennard, M., Chen, Q., Tsai, S., Yang, J., Schoorl, W., Vitalis, T.Z., Jefferies, W.A., 2005. Development of a potential protein vector (NeuroTrans)to deliver drugs across the blood–brain barrier. Int. Congr. Ser. 1277, 171–184.

Garcia-Garcia, E., Andrieux, K., Gil, S.,Couvreur, P., 2005.Colloidal carriers and blood–brain barrier (BBB) translocation: a way to deliver drugs to the brain? Int. J.Pharm., 298: 274–292.

Gaillard, P.J., Brink, A., de Boer, A.G., 2005. Diphtheria toxin receptor-targeted brain drugdelivery, Int. Congr. Ser. 1277, 185–198.

Gaillard, P.J., Voorwinden, H.V., Nielsen, J.L., Ivanov, A., Atsumi, R., Engman, H., Rinbom, C., De Boer, A.G., Breimer, D.D., 2001. Establishment and functional characterization of an *in vitro* model of the blood–brain barrier comprising a co-culture of brain capillary endothelial cells and astrocytes, Eur. J .Pharm. Sci., 12, 215–222.

Giannini, G., Rappuoli, R., Ratti, G., 1984. The amino-acid sequence of two non-toxicmutants of diphtheria toxin: CRM45 and CRM197. Nucleic Acids Res., 12: 4063–4069.

Gong, C., Li, X., Xu, L., Zhang, Y.H., 2012. Target delivery of a gene into the brain using the RVG29-oligoarginine peptide, Biomaterials, 33, 3456-3463.

Gref, R. Minamitake, Y., Peracchia, M.T., Trubetskoy, V., Torchilin, V., Langer, R., Biodegradablelong-circulating polymeric nanospheres, Science (Wash DC) 263, 1600–1603.

Grislain, L., Couvreur, P., Lenaerts, V., Roland, M., Deprez-Decampeneere, D., Speiser, P., 1983.Pharmacokinetics and distribution of a biodegradable drug-carrier, Int. J. Pharm., 15, 335–345.

Guliyeva, U., Oner, F., Ozsoy, S., Lu, R.H., 2006. Chitosan microparticles containing plasmid DNA as potential oral gene delivery system, Eur. J. Pharm. Biopharm., 62, 17–25.

Gupta, B., Levchenko, T., Torchilin, V.P., 2007. TAT peptide-modified liposomes provide enhanced gene delivery to intracranial human brain tumor xenografts in nude mice, Oncol. Res., 16, 351–359.

Gupta, B., Levchenko, T.S., Torchilin, V.P., 2005. Intracellular delivery of large molecules and small particles by cell-penetrating proteins and peptides, Adv. Drug Deliv. Rev., 57, 637–51.

Gutman, R.L., Peacock, G., Lu, D.R., Targeted drug delivery for brain cancer treatment, J. Control, Release, 65, 31–41.

Guo, L., Fan, L., Pang, Z., Ren, J., Ren, Y., Li, J., Chen, J., Wen, Z., Jiang, X., 2011. TRAIL and doxorubicin combination enhances anti-glioblastoma effect based on passive tumor targeting of liposomes, J. Control. Release, 154, 93–102.

Ha¨llbrink, M., Floren, A., Elmquist, A., Pooga, M., Bartfai, T., Langel. U., 2001. Cargo delivery kinetics of cell-penetrating peptides. Biochim. Biophys.Acta., 1515, 101–109.

Haque, N., Isacson, O., 1997. Antisense gene therapy for neurodegenerative disease?Exp. Neurol., 144, 139–146.

Harasyma, T.O., Ballya, M.B., Tardid, P., 1998. Clearance properties of liposomes involving conjugated proteins for targeting, Adv. Drug Deliv. Rev., 32, 99–118.

Hatakeyama, H., Akita, H., Ishida, E., Hashimoto, K., Kobayashi, H., Aoki, T., Yasuda, J., Obata, K., Kikuchi, H., Ishida, T., Kiwada, H.,Harashima, H., 2007.Tumor targeting ofdoxorubicin by anti-MT1-MMP antibody-modified PEG liposomes, Int. J.Pharm. 342, 194–200.

Hawkins, B.T., Egleton, R.D., 2008. Pathophysiology of the blood–brain barrier: animal models and methods, Curr.Top. Dev. Biol., 80, 277–309.

Hayashi, Y., Yamauchi, J., Khalil, I.A., Kajimoto, K., Akita, H., Harashima, H., 2011. Cell penetrating peptide-mediated systemic siRNA delivery to the liver, Int. J. Pharm., 419, 308–313.

Hirai, Y., Kuwada, M., Yasuhara, T., Yoshida, H., Nakajima, T., 1979.A new mast cell degranulating peptide homologous to mastoparan in the venom of Japanese hornet (Vespa xanthoptera), Chem. Pharm. Bull., 27, 1945–1946.

Hu, K., Li, J., Shen, Y., Lu, W., Gao, X., Zhang, Q., Jiang, X., 2009. Lactoferrin-conjugated PEGPLAnanoparticles with improved brain delivery: *In vitro* and *in vivo* evaluations, J. Control. Release, 134, 55–61.

Huang, R.Q., Ke, W.L., Qu, Y.H., Zhu, J.H., Pei, Y.Y., Jiang, C., 2007. Characterization of lactoferrin receptor in brain endothelial capillary cells and mouse brain. J. Biomed. Sci., 14, 121–128.

Huang, R. Q., Ke, W., Han, L., Liu, Y., Shao, K., Jiang, C., Pei, Y., 2010. Lactoferrin-modified nanoparticles could mediate efficient gene delivery to the brain *in vivo*, Brain Res. Bull., 81, 600–604.

Huwyler, J., Wu, D., Pardridge, W.M., 1996. Brain drug delivery of small molecules using immunoliposomes, Proc. Natl. Acad. Sci. USA, 93, 14164–14169.

Hynynen, K., 2008. Ultrasound for drug and gene delivery to the brain. Adv. Drug Deliv. Rev., 60, 1209–1217.

Kamata, H., Tasaka, S., Inoue, K., Miyamoto, K., Nakano, Y., Shinoda, H., Kimizuka, Y., Fujiwara, H., Ishii, M., Hasegawa, N., Takamiya, R., Fujishima, S., Takano, H., Ishizaka, A., 2011. Carbon black nanoparticles enhance bleomycin-induced lung inflammatory and fibrotic changes in mice, Exp. Biol. Med., 236, 315–324.

Iden, D.L., Allen, T.M., 2001. *In vitro* and *in vivo* comparison of immunoliposomes made by conventional coupling techniques with those made by a new post-insertion approach, Biochim. Biophys. Acta., 1513, 207–216.

Isacson, O., Behavioral effects and gene delivery in a rat model of Parkinson's disease,1995. Science, 269, 856–857.

Ishihara, H., Kubota, H., Lindberg, R.L., Leppert, D., Gloor, S.M., Errede, M., Virgintino, D., Fontana, A., Yonekawa, Y., Frei, K., 2008. Endothelial cell barrier impairment induced by glioblastomas and transforming growth factor beta2 involves matrix metalloproteinases and tight junction proteins, J Neuropathol Exp Neurol., 67, 435–48.

Ishiwata, H., Suzuki, N., Ando, S., Kikuchi, H., Kitagawa, T., 2000. Characteristics and biodistribution of cationic liposomes and their DNA complexes, J. Control. Release, 69, 139–148.

Jalali, N., Moztarzadeh, F., Mozafari, M., Asgari, S., Motevalian, M., Alhosseini, S.N., 2011.Surface modification of poly(lactide-co-glycolide) nanoparticles by d-α-tocopheryl polyethylene glycol 1000 succinate as potential carrier for the delivery of drugs to the brain. Colloids and Surfaces A: Physicochem. Eng. Aspects,392, 335– 342.

Janzer, R.C., Raff, M.C., 1987. Astrocytes induce blood–brain barrier properties in endothelial cells, Nature, 325, 253–257.

Jaspreet, K., Gurpreet, S.,Seema, S., Rana, A.C., 2012.Innovative growth in developing new methods for formulating solid lipid nanoparticles and microparticles. J. Drug Deliv. Therapeutics, 2, 146-150.

Jefferies, W.A., Brandon, M.R., Hunt, S.V., Williams, A.F., Gatter, K.C., Mason, D.Y., 1984. Transferrin receptor on endothelium of brain capillaries, Nature, 312, 162–163.

Ji, B., Maeda, J., Higuchi, M., Inoue, K., Akita, H., Harashima, H., Suhara, T., 2006. Pharmacokinetics and brain uptake of lactoferrin in rats, Life Sci., 78, 851–855.

Jin, K., Sun, Y., Xie, L., Childs, J., Mao, X.O., Greenberg, D.A., 2004. Post-ischemic administration of heparin-binding epidermal growth factor-like growth factor (HB-EGF) reducesinfarct size and modifies neurogenesis after focal cerebral ischemia in the rat. J. Cereb. Blood Flow Metab., 24: 399–408.

Johanson, C.E., Duncan III, J.A., Kling, P.M., Brinker, T., Stopa, E.G., Silverberg, G.D., 2008. Multiplicity of cerebrospinal fluid functions: new challenges in health and disease. Cerebrospinal Fluid Res. 5, 10.

Johanson, C.E., Duncan, J.A., Stopa, E.G., Baird, A., 2005. Enhanced prospects for drug delivery and brain targeting by the choroid plexus-CSF route. Pharm. Res. 22, 1011–1037.

Johnson, P.A., Miyanohara, A., Levine, F., Cahill, T., Friedmann, T., 1992. Cytotoxicity of are plication-defective mutant of herpes simplex virus type 1, J.Virol. 1992, 2952–2965.

Jones, S.W., Christison, R., Bundell, K., Voyce, C.J., Brockbank, S.M.V., Newham, P., Lindsay, M.A., 2005. Characterisation of cell-penetrating peptide-mediated peptide delivery, Br. J. Pharmacol., 145, 1093–1102.

Kabanov, A.V., Batrakova, E.V., Miller, D.W., 2003. Pluronic block copolymers as modulatorsof drug efflux transporter activity in the blood–brain barrier, Adv. DrugDeliv. Rev. 55, 151–164.

Kaefer, M., Vemulapalli, S., Freeman, M.R., 2000.A nontoxic diphtheria toxin analogue inhibits neonatal bladder smooth muscle cell proliferation. J. Urol., 163: 580–584.

Kalaria, R.N., Sromek, S.M., Grahovac, I., Harik, S.I., 1992. Transferrin receptors of rat andhuman brain and cerebral microvessels and their status in Alzheimer's disease. Brain Res., 585, 87–93.

Kanth, S.B.M., Kalishwaralal, K., Sriram, M., Pandian, S.R., Youn, H., Eom, S.H., Gurunathan, S., 2010. Anti-oxidant effect of gold nanoparticles restrains hyperglycemic conditions in diabetic mice, J. Nanobiotechnol., 8, 16.

Kaplitt, M.G., Feigin, A., Tang, C., Fitzsimons, H.L., Mattis, P.,Lawlor, P.A., Bland, R.J., Young, D., Strybing, K., Eidelberg, D., During, M.J., 2007. Safety and tolerability of gene therapy with an adeno-associated virus (AAV) borne GAD gene for Parkinson'sdisease: an open label, phase I trial. Lancet, 369, 2097–2105.

Kawahara, N., Mishima, K., Higashiyama, S., Taniguchi, N., Tamura, A., Kirino, T., 1999. Thegene for heparin-binding epidermal growth factor-like growth factor is stressinducible:its role in cerebral ischemia, J. Cereb. Blood Flow Metab., 19: 307–320.

Kateb, B., Chiu, K., Black, K.L., Yamamoto, V., Khalsa, B., Ljubimova, J.Y., Ding, H., Patil, R., Portilla-Arias, J.A., Modo, M., Moore, D.F., Farahani, K., Okun, M.S., Prakash, N., Neman, J., Ahdoot, D., Grundfest, W., Nikzad, S., Heiss, J.D., 2011. Nanoplatforms for constructingnew approaches to cancer treatment, imaging, and drug delivery:what should be the policy? Neuroimage.S106–S124.

Ke, W., Shao, K., Huang, R., Han, L., Liu, Y., Li, J., Kuang, Y., Ye, L., Lou, J., Jiang, C., 2009.Genedelivery targeted to the brain using an Angiopep-conjugated polyethylene glycol modifiedpolyamidoaminedendrimer. Biomaterials, 30, 6976–6985.

Kibria, G., Hatakeyama, H., Ohga, N., Hida, K., Harashima, H., 2011. Dual ligand modification of PEGylated liposomes shows better cell selectivity and efficient gene delivery. J. Control. Release, 153,141–148.

Kim, H.H., Choi, H.S., Yang, J.M., Shin, S., 2007. Characterization of gene delivery *in vitro* and *in vivo* by the arginine peptide system, Int. J. Pharm., 335, 70–78.

Kim, H.K., Davaa, E., Myung, C.S., Park, J.S., 2010. Enhanced siRNA delivery using cationic liposomes with new polyarginine conjugated PEG-lipid. Int. J. Pharm. 392, 141–147.

Kim, J.Y., Choi, W., Kim, Y.H., Tae, G., 2013. Brain-targeted delivery of protein using chitosan- and RVG peptide-conjugated, pluronic-based nano-carrier, Biomaterials, 34, 1170-1178

Kim, J.B., 2005. Three-dimensional tissue culture models in cancer biology. Seminars in Cancer Biology., 15, 365–377.

Kilk, K., Andaloussi, S.E.L., Jarver, P., Meikas, A., Valkna, A., Bartfai, T., Kogerman, P., Metsis, M., Langela, U., 2005. Evaluation of transportan 10 in PEI mediated plasmid delivery assay,J. Control.Release, 103, 511– 523.

Klibanov, A., Mayurama, K., Torchillin, V.P., Huang, L., 1990. Amphipathic polyethylene glycols effectively prolong the circulation time of liposomes. FEBS Lett. 268, 235-237.

Kreuter, J. 2005. Application of nanoparticles for the deliveryof drugs to the brain. International Congress Series, 1277: 85– 94.

Kreuter ,J., Petrov, V.E., Kharkevich, D.A., Alyautdin, R.N., 1997. Influence of the type of surfactant on the analgesic effects induced by the peptide dalargin after its delivery across the blood–brain barrier using surfactant-coated nanoparticles,J. Control. Release, 49, 81–87.

Kreuter, J., Alyautdin, R.N., Kharkevich, D.A., Ivanov, A.A., 1995. Passage of peptides through the blood–brain barrier with colloidal polymer particles (nanoparticles), Brain Res., 674, 171–174.

Krex, D., Klink, B., Hartmann, C., Deimling, A.V., Pietsch, T., Simon, M., Sabel, M., Steinbach, J.P., Heese, O., Reifenberger, G., Weller, M., Schackert, G., German Glioma Network, German Glioma Network, 2007. Long-term survival with glioblastoma multiforme, Brain, 130, 2596–606.

Kohane, D.S., Plesnila, N., Thomas, S.S., Le, D., Langer, R., Moskowitz, M.A., 2002. Lipid–sugar particles for intracranial drug delivery: safety and biocompatibility. Brain Res., 946, 206–213.

Koo, Y.E.L., Reddy, G.R., Bhojani, M., Schneider, R., Philbert, M.A., Rehemtulla, A., Ross, B.D., Kopelman, R., 2006.Brain cancer diagnosis and therapy with nanoplatforms. Adv.DrugDeliv. Rev., 58: 1556–1577.

Kuang, Y., Lackay, S.N., Zhao, L., Fu, Z.F., 2009. Role of chemokines in the enhancement of BBB permeability and inflammatory infiltration after rabies virus infection. Virus Res., 144, 18–26.

Kuo, Y.C., Kuo, C.Y., 2008. Electromagnetic interference in the permeability of saquinaviracross the blood–brain barrier using nanoparticulate carriers, Int. J. Pharm., 351, 271–281.

Knopf, P.M., Cserr, H.F., Nolan, S.C., Wu, T.Y., Harling-Berg, C.J., 1995. Physiology and immunology of lymphatic drainage of interstitial and cerebrospinal fluid from the brain.Neuropathol. Appl. Neurobiol., 21, 175–180.

Lafon, M., Rabies virus receptors, J. Neurovirol., 2005, 82-87.

Lee, D., Powers, K., Baney, R., 2004. Physicochemical properties and blood compatibility of acylated chitosan nanoparticles, Carbohydr. Polym., 58, 371–377.

Lee, H.B., Blaufox, M.D., 1985. Blood Volume in the Rat, J. Nucl. Med., 26, 72–76.

Lee, H.J., Engelhardt, B., Lesley, J., Bickel, U., Pardridge, W.M., 2000. Targeting rat anti mouse transferrin receptor monoclonal antibodies through blood–brain barrierin mouse, J. Pharmacol. Exp. Ther., 292, 1048–1052.

Lee, Y., Messing, A., Su, M., Brenner, M., 2008. GFAP promoter elements required for region-specific and astrocyte-specific expression, Glia, 56, 481–493.

Lentz, T.L., Burrage, T.G., Smith, A.L., Crick, J., Tignor, G.H., 1982. Is the acetylcholinereceptor a rabies virus receptor? Science 1982, 215-182-4.

Leveugle, B.,Spik, G., Perl, D.P.,Bouras, C., Fillit, H.M., Hof, P.R., 1994. The iron-bindingproteinlactotransferrin is present in pathologic lesions in a variety of neurodegenerativedisorders: a comparative immunohistochemical analysis. Brain Res., 650, 20–31.

Levin, V.A., 1980. Relationship of octanol-water partition coefficient and molecular weight to rat brain capillary permeability. J. Med. Chem. 23, 682-684.

Lewin, M., Carlesso, N., Tung, C.H., Tang, X.W., Cory, D., Scadden, D.T., Wessleder, R., 2000.Tat peptide-derivatized magnetic nanoparticles allow *in vivo* tracking and recovery of progenitor cells, Nat. Biotechnol., 18, 410–414.

Li, H., Zhao, X., Ma, Y., Zhai, G., Li, L., Lou, H., 2009. Enhancement of gastrointestinal absorption of quercetin by solid lipid nanoparticles, J. Cont. Release, 133, 238-244.

Li, X., Ding, L., Xu, Y., Wang, Y., Ping, Q., 2009.Targeted delivery of doxorubicin using stealth liposomes modified with transferrin, Int. J. Pharm. 373: 116–123.

Lila, A.S.A., Kizuki, S., Doi ,Y., Suzuki, T., Ishida, T., Kiwada, H., 2009. Oxaliplatin encapsulated in PEG-coated cationic liposomes induces significant tumor growth suppression via a dual-targeting approach in a murine solid tumor model, J. Control. Release, 137, 8–14.

Liu, X.M., Pramoda, K.P., Yang, Y.Y., Chow, S.Y., He, C., 2004.Cholesteryl-grafted functionalamphiphilicpoly(N-isopropylacrylamide-co-N-hydroxylmethylacrylamide):synthesis, temperature-sensitivity, self-assembly and encapsulation of a hydrophobicagent, Biomaterials 25: 2619–2628.

Liu, Y., Huang, R., Han, L., Ke, W., Shao, K., Ye, L., Lou, J., Jiang, C., 2009.Brain-targeting gene deliveryand cellular internalization mechanisms for modified rabies virus glycoproteinRVG29 nanoparticles, Biomaterials, 2009, 4195-202.

Lindgren, M., Hallbrink, M., Prochiantz, A., Langel, U., 2000.Cell-penetrating peptides.TrendsPharmacol. Sci., 21, 99–103.

Liu, H.L., Pan, C. H., Ting, C.Y., Hsiao, M.J., 2010. Opening of the blood–brain barrier bylow-frequency (28-kHz) ultrasound: a novel pinhole-assisted mechanical scanningdevice, Ultrasound Med. Biol., 36, 325–335.

Loxley, A., 2009. Solid Lipid Nanoparticles for the Delivery of Pharmaceutical Actives.Drug Deliv. Technol., 9, 1-5.

Lu, W., Wan, J., She, Z., Jiang, X., 2007.Brain delivery property and accelerated bloodclearance of cationic albumin conjugated pegylated nanoparticle. J. Control.Release, 118, 38–53.

Lu, W., Wan, J., Zhang, Q., She, Z., Jiang, X., 2007. Aclarubicin-loaded cationic albuminconjugatedpegylated nanoparticle for glioma chemotherapy in rats, Int. J. Cancer 120, 420–431.

MacKaya, J.A., Deenb, D.F., Szoka, F.C., 2005. Distribution in brain of liposomes after convection enhanced delivery; modulation by particle charge, particle diameter and presence of steric coating, Brain Res., 1035, 139–153.

Madan, J., Pandey, R.S., Jain, V., Katare, O.P., Chandra, R., Katyal, A., 2013. Poly (ethylene)-glycol conjugated solid lipid nanoparticles of noscapine improve biological half-life, brain delivery and efficacy in glioblastoma cells, Nanomed.Nanotech. Biol. Med., 9, 492–503

Mae, M., Myrberg, H., EI-Andaloussi, S., Langel, U., 2009. Design of a tumor homing cell penetrating peptide for drug delivery, Int. J. Pept. Res. Ther., 15, 11–15.

Mak, M., Fung, L., Strasser, J.F., Saltzman, W.M., 1995.Distribution of drugs following controlled delivery to the brain interstitium, J. Neuro-Oncol., 26, 91–102.

Malina, K.C.K., Cooper, I., Teichberg, V.I., 2009. Closing the gap between the *in vivo* and *in vitro* blood–brain barrier tightness, Brain Res., 1284, 12–21.

Manfredsson, F.P., Mandel, R.J., 2010, Development of gene therapy for neurological disorders, Discov. Med., 9, 204–211.

Markoutsa, E., Pampalakis, G., Niarakis, A., Romero, I.A., Weksler, B., Couraud, P.O., Antimisiaris, S.G., 2011.Uptake and permeability studies of BBB-targeting immunoliposomesusing the hCMEC/D3 cell line, Eur. J. Pharm. Biopharm., 77, 265–274.

Marshall, E., 1999. Gene therapy death prompts review of adenovirus vector, Science, 286, 2244–2245.

Martins, S., Tho, I.,Reimold, I., Fricker, G., Souto, E., Ferreira, D.,Brandl, M., 2012. Brain delivery of camptothecin by means of solid lipid nanoparticles: Formulation design, *in vitro* and *in vivo* studies. Int. J. Pharm., 439, 49– 62

Massodi, I., Bidwell III, G.L., Raucher, D., 2005. Evaluation of cell penetrating peptides fused to elastin-like polypeptide for drug delivery. J. Control.Release, 108, 396– 408.

Mayurama K., 2011. Intracellular targeting of liposomal drugs to solid tumors based on the EPR effects. Adv. drug deliv.Rev. 63:161-169.

Mazor, L.P., Dakwar ,G.R., Popov, M., Kolusheva, S., Shames, A., Linder, C., Grinberg, S., Heldman, E., Stepensky, D., Jelinek, R., 2013. Bolaamphiphilic vesicles encapsulating iron oxide nanoparticles: new vehicles for magnetically-targeted drug delivery, Int.J. Pharm.http://dx.doi.org/10.1016/j.ijpharm.2013.04.017.

Maeda, H., Wu, J., Sawa, T., Matsumura, Y., Hori, K., 2000. Tumor vascular permeability and the EPR effect in macromolecular therapeutics: a review, J. Control. Release, 65, 271–284.

McNeil, D.E., Cote, T.R., Clegg, L., Rorke, B.L., 2002. Incidence and trends in pediatric malignancies medulloblastoma/primitive neuroectodermal tumor: a SEER update: surveillance epidemiology and end results, Med. Pediatr. Oncol., 39, 190–4.

Mehnert, W., Mader.K., 2001.Solid lipid nanoparticles Production, characterization and applications.Adv. Drug Deliv. Rev. 47, 165–196.

Miedel, M.C., Hulmes, J.D., Pan, Y.E.C., 1989. The use of fluorescamine as a detection reagent in protein microcharacterization, J. Biochem. Biophys. Methods, 18, 37–52.

Mishima, K., Higashiyama, S.,Nagashima, Y., Miyagi, Y., Tamura, A., Kawahara, N., Taniguchi, N., Asai, A., Kuchino, Y., Kirino, T., 1996. Regional distribution of heparin-bindingepidermal growth factor-like growth factor mRNA and protein in adult rat forebrain. Neurosci.Lett., 213, 153–156.

Moos, T., Morgan, E.H., 2000.Transferrin and transferrin receptor function in brain barriersystems.Cell. Mol. Neurobiol., 20, 77–95.

Moos, T., Morgan, E.H., 2004.The metabolism of neuronal iron and its pathogenic role in neurological disease: review. Ann. N. Y. Acad. Sci., 1012, 14–26.

Moreira, J.N., Ishida, T., Gaspar, R., Allen, T.M., 2002. Use of the post-insertion technique to insert peptide ligands into preformed stealth liposomes with retention of binding activity and cytotoxicity., Pharm. Res., 19, 265–269.

Moriyama, E., Salcman, M., Broadwell, R.D., 1991.Blood–brain barrier alteration aftermicrowave-induced hyperthermia is purely a thermal effect: I, temperatureand power measurements. Surg. Neurol., 35, 177–182.

Morris, C.M., Candy, J.M.,Kerwin, J.M., Edwardson, J.A., 1994. Transferrin receptors in thenormal human hippocampus and in Alzheimer's disease.Neuropathol.Appl.Neurobiol., 20, 473–477.

Mudhakir, D., Akita, H., Khalil, I.A., Futaki, S., Harashima, H., 2005. Pharmacokinetic analysis of the tissue distribution of octaarginine modified liposomes in mice, Drug Metab. Pharmacokinet., 20, 275–281.

Muhlen, A., Schwarz, C., MehnertW., 1998. Solid lipid nanoparticles (SLN) for controlled drug delivery – Drug release and release mechanism. Eur. J. Pharm.Biopharm. 45, 149–155.

Muller, R.H., Mader, K., Gohla, S., 2000, Solid lipid nanoparticles (SLN) for controlled drug delivery—a review of the state of the art, Eur. J. Pharm. Biopharm., 50, 161–177.

Nakagawa, S., Deli, M.A., Kawaguchi, H., Shimizudani, T., Shimono, T., Kittel, A., Tanaka, K., Niwa, M., 2009. A new blood–brain barrier model using primary rat brain endothelial cells, pericytes and astrocytes, Neurochem. Int., 54, 253–263.

Nakano K, Tozuka Y, Yamamoto H, Kawashima Y, Takeuchi H. 2008. A novel method for measuring rigidity of submicronsize liposomes with atomic force microscopy. Int J Pharm 355:203–209.

Oba, M., Fukushima, S., Kanayama, N., Aoyagi, K., Nishiyama, N.,Koyama, H., Kataoka, K., 2007. Cyclic RGD peptide-conjugatedpolyplex micelles as a targetable gene delivery system directedto cells possessing alphavbeta3 and alphavbeta5 integrins. BioconjugChem., 18, 1415–1423.

Oldendorf, W.H., Cornford, M.E., Brown, W.J. 1997.The large apparent work capability of the blood–brain barrier: a study of the mitochondrial content of capillary endothelial cells in brain and other tissues of the rat, Ann. Neurol. 1 (1977) 409–417.

Opanashuk, L.A., Mark, R.J., Porter, J., Damm, D., Mattson, M.P., K.B. Seroogy, Heparinbindingepidermal growth factor-like growth factor in hippocampus: modulationof expression by seizures and anti-excitotoxic action, J. Neurosci. 19 (1999)133–146.

Opanasopit, P., Tragulpakseerojn, J., Apirakaramwong, A., Ngawhirunpat, T., Rojanarata, T., Ruktanonchai, U., 2011.The development of poly-L-arginine-coated liposomes for gene delivery, Int. J. Nanomed., 6, 2245–2252.

Pang, Z., Lu, W., Gao, H., Hu, K., Chen, J., Zhang, C., Gao, X., Jiang, X., Zhu, C., 2008. Preparation and brain delivery property of biodegradable polymersomes conjugated with OX26,J. Control. Release, 128, 120-127.

Pardridge, W.M., 1980. CNS drug design based on principles of blood-brain barrier transport, J.Neurochem., 70, 1781-1792.

Pardridge, W.M., 1995. Transport of small molecules through the blood-brain barrier: biology and methodology, Adv. Drug Deliv. Rev., 15, 5–36.

Pardridge, W.M.,1999. Vector-mediated drug delivery to the brain, Adv. Drug Deliv. Rev. 36, 299–321

Pardridge, W. M., 2002. Drug and gene delivery to the brain: the vascular route, Neuron, 36, 555–558

Pardridge, W. M., 2001, Brain drug targeting and gene technologies, Jpn. J. Pharmacol., 87, 97–103

Pardridge, W.M., 2002. Drug and gene targeting to the brain with molecular Trojan horses, Nat. Rev. Drug Discov., 1, 131–139.

Pardridge, W.M., 2003. Blood–brain barrier drug targeting: the future of brain drug development. Mol. Interv., 3, 90–105.

Pardridge, W.M., Eisenberg, J., Yang, J., 1985. Human blood–brain barrier insulin receptor. J.Neurochem., 44, 1771–1778.

Pardridge, W.M., Boado, R.J., Farrell, C.R., 1990. Brain-type glucose transporter (GLUT-1) is selectively localized to the blood-brain barrier. Studies with quantitative western blotting and in situ hybridization, J. Biol. Chem., 265, 18035–18040.

Pardridge, W.M., Kang, Y.S., Buciak, J.L., Yang, J., 1995. Human insulin receptor monoclonalantibody undergoes high affinity binding to human brain capillaries *in vitro* and rapid transcytosis through the blood–brain barrier *in vivo* in the primate. Pharm. Res., 12, 807–816.

Pathan, S.A., Iqbal, Z., Zaidi, S.M., Talegaonkar, S., Vohra, D., Jain, G.K., Azeem, A., Jain, N., Lalani, J.R., Khar, R.K., Ahmad,F.J., 2009. CNS drug delivery systems: novel approaches.Recent Pat.Drug Deliv.Formul., 3, 71–89.

Peer, D., Karp, J.M., Hong, S., Farokhzad, O.C., Margalit, R., Langer, R., 2007. Nanocarriers as an emerging platform for cancer therapy. Nat.Nanotechnol., 12, 751-760.

Peracchia, M., Gref, R., Minamitake, Y.,Domb, A., Lotan, N., Langer, R., 1997.PEG-coatednanospheres from amphiphilic diblock and multiblock copolymers: investigationof their drug encapsulation and release characteristics, J. Control. Release, 46, 223–231.

Pfeiffer, D.R., Gudz, T.I., Novgorodov, S.A., Erdahl, W.L., 1995. The peptide mastoparan is a potent facilitator of the mitochondrial permeability transition, J. Biol. Chem., 270, 4923–4932.

Poduslo, J.F., Curran, G.L., 1996. Polyamine modification increases the permeability ofproteins at the blood–nerve and blood–brain barriers. J. Neurochem, 66, 1599–1609.

Pooga, M., But, C., Kihlmark, M., Ha¨llbrink, M., Fernaeus, S., Raid, R., Land, T., Hallberg, E., Bartfai, T., Langel, U., 2001. Cellular translocation of proteins by transportan. FASEB J., 15, 1451–1453.

Prabhakar, K., Afzal, S.M., Kumar, P.U., Rajanna, A., Kishan, V., 2011. Brain delivery of transferrin coupled indinavir submicron lipid emulsions—Pharmacokinetics and tissue distribution, Colloids Surf., B, 86, 305–313.

Provenzale, J.M., Mukundan, S., Dewhirst, M., 2005. The role of blood–brain barrier permeability in brain tumor imaging and therapeutics, Am. J. Roentgenol., 185, 763–7.

Qian, Y., Zha, Y., Feng, B., Pang, Z., Zhang, B., Sun, X., Ren, J., Zhang, C., Shao, X., Zhang, Q., Jiang, X., 2013.PEGylatedpoly(2-(dimethylamino) ethyl methacrylate)/DNA polyplex micelles decorated with phage-displayed TGN peptide for brain-targeted gene delivery, Biomaterials, 34, 2117-2129.

Qian, Z.M., Li, H., Sun, H., Ho, K., 2002. Targeted drug delivery via the transferrin receptor-mediated endocytosis pathway, Pharmacol. Rev., 54, 561–587.

Qin, Y., Chen, H., Yuan, W., Kuai, R., Zhang, Q., Xie, F., Zhang, L., Zhang, Z., Liu, J., He, Q., 2011. Liposome formulated with TAT-modified cholesterol for enhancing the brain delivery, Int. J. Pharm., 419, 85–95.

Qin, Y., Chen, H., Yuan, W., Kuai, R., Zhang, Q., Xie, F., Zhang, L., Zhang, Z., Liu, J., Qin, H., 2011.Liposome formulated with TAT-modified cholesterol for enhancing the brain delivery..Int. J. Pharm, 419, 85–95.

Qiu, L.B., Ding, G.R., Li, K.C., Wang, X.W., Zhou, Y., Zhou, Y.C., Li, Y.R., Guo, G.Z., 2010. Therole of protein kinase C in the opening of blood–brain barrier induced by electromagnetic pulse. Toxicology, 273, 29–34.

Raab, G., Klagsbrun, M., 1997.Heparin-binding EGF-like growth factor, Biochim.Biophys.Acta, 1333, F179–F199.

Ramge, P., Kreuter, J., Lemmer, B., 1999. Circadian phase-dependent antinociceptive reaction in mice after i.v. injection of dalargin-loaded nanoparticles determined by the hot-plate test and the tail-flick test, Chronobiol. Int., 17, 767–777.

Ramana, L.N., Sethuraman, S., Ranga, U., Krishnan, U.M., 2010. Development of a liposomalnano delivery system for nevirapine, J. Biomed. Sci., 17, 57.

Ramsauer, M., Kunz, J., Krause, D., Dermietzel, R., 1998.Regulation of a blood–brain barrier-specific enzyme expressed by cerebral pericytes (pericyticaminopeptidase N/pAPN) under cell culture conditions. J Cereb Blood Flow Metab., 18, 1270–1281.

Ramsauer, M., Krause, D., Dermietzel, R.,2002.Angiogenesis of the blood–brain barrier *in vitro* and the function of cerebral pericytes. FASEB J., 16, 1274–1276.

Raymon, H., Thode, S., Gage, F., 1997. Application of *ex vivo* gene therapy in the treatment of Parkinson's disease, Exp. Neurol., 144, 82–91.

Recht, L., Torres, C.O., Smith, T.W., Raso, V., Griffin, T.W., 1990. Transferrin receptor innormal and neoplastic brain tissue: implications for brain-tumor immunotherapy. J Neurosurg., 72, 941–945.

Regina, A., Demeule, M., Che, C., Lavallee, I., Poirier, J., Gabathuler, R., Beliveau, R., Castaigne, J.P., 2008.Antitumour activity of ANG1005, a conjugate between paclitaxel andthe new brain delivery vector Angiopep-2. Br. J. Pharmacol., 155, 185–197.

Rea, J.C., Barron, A.E., Shea, L.D., 2008, Peptide-mediated lipofection is governed by lipoplex physical properties and the density of surfacedisplayed amines, J. Pharm. Sci., 97, 4794–806.

Ren, J., Shen, S., Wang, D., Xi, Z., Guo, L., Pang, Z., Qian, Y., Sun, X., Jiang, X., 2012. The targeted delivery of anticancer drugs to brain glioma by PEGylated oxidized multi-walled carbon nanotubes modified with angiopep-2, Biomaterials, 33, 3324-3333.

Rip, J., Schenk, G.J., de Boer, A.G., 2009. Differential receptor-mediated drug targeting to the diseased brain. Expert Opin. Drug Deliv., 6, 227–237.

Rodal, S,K,, Skretting, G.,Garred, O., Vilhardt, F., Deurs, B.V., Sandvig,K., 1999. Extraction of cholesterol with Methyl-b-Cyclodextrin perturbs formation of clathrin-coated endocytic vesicles. Mol Biol Cell., 10, 961–74.

Rooy, I., Mastrobattista, E., Storm, G., Hennink, W.E., Schiffelers, R.M., 2011. Comparisonof five different targeting ligands to enhance accumulation of liposomes into the brain. J. Control. Release, 150, 30–36.

Roney, C., Kulkarni, P., 2005. Targeted nanoparticles for drug delivery through the blood–brain barrier for Alzheimer's disease. J. Control. Release, 108, 193-214.

Rousselle, C., Clair, P., Lefauconnier, J.M., Kaczorek, M.,Scherrmann, J.M., Temsamani, J., 2000.New advances in the transport of doxorubicin through theblood–brain barrier by a peptide vector-mediated strategy. Mol. Pharmacol., 57, 679–686.

Rousselle, C., Clair, P., Smirnova, M., Kolesnikov, Y., Pasternak, G.W., Gac-Breton, S., Rees, A.R., Scherrmann, J.M., Temsamani, J., 2003.Improved brain uptake and pharmacologicalactivity of dalargin using a peptide-vector-mediated strategy. J. Pharmacol.Exp. Ther., 306, 371–376.

Roth, L.J., Barlow, C.F., 1961. Drugs in the brain.Science. 134, 22–31.

Rudolph, C., Schillinger, U., Ortiz, A., Tabatt, K., Plank, C., Müller, R.H., Rosenecker, J., Application of novel solid lipid nanoparticle (SLN)- gene vector formulations based on a dimeric HIV-1 TAT-peptide *in vitro* and *in vivo*, 2004. Pharm. Res., 21, 1662–1669.

Saar, K., Lindgren, M., Hansen, M., Eiriksdottir, E., Jiang, Y., Rosenthal-Aizman, K., Sassian, M., Langel, U., 2005.Cell-penetrating peptides: a comparative membrane toxicity study. Anal.Biochem., 345, 55–65.

Sabatier, J.M., Vives, E., Mabrouk, K., Benjouad, A., Rochat, H., Duval, A., Hue, B., Bahraoui, E., 1991.Evidence for neurotoxic activity of tat from human immunodeficiencyvirus type 1. J. Virol., 65, 961–967.

Sadzuka, Y., Nakade, A., Hirama, R., Miyagishima, A., Nozawa, Y., Hirota, S., Sonobe, T., 2002. Effects of mixed polyethyleneglycol modification on fixed aqueous layer thickness and antitumor activity of doxorubicin containing liposome. Int. J. Pharm 238, 171-180.

Szoka, F., Papahadjopoulos, D., 1980.Comparative properties and methods of preparation of lipid vesicles (liposomes), Annu. Rev. Biophys. Bioeng., 9, 467–508

Scheller A., Wiesner,B., Melzig,M., Bienert,M. and Oehlke,J., 2000.Evidence for an amphipathicity independent cellular uptake of amphipathic cell-penetrating peptides. Eur. J. Biochem., 267, 6043–6050.

Scherrmann, J.M., 2002. Drug delivery to brain via the blood–brain barrier. Vascular Pharmacology, 38, 349 – 354.

Schlachetzki, F., Zhang, Y., Boado, R., and Pardridge, W. M., 2004. Gene therapy of the brain: the trans-vascular approach, Neurology, 62, 1275–1281.

Schmidt, N., Mishra, A., Lai, G.H., Wong, G.C.L., 2010. Arginine-rich cell-penetrating peptides, FEBS Lett., 584, 1806–1813.

Schroeder, U., Sabel, B.A., 1996. Nanoparticles, a drug carrier system to pass the blood–brain barrier, permit central analgesic effects of i.v. dalargin injections, Brain Res., 710, 121–124.

Schnyder, A., Huwyler, J., 2005. Drug Transport to Brain with Targeted Liposomes.J. Am. Soc. Exp. Neu. Therap. 2, 99–107.

Schröder, U., Sabel, B.A., 1996. Nanoparticles, a drug carrier system to pass the blood–brain barrier, permit central analgesic effects of i.v.dalargin injections.BrainRes., 710, 121–124.

Seju, U., Kumar, A., Sawant, K.K., 2011. Development and evaluation of olanzapine-loaded PLGA nanoparticles for nose-to-brain delivery: *In vitro* and *in vivo* studies, ActaBiomater., 7, 4169–4176.

Semete, B., Booysen, L., Lemmer, Y., Kalombo, L., Katata, L., Verschoor, J., Swai, H.S., 2010. *In vivo* evaluation of the biodistribution and safety of PLGA nanoparticles as drug delivery systems, Nanomedicine, 6, 662–671.

Serwer, L.P., James, C.D., 2012. Challenges in drug delivery to tumors of the central nervous system: An overview of pharmacological and surgical considerations. Adv. Drug Deliver. Reviews, 64, 590–597.

Shao, K., Huang, R., Li, J., Han, L., Ye, L., Lou, J., Jiang, C., 2010.Angiopep-2 modified PE-PEGbased polymeric micelles for amphotericin B delivery targeted to the brain.J. Control. Release, 147, 118–126.

Sharma, G., Modgil, A., Sun, C., Singh, J., 2012. Grafting of Cell-Penetrating Peptide to Receptor-TargetedLiposomes Improves their Transfection Efficiency and Transportacross Blood–Brain Barrier Model. J. Pharm. Sci.,2012, 2468–2478.

Sharma, G., Modgil, A., Layek, B., Arora, K., Sun, C., Law, B., Singh, J., 2013. Cell penetrating peptide tethered bi-ligand liposomes for delivery to brain *in vivo*: Biodistribution and transfection. J. Control. Release, 167, 1–10.

Shek, P.N., Lopez, N.G., Heath, T.D., 1986. Immune response mediated by liposomeassociatedprotein antigens. IV. Modulation of antibody formation by vesicleencapsulated methotrexate, Immunology 57, 153–157.

Shi, N., Boado, R.J., Pardridge, W.M., 2001. Receptor-mediated gene targeting to tissues *in vivo* following intravenous administration of Pegylated immunoliposomes, Pharm. Res., 18, 1091–1095.

Shir, A., Ogris, M., Wagner, E., Levitzki, A., 2006.EGF receptor-targeted synthetic doublestrandedRNA eliminates glioblastoma, breast cancer, and adenocarcinomatumors in mice, PLoS Med., 3, 6.

Snyder, E.L., Dowdy, S.F., 2004. Cell penetrating peptides in drug delivery. Pharm. Res., 21, 389–393.

Son, S., Hwang, D.W., Singha, K., Jeong, J.H., Park, T.G., Lee, D.S., Kim, W.J., 2011. RVG peptide tethered bioreduciblepolyethylenimine for gene delivery to brain. J. Control. Release, 155, 18–25.

Sourla, A., Doillon, C., Koutsilieris, M., 1996. Three-dimensional type I collagen gel system containing MG-63 osteoblasts-like cells as model for studying local bone reaction caused by metastatic cancer cells. Anticancer Res.,16, 2773–80.

Stam, R., 2010. Electromagnetic fields and the blood–brain barrier. Brain Res. Rev., 65, 80–97.

Stewart, P.A., 2000. Endothelial vesicles in the blood–brain barrier: are they related to permeability? Cell. Mol. Neurobiol., 20, 149–163.

Streit, W.J.,Conde, J.R., Fendrick, S.E., Flanary, B.E.,Mariani, C.L., 2005. Role of microglia in the central nervous system's immune response. Neurol. Res. 27, 685–691.

Stolnik, S., Illum, L., Davis, S.S., 1995.Long circulating microparticulate drug carriers,Adv. Drug Deliv. Rev. 16, 195–214.

Suka, J.S., Suha, J., Choya, K., Laib, S.K., Fub, J., Hanesa, J., 2006. Gene delivery to differentiated neurotypic cells with RGD and HIV Tat peptide functionalized polymeric nanoparticles, Biomaterials 27,5143–5150.

Tan, P.H., Manunta, M., Ardjomand, N., Xue, S.A., Larkin, D.F., Haskard, D.O., Taylor, K.M., George, A.J., 2003. Antibody targeted gene transfer to endothelium. J. Gene Med., 5, 311–323.

Temsamani, J., Vidal, P., 2004. The use of cell-penetrating peptides for drug delivery.DrugDiscov. Today, 9, 1012–1019

Terasaki, T., Ohtsuki, S., Hori, S., Takanaga, H., Nakashima, E., Hosoya, K., 2003.New approaches to *in vitro* models of blood–brain barrier drug transport. Drug Discovery Today. 8, 944-954.

Thomas, F.C., Taskar, K., Rudraraju, V., Goda, S., Thorsheim, H.R., Gaasch, J.A., Mittapalli, D. Palmieri, R.K., Steeg, P.S., Lockman, P.R., Smith, Q.R., 2009.Uptake ofANG1005, a novel paclitaxel derivative, through the blood–brain barrier intobrain and experimental brain metastases of breast cancer. Pharm. Res., 26, 2486–2494.

Tian, W., Ying, X., Du, J., Guo, J.,Men, Y., Zhang, Y., Li ,R.J., Yao, H.J., Lou, J.N., Zhang, L.R., Lu W.L., 2010. Enhanced efficacy of functionalized epirubicin liposomes in treating brainglioma-bearing rats.Eur. J. Pharm. Sci. 41: 232–243.

Tilloy, S., Monnaert, V., Fenart, L., Bricout, H., Cecchelli, R., Monflier, E., 2006. Methylatedbeta-cyclodextrin as P-gp modulators for deliverance of doxorubicin across an *in vitro* model of blood–brain barrier, Bioorg. Med. Chem. Lett., 16, 2154–2157.

Tontsch, U., Bauer, H.C., 1991. Glial cells and neurons induce blood–brain barrier related enzymes in cultures cerebral endothelial cells, Brain, 593, 247–253.

Torchilin, V.P., Levchenko, T.S., Rammohan, R., Volodina, N., Sternberg, B.P., D'Souza, G.G.M., 2003. Cell transfection *in vitro* and *in vivo* with nontoxic TAT peptide–liposome–DNA complexes, Proc. Natl. Acad. Sci.,100, 1972–1977.

Torchilin, V.P., Rammohan, R., Weissig, V., Levchenko, T.S., 2001. TAT peptide on the surface of liposomes affords their efficient intracellular delivery even at low temperature and in the presence of metabolic inhibitors, Proc. Natl. Acad. Sci., 98, 8786–8791.

Tosi, G., Vergoni, A.V., Ruozi, B., Bondioli, L., Badiali, L., Rivasi, F.,Costantino, L., Forni, F., Vandelli, M.A., 2010.Sialic acid and glycopeptides conjugated PLGA nanoparticlesfor central nervous system targeting: *in vivo* pharmacological evidenceand biodistribution, J. Control. Release, 145, 49–57.

Townsend, S.A., Evrony, G.D., Gu, F.X., Schulz, M.P., Brown Jr, R.H., Langer, R., 2007. Tetanus toxin C fragment-conjugated nanoparticles for targeted drug delivery to neurons, Biomaterials 28, 5176–5184.

Trabulo, S., Cardoso, A.L., Mano, M., de Lima, M.C.P., 2010.Cell penetrating peptides—Mechanisms of cellular uptake and generation of delivery systems, Pharmaceuticals, 3, 961–993.

Tseng, M.T., Lu, X., Duan, X., Hardas, S.S., Sultana, R., Wu, P., Unrine, J.M., Graham, U., Butterfield, D.A., Grulke,E.A., Yokel, R.A., 2012. Alteration of hepatic structure and oxidative stress induced by intravenous nanoceria, Toxicol. Appl. Pharmacol., 260, 173–182.

Tsuji, A., 2005. Small molecular drug transfer across the blood-brain barrier via carrier mediated transport systems, NeuroRx, 2, 54–62.

Tsuji, A., Tamai, I.I., 1999. Carrier-mediated or specialized transport of drugs across the blood–brain barrier, Adv. Drug Deliv. Rev., 36, 277–290.

Ulbrich, K., Hekmatara, T., Herbert, E., Kreuter, J., 2009.Transferrin- and transferrinreceptor-antibody-modified nanoparticles enable drug delivery across the blood–brain barrier (BBB), Eur. J. Pharm. Biopharm., 71, 251–256.

Varga, C.M., Wickham, T.J., Lauffenburger, D.A., 2000. Receptor mediated targeting of gene delivery vectors: insights from molecular mechanisms for improved vehicle design, Biotechnol. Bioeng., 70, 593–605.

Vauthier, C., Bouchemal, K., 2009. Methods for the preparation and manufacture of polymeric nanoparticles, Pharm. Res., 26, 1025–1058.

Vasir, J.K., Reddy, M.K., Labhasetwar, V.D., 2005. Nanosystems in Drug Targeting: Opportunities and Challenges, Curr. Nanosci., 1, 47–64.

Venishetty, V.K., Samala, R., Komuravelli, R., Kuncha, M., Sistla, R., Diwan, P.V., 2013.β-Hydroxybutyric acid grafted solid lipid nanoparticles: A novel strategy to improve drug delivery to brain, Nanomed.Nanotech. Biol. Med., 9, 388–397.

Veszelka, S., Paszto,´ I.M., Farkas, A.E., Krizbai, I., Ngo, T.K., Niwa, M., Abraham, C.S., Deli, M.A., 2007. Pentosan polysulfate protects brain endothelial cells against bacterial lipopolysaccharide induced damages, Neurochem. Int., 50, 219–228.

Visser, C.C., Stevanovi, S., Voorwinden, L.H., Bloois, L.V., Gaillard, P.J., Danhof, M., Crommelin, D.J.A., Boer, A.G., 2005. Targeting liposomes with protein drugs to the blood–brain barrier *in vitro*, Eur. J. Pharm. Sci., 25, 299–305.

Wade, L.A., Katzman, R., 1975. 3-O-methyldopa uptake and inhibition of L-dopa at theblood–brain barrier, Life Sci., 17, 131–136.

Wallje, E.B., Keller, S., Serowy, S., Geibel, S., Pohl, P., Bienert M., Dathe, M., 2005. A Critical Reassessment of Penetratin Translocation Across Lipid Membranes,Biophys. J., 89, 2513–2521.

Wang, Y., Sub, W., Li, Q., Li, C., Wang, H., Li, Y., Cao, Y., Chang, J., Zhang, L., 2013. Preparation and evaluation of lidocaine hydrochloride-loaded TAT-conjugated polymeric liposomes for transdermal delivery, Int. J. Pharm., 441, 748– 756.

Wen, Z., Yan, Z., Hu, K., Pang, Z., Cheng, X., Guo, L.R., Zhang, Q., Jiang, X., Fang, L., Lai, R., 2011. Odorranalectin-conjugated nanoparticles: Preparation, brain delivery and pharmacodynamic study on Parkinson's disease following intranasal administration, J. Control. Release, 151, 131–138.

Weyhers, H., Mehnert, W., Hahn, H., Müller, R.H., 1995. Solid lipid nanoparticles—determination of *in vivo* toxicity, Proc. First World Meeting APGI/APV, 1995, 489–490.

Wekerle, H., 2002. Immune protection of the brain-efficient and delicate, J. Infect.Dis., 186 (Suppl 2), S140–S144.

Williams, K., Alvarez, X., Lackner, A.A., 2001. Central nervous system perivascular cells are immunoregulatory cells that connect the CNS with the peripheral immune system, Glia 36, 156–164.

Williams, W.M., Hoss, W., Formaniak, M., Michaelson, S.M., 1984.Effect of 2450 MHz microwaveenergy on the blood–brain barrier to hydrophilic molecules, A. Effecton the permeability to sodium fluorescein, Brain Res., 319, 165–170.

Wilson, B., Samant, M.K., Santhi, K., Kumar, K.P.S., Paramakrishnan, N., Suresh, B., 2008.Poly(n-butylcyanoacrylate) nanoparticles coated with polysorbate 80 for the targeted delivery of rivastigmine into the brain to treat Alzheimer's disease, Brain Res.,1200,159-168.

Wohlfart, S., Gelperina, S., Kreuter, J., 2012.Transport of drugs across the blood–brain barrier by nanoparticles, J Control. Release, 161, 264–273.

Woodle, M.C., 1995. Sterically stabilized liposome therapeutics, Adv. Drug Deliv. Rev., 16: 249–265.

Woodle, M.C., Engberg, C.M., Zalipsky, S., 1994. New amphipathic polymer–lipid conjugates forming long-circulating reticuloendothelial system-evading liposomes, Bioconjug. Chem., 5, 493–496.

Wu, D., Yang, J., Pardridge, W.M., 1997. Drug targeting of a peptide radiopharmaceutical through the primate blood–brain barrier *in vivo* with a monoclonal antibody tothe human insulin receptor, J. Clin.Invest., 100, 1804–1812.

Wu, J., Hua, Y., Keep, R.F., Nakamura, T., Hoff, J.T., Xi, G., 2003. Iron and iron-handling proteinsin the brain after intracerebral hemorrhage, Stroke 34, 2964–2969.

Xia, C.F., Boado, R.J., Pardridge, W.M., 2009. Antibody-mediated targeting of siRNAviathe human insulin receptor using avidin–biotin technology, Mol. Pharm., 6, 747–751.

Xia, H., Gao, X., Gu, G., Liu, Z., Hu, Q., Tu, Y., Song, Q., Yao, L., Pang, Z., Jiang, X., Chen, J., Chen, H., 2012. Penetratin-functionalized PEG–PLA nanoparticles for brain drug delivery, Int J Pharm., 436, 840–850.

Xiang, Y., Liang, L., Wang, X., Wang, J., Zhang, X., Zhang, Q., 2011.Chloride channel-mediated brain glioma targeting of chlorotoxin-modified doxorubicin-loaded liposomes.J. Control. Release, 152, 402–410.

Xie, Y., Ye, L., Zhang, X., Cui, W., Lou, J., Nagai, T., Hou, X., 2005.Transport of nerve growth factor encapsulated into liposomesacross the blood–brain barrier: *In vitro* and *in vivo* studies. J. Control. Release, 105,106-119.

Xu, Y., Szoka, F.C., 1996. Mechanism of DNA Release from Cationic Liposome/DNA Complexes Used in Cell Transfection, Biochemistry, 35, 5616–5623.

Yamada, Y., Harashima, H., 2008. Mitochondrial drug delivery systems for macromolecule and their therapeutic application to mitochondrial diseases.Adv. Drug Deliv. Rev. 60, 1439–1462.

Yamamoto, M., Ikeda, K., Ohshima, K., Tsugu, H., Kimura, H., Tomonaga, M., 1997.Increased expression of low density lipoprotein receptor–protein /alpha2–macroglobulin receptor in human malignant astrocytomas, Cancer Res., 57, 2799–2805.

Yamano, S., Dai, J., Yuvienco, C., Khapli, S., Moursi, A.M., Montclare, J.K., 2011. Modified Tat peptide with cationic lipids enhances gene transfection efficiency via temperature-dependent and caveolae-mediated endocytosis, J. Control. Release, 152, 278–85.

Yandek, L.E., Pokorny, A., Floren, A., Knoelke, K., Langel, U., Almeida, P.F.F., 2007. Mechanism of the Cell-Penetrating Peptide Transportan 10 Permeation of Lipid Bilayers. Biophys J., 92, 2434-44.

Yang, S.C., Zhu, J.B., Lu, Y., Liang, B.W., Yang, C.Z., 1999.Body distribution of camptothecin solid lipid nanoparticles after oral administration, Pharm. Res., 16, 751–757.

Yang, F.Y., Fu, W.M., Yang, R.S.,Liou, H.C., Kang, K.H., Lin, W.L., 2007.Quantitative evaluationof focused ultrasound with a contrast agent on blood–brain barrier disruption,Ultrasound Med. Biol., 33, 1421–1427.

Ying, X., Wen, H., Lu, W.L., Du, J., Guo, J., Tian, W., Men, Y., Zhang, Y., Li, R.J., Yang, T.Y., Shang, D.W., Lou, J.N., Zhang, L.R., Zhang, Q., 2010. Dual-targeting daunorubicin liposomes improve the therapeutic efficacy of brain glioma in animals. J. Control. Release, 141, 183–192.

Yoon, D.J., Chu, D.S., Ng, C.W., Pham, E.A., Mason, A.B., Hudson, D.M., Smith, V.C., MacGillivray, R.T., Kamei, D.T., 2009. Genetically engineering transferrin to improve its *in vitro* ability to deliver cytotoxins, J. Control. Release, 133, 178–184.

Yuba, E., Kojima, C., Sakaguchi, N., Harada, A., Koiwai, K., Kono, K., 2008. Gene delivery to dendritic cells mediated by complexes of lipoplexes and pH-sensitive fusogenic polymer-modified liposomes, J. Control. Release, 130, 77–83.

Yuan, S.Y., 2006. New insights into eNOS signaling in microvascularpermeability.Am.J.Physiol. Heart Circ. Physiol., 291, H1029–H1031.

Zara, G.P., Cavalli, R., Fundarò, A., Bargoni, A., Caputo, O., Gasco, M.R., 1999. Pharmacokinetics of doxorubicin incorporated in solid lipid nanospheres (SLN), Pharmacol. Res., 40, 281–286.

Ziegler, A., Nervi, P., Durrenberger, M., Seelig, J., 2005.The cationic cell-penetrating peptide CPP TAT derived from the HIV-1 protein Tat is rapidly transported into living fibroblasts: optical, biophysical and metabolic evidence, Biochemistry, 44, 138–148.

Zimmerberg, J., Parsegian, V.A., 1986. Polymer inaccessible volume changes during opening and closing of a voltage-dependent ionic channel, Nature 323, 36–39.

Zensi, A., Begley, D., Pontikis, C., Legros, C., Mihoreanu, L., Wagner, S.,Buchel, C., Briesen, H.,Kreuter, J., 2009. Albumin nanoparticles targeted with Apo E enter the CNS bytranscytosis and are delivered to neurons. J. Control. Release, 137, 78–86.

Zhang, H.W., Zhang, L., Sun, X., Zhang, Z.R., 2007. Successful transfection of hepatoma cells after encapsulation of plasmid DNA into negatively charged liposomes. Biotechnol. Bioeng., 96, 118–124.

Zhang, Y., Boado, R.J., Pardridge, W.M., 2003. Marked enhancement in gene expression by targeting the human insulin receptor. J. Gene Med., 5, 157–163.

Zhang, C., Tang, N., Liu, X.J., Liang, W., Xu, W., Torchilin, V.P., 2006. siRNA-containing liposomes modified with polyarginine effectively silence the targeted gene. J. Control. Release, 112, 229–239.

Zhao, H., Li, G.L., Wang, R.Z., Li, S.F., Wei, J.J., Feng, M., Zhao, Y.J., Ma, W.B., Yang, Y., Li, Y.N., Kong, Y.G., 2010. A comparative study of transfection efficiency between liposomes, Immunoliposomes and brain-specific immunoliposomes, J. Int. Med. Res., 38, 957–966.

Zhong, M.Q., Hongyan, L., Hongzhe, U., Kwokping, H. 2002. Targeted drug delivery via the transferrin receptor-mediated endocytosis pathway. Pharmacol. Rev., 54, 561–87.

Zhu, S., Qian, F., Zhang, Y., Tang, C., Yin, C., 2007. Synthesis and characterization of PEG modified N-trimethyl amino ethyl methacrylate chitosan nanoparticles, Eur. Polymer J., 43, 2244–2253.

Zorko, M., Langel, U., 2005.Cell-penetrating peptides: mechanism and kinetics of cargodelivery, Adv. Drug Deliv. Rev., 57, 529–545.